MOUSE MUSCLEBLIND-LIKE COMPOUND KNOCKOUT MODELS OF MYOTONIC DYSTROPHY

By

KUANG-YUNG LEE

A DISSERTATION PRESENTED TO THE GRADUATE SCHOOL
OF THE UNIVERSITY OF FLORIDA IN PARTIAL FULFILLMENT
OF THE REQUIREMENTS FOR THE DEGREE OF
DOCTOR OF PHILOSOPHY

UNIVERSITY OF FLORIDA

2013

To my family: Sarah, Hubert, Jasper and Nathaniel

ACKNOWLEDGMENTS

I thank my boss, Dr. Maurice Swanson, for helping me complete my graduate career. He is a perfect role model and I was motivated every day hoping that one day I will also be an outstanding scientist. I appreciate the help from my wife Sarah, a master biologist, who received her degree from Stanford University and understands the difficulty of a biomedical career path. Without her support and the care of our three lovely boys, Hubert, Jasper and Nathaniel, it would have been impossible for me to survive these challenging years in graduate school. I appreciate my parents, who are my best listeners at every glorious and frustrated moment. I thank my committee members at Chang-Gung Memorial Hospital in Keelung, Taiwan, who provided me the flexibility to make my research dream come true. I am grateful to have the support of many colleagues: Dr. Moyi Li (my mentor and partner on my major projects), Dr. Mike Poulos (for his instruction and assistance during my rotation project), Mini Manchanda, Drs. Chris Chamberlain and Kostas Charizanis, Apoorva Mohan, Dustin Finn, Hannah Hong and Drs. Ashok Kumar, Tom Foster, Laura Ranum (for assistance with the *Mbnl* double knockout project). I also thank my collaborators Drs. Takashi Kimura, Chaolin Zhang, Mario Gomes-Pereira, Seiji Nishino, Nicolas Charlet-Berguerand for papers published or in preparation. I acknowledge my committee members Drs. Jim Resnick, Brian Harfe and Sergei Zolotukhin for their helpful advice. Finally, I appreciate all the former and current Swanson/Ranum lab members, mouse house veterinarians and technicians, departmental administrative members, mentors during rotations, IDP office staff, and church brothers and sisters that I have not mentioned individually for their kind support throughout these years.

TABLE OF CONTENTS

page

LIST OF TABLES

LIST OF FIGURES

LIST OF ABBREVIATIONS

1KO	*Mbnl1* knockout
1KO2HET	*Mbnl1* knockout; *Mbnl2* heterozygous knockout
2KO1HET	*Mbnl2* knockout; *Mbnl1* heterozygous knockout
AAV	Adeno-associated virus
AChR	Acetylcholine receptor
Add1	Adducin 1
Ank1	Ankyrin 1, erythroid
App	Amyloid beta precursor protein
Arhgef7	Rho guanine nucleotide exchange factor (GEF7)
AS	Alternative splicing
Atp2a1	ATPase calcium transporting, cardiac muscle, fast twitch 1(Serca1)
AV	Atrioventricular
Bin1	Bridging integrator 1
Cacna1d	Calcium channel, voltage dependent, L-type, alpha 1D subunit
Cacna1s	Calcium channel, voltage dependent, L-type, alpha 1S subunit
Camk2d	Calcium/calmodulin-dependent protein kinase II delta
Camkk2	Calcium/calmodulin-dependent protein kinase kinase 2, beta CDM Congenital myotonic dystrophy
CELF1	CUGBP1 and ETR like factor 1
Clasp2	CLIP associating protein 2
Clcn1	Chloride channel 1
CNBP	Cellular nucleic acid binding protein (Znf9)
CNS	Central nervous system
Csda	Cold shock domain protein A (Ybx3)

CSNK1D	Casein kinase 1 delta
cTNT	Cardiac troponin T (troponin T2)
CUGBP	CUG binding protein
DCLK1	Doublecortin-like kinase 1
dCTP	Deoxycytidine triphosphate
DDX5	Dead box polypeptide 5
DGKH	Diacylglycerol kinase eta
DKO	Double knockout
DM	Myotonic dystrophy
DM1	Myotonic dystrophy type 1
DM2	Myotonic dystrophy type 2
DMPK	Myotonic dystrophy protein kinase
EC	Excitation contraction
ECG	Electrocardiography
EMG	Electromyography
FMR-1	Fragile X mental retardation syndrome
FTD-ALS	Frontal temporal dementia and amyotrophic lateral sclerosis
FXTAS	Fragile X tremor and ataxia syndrome
GA	Gastrocnemius
GABA	Gamma-aminobutyric acid
Grin1	Glutamate receptor, ionotropic, NMDA1
HITS-CLIP	High throughput sequencing crossed linked immunoprecipitation
hnRNP	Heterogeneous nuclear ribonucleoprotein
HSA	Human skeletal actin
HTT	Huntingtin

KCNMA1	Potassium large conductance calcium-activated channel, subfamily M, alpha member 1
LDB3	LIM domain binding 3
LNP	Limb and neural patterns
MAPT	Microtubule associated protein Tau
MBNL	Muscleblind-like
MHC	Myosin heavy chain
MPRIP	Myosin phosphatase Rho interacting protein
MRI	Magnetic resonance image
MTMR	Myotubularin related protein
NDRG4	N-myc downstream regulated gene 4
Nestin DKO	(*Mbnl1*$^{\Delta E3/\Delta E3}$; *Mbnl2*$^{cond/cond}$; *Nestin*$^{+/-}$)
NFIX	Nuclear factor I/X
NLS	Nuclear localization signal
NMJ	Neuromuscular junction
NREM	Non rapid eye movement
PER1	Period circadian clock 1
PPP1R12A	Protein phosphatase 1, regulatory subunit 12a
PSG	Polysomnography
PTBP	Polypyrimidine tract binding protein
PTZ	Pentylenetetrazole
RAN	Repeat associated non-ATG initiated translation
RBFOX	RNA binding protein fox-1 homolog
RBP	RNA binding protein
REM	Rapid eye movement
RNA SEQ	RNA sequencing

RT-PCR	Reverse transcription polymerase chain reaction
RTTA	Reverse tetracycline transactivation
RYR1	Ryanodine receptor 1
SCA8	Spinal cerebellar ataxia type 8
SCN	Suprachiasmatic nucleus
SE	Splicing enhancer
SERCA1	Sarcoplasmic/endoplasmic calcium ATPase 1 (Atp2a1)
SLAIN2	SLAIN motif family member 2
SLITRK4	SLIT and NTRK-like family, member 4
SORBS1	Sorbin and SH3 domain containing 1
SPAG9	Sperm associated antigen 9
SPNA2	Spectrin alpha 2
SS	Splicing silencer
ST3GAL3	ST3 beta-galactoside alpha-2,3-sialyltransferase 3
TA	Tibialis anterior
TANC2	Tetratricopeptide repeat, ankyrin repeat, and coiled-coil containing 2
Tmem63b	Transmembrane protein 63b
TNNT2	Cardiac troponin T (cTNT)
TNNT3	Troponin T3
TTN	Titin
UTR	Untranslated region
VF	Ventricular fibrillation
VT	Ventricular tachycardia

Abstract of Dissertation Presented to the Graduate School
of the University of Florida in Partial Fulfillment of the
Requirements for the Degree of Doctor of Philosophy

MOUSE MUSCLEBLIND-LIKE COMPOUND KNOCKOUT MODELS OF MYOTONIC DYSTROPHY

By

Kuang-Yung Lee

August 2013

Chair: Maurice Swanson
Major: Medical Sciences – Genetics

Myotonic dystrophy (DM), which is the most common adult onset muscular dystrophy, is caused by an unstable $(CTG)_n$ repeat expansion in the 3' UTR of the *DMPK* gene (DM1), or a $(CCTG)_n$ intronic repeat expansion in the *CNBP* gene (DM2). When transcribed, these repeat expansions generate toxic C(C)UG RNAs that directly sequester the muscleblind-like (MBNL) proteins. MBNL proteins regulate alternative splicing during the developmental transition from fetal to adult life. Among the three paralogs of the MBNL family, MBNL1 is expressed abundantly in skeletal muscle while MBNL2 expression is higher in the central nervous system (CNS). *Mbnl1* knockout mice recapitulate (DM)-relevant skeletal muscle symptoms including myotonia, but show only mild CNS phenotypes. In contrast, *Mbnl2* knockout mice exhibit DM-associated CNS abnormalities, including sleep dysregulation without major skeletal muscle deficits. To evaluate the effect of compound loss of *Mbnl* gene expression, we crossed *Mbnl1* and *Mbnl2* knockout lines but double knockout mice were inviable. Interestingly, we discovered that *Mbnl1*$^{\Delta E3/\Delta E3}$; *Mbnl2* $^{+/\Delta E2}$ homozygous; heterozygous double knockout mice exhibited a shorter life span, severe myotonia, muscle weakness, enhanced histopathology and neuromuscular junction (NMJ) deficits. Additionally, *Mbnl1*$^{\Delta E3/\Delta E3}$;

Mbnl2 $^{+/\Delta E2}$ knockouts developed cardiac conduction block accompanied by fibrosis and cardiomyopathy in the heart consistent with the heart phenotype in DM. In both skeletal and cardiac muscles, enhanced splicing alterations could underlie these pathological changes. To overcome the embryonic lethality of *Mbnl1*$^{\Delta E3/\Delta E3}$; *Mbnl2* $^{\Delta E2/\Delta E2}$ double knockouts, we employed a conditional knockout strategy and created *Mbnl1*$^{\Delta E3/\Delta E3}$; *Mbnl2*$^{cond/cond}$; Nestin$^{+/-}$ mice with constitutive loss of Mbnl1 but neuron-specific depletion of Mbnl2. These mice also showed reduced lifespan, muscle weakness and severe motor deficits. Moreover, pronounced splicing alterations in the brain were detected and hippocampal dysfunction was uncovered by electrophysiological analysis. We conclude that both Mbnl1 and Mbnl2 play critical roles in skeletal muscle, heart and brain during development and their depletion by CUG and CCUG expansion RNA in DM leads to the characteristic multisystemic manifestations of this neuromuscular disease. These results suggest that alternative therapeutic approaches should be developed which are designed to restore the totality of MBNL activity in DM tissues.

CHAPTER 1
OVERVIEW OF MYOTONIC DYSTROPHY AND ALTERNATIVE RNA PROCESSING

Introduction

Myotonic Dystrophy (DM) is a Microsatellite Expansion Disorder

Myotonic dystrophy (DM) is the most common adult onset muscular dystrophy with a prevalence of 1 in 8000 (Harper, 2001; Lee and Cooper, 2009). Along with skeletal muscle weakness and atrophy, the characteristic feature of this disease is myotonia, a delay in relaxation after muscle contraction (Barroso and Nogues, 2009; Wang and Huang, 2011). However, skeletal muscle is not the only system affected in DM. Patients also develop neuropsychiatric symptoms, cardiac conduction block and sudden death, insulin resistance, testicular atrophy, gastrointestinal symptoms and cataract. Twenty-one years ago, when the type 1 DM (DM1) genetic locus and causative mutation was first described, it was unclear how a single mutation in a single gene could account for all of these symptoms.

DM belongs to a group of diseases called microsatellite expansion disorders. Microsatellites are short tandem nucleotide repeats and their sizes are variable (polymorphic) among normal individuals. More than twenty diseases are caused by microsatellite repeats when the repeats expand beyond a certain threshold (Batra et al., 2010). These repeats are located in different gene regions and generate pathologic effects through protein gain-of-function, transcriptional interference or RNA gain-of-function mechanisms (Nelson et al., 2013). For example, Huntington disease is caused by protein gain-of-function in which pathological $(CAG)_n$ repeats located in the coding region of the *HTT* gene generate toxic huntingtin protein which accumulates in intranuclear inclusions (La Spada and Taylor, 2010). When repeats are located in a

non-coding region, such as $(CGG)_n$ (full mutation, n>200) repeats in the 5'UTR of *FMR1* gene in Fragile X mental retardation syndrome (FRAXA), they adversely affect gene expression through hypermethylation (Swanson and Orr, 2007). Repeats in non-coding regions may also generate toxicity through an RNA gain-of-function mechanism. An interesting example is Fragile X tremor ataxia syndrome (FXTAS), which is caused by *FMR1* $(CGG)_n$ (permutation, n=55~200) expansions. These repeats are shorter than those present in FRAXA but expression of these $(CGG)_{55\text{-}200}$ expansions leads to upregulation of FMR1 mRNA levels, nuclear retention of these mutant RNAs in the nucleus and sequestration of several RNA binding proteins (RBP) including hnRNP A2/B1 and PURA. (Jin et al., 2007; Sofola et al., 2007). Interestingly, sense and antisense transcription of repeat expansion regions may contribute in different ways to pathogenesis. In spinal cerebellar ataxia type 8 (SCA8), protein gain-of-function and RNA gain-of-function mechanisms have been suggested to be associated with disease with both sense (coding, *ATXN8* gene) and antisense (non-coding, *ATXN8OS*) RNAs expressed (Daughters et al., 2009; Moseley et al., 2006; Ranum and Cooper, 2006). In 2011, a $(GGGGCC)_n$ (G_4C_2) repeat in the first intron of the *C9ORF72* gene was reported in families affected by frontal temporal dementia and amyotrophic lateral sclerosis (FTD/ALS) (DeJesus-Hernandez et al., 2011; Renton et al., 2011) One of the proposed mechanisms for this disease is that (G_4C_2) repeats may trap RBPs and two groups have reported potential sequestered factors (Mori et al., 2013; Polymenidou et al., 2012; Xu et al., 2013). These new findings have drawn more attention to the field of microsatellite expansion disorders.

DM type 1 (DM1) is the first example of an RNA gain-of-function disease and DM type 2 (DM2) is a perfect example of a different, but structurally related, repeat on a different gene that causes similar pathological symptoms via the same molecular mechanism. For DM1, unstable $(CTG)_n$ expansions containing >50 repeats are located in the 3'UTR region of the *DMPK* gene (Brook et al., 1992; Buxton et al., 1992; Fu et al., 1992; Mahadevan et al., 1992). In DM2, unstable $(CCTG)_n$ expansions containing >75 repeats are located in the first intron of *CNBP/ZNF9* (Liquori et al., 2001; Ranum et al., 1998; Ricker et al., 1994). The congenital form of DM is referred to as CDM, which is caused by $(CTG)_{>1,000}$ expansions in *DMPK*. (O'Rourke and Swanson, 2009; Poulos et al., 2011; Ranum and Cooper, 2006; Ranum and Day, 2002, 2004; Shin et al., 2009). In both of these cases, $(CUG)_n$ or $(CCUG)_n$ transcripts accumulate in ribonuclear foci and these foci colocalize with several RBPs, most prominently the muscleblind-like (Mbnl) proteins (Fardaei et al., 2001; Fardaei et al., 2002; Mankodi et al., 2003).

Myotonic Dystrophy (DM) is a Multisystemic Disease

While muscle pathologies may be considered as the most overt symptoms of DM, this disease is multisystemic in nature. In addition to skeletal muscle symptoms, DM patients also experience problems involving the central nervous system (CNS), cardiovascular functions, metabolic and endocrine systems, as well as the reproductive and visual systems (Ashizawa and Sarkar, 2011; Wells and Ashizawa, 2006). These systemic manifestations could be the presenting features and impose additional physiological and psychological burdens on patients and their families. Therefore, rather than muscle symptoms, these non-muscle symptoms may cause a more profound impact on their quality of life. The presentation of these various symptoms also causes mis-diagnosis and increases the chance of a medical emergency. On the other hand,

this disease presented a significant challenge for scientists to generate a pathogenic model to explain this multisystemic disease.

DM-associated CNS involvement includes excessive daytime sleepiness (hypersomnia) (Dauvilliers and Laberge, 2012), spatial learning deficits, executive dysfunction, cognitive and linguistic impairment, apathy and social phobia, anxiety and depression, attention deficits and hyperactivity in the case of children (Meola and Sansone, 2007; Modoni et al., 2008; Sansone et al., 2007). These symptoms are a major concern of patients and their partners and have a profound impact on their daily performance and quality of life (Ashizawa, 1998). Arrhythmia is the most common cardiac symptom. Although most DM1 patients develop first degree AV block without any overt signs of heart failure, these mild AV blocks could suddenly evolve into advanced ventricular tachycardia (VT) and ventricular fibrillation (VF), resulting in sudden death (Groh et al., 2008; Petri et al., 2012; Wahbi et al., 2012). Other symptoms include insulin resistance, testicular atrophy (infertility) and subcapsular ocular cataracts. Subjective complaints from DM patients include hand and arm problems, fatigue and sleep disturbance (Heatwole et al., 2012). Patients with CDM are hypotonic and appear as floppy infants. Assisted ventilation is frequently required and club feet (talipes) and mental retardation are commonly observed (Campbell et al., 2004; Roig et al., 1994). DM patients are also sensitive to benzodiazepines, barbiturates (Harper, 2001) and neuromuscular blocking drugs. Surgical complications are frequently encountered and the risks of anesthesia are higher than in normal individuals (Kashiwai et al., 2012; Mathieu et al., 1997; Nishi et al., 2004). DM patients also have higher risks of sleep apnea (Kiyan et al., 2010) and fracture (de Die-Smulders et al., 1998).

Mouse Models for Studying Myotonic Dystrophy

Since the discovery of the $(CTG)_n$ expansion in the *DMPK* 3'UTR, a number of mouse models have been generated to clarify DM1 disease mechanisms (Gomes-Pereira et al., 2011). They can be categorized into four groups: 1) *Dmpk* knockout mice; 2) $(CUG)_n$ expansion or poly(CUG) mice; 3) CUGBP1 overexpression mice; 4) *Mbnl* knockout mice. Initial pathogenic models proposed that $(CTG)_n$ repeats alter the transcription of the *DMPK* gene (Krahe et al., 1995). Therefore, *Dmpk* knockout mice were created to determine if loss of *Dmpk* expression could reproduce the characteristic manifestations of DM disease. However, *Dmpk* knockout mice failed to develop myotonia and showed only a modest late-onset myopathy (Jansen et al., 1996). Since loss of *Dmpk* expression failed to recapitulate DM phenotypes, another possibility was that the $(CUG)_n$ expansion itself could generate the pathological effects regardless of the gene context. To test this hypothesis, the HSA^{LR} transgenic model for DM was generated in which a $(CTG)_{250}$ repeat expansion was cloned into the 3'- UTR of the human skeletal actin (*HSA*) gene. This $(CTG)_{250}$ transgene was expressed specifically in skeletal muscle by the α-actin promoter. The HSA^{LR} model developed myotonia while control short repeat, or $(CTG)_5$, mice (HSA^{SR}) remained asymptomatic (Mankodi et al., 2000). To simulate the multi-system expression of *DMPK* in humans, several mutant *DMPK* $(CTG)_n$ transgenic lines were created. The DM300-328 line contains a 45 kb genomic fragment from a DM1 patient with a $(CTG)_{300}$ expansion mutation (Lia et al., 1998; Seznec et al., 2001; Seznec et al., 2000). Surprisingly, this repeat size jumped to around 600 repeats in DMXL, and later on more than 1000 in DMSXL, lines, which recapitulates the intergenerational instabilities seen in DM1 patients (Gomes-Pereira et

al., 2007; Huguet et al., 2012). The SXL model also shows splicing alterations in multiple systems although the degree of mis-splicing is very modest since the expression of transgenes with large expansions is repressed. In skeletal muscle, weakness/atrophy was detectable (Huguet et al., 2012) and in the CNS behavioral abnormalities and synaptic defects were present (Hernandez-Hernandez et al., 2013).The main limitation of these transgenic mouse lines is they exhibit individual variability and are time-consuming to generate (Gomes-Pereira et al., 2011). The EpA960 transgenic line contains an interrupted CTG repeat cloned into the *DMPK* 3' UTR which can be crossed to a tamoxifen-inducible transgenic Cre line. Two mouse models have been created that express the *DMPK* $(CUG)_{960}$ transgene in skeletal muscle and in heart in a spatial and temporal manner. The skeletal muscle transgenic mouse EpA960/HSA-Cre-ER^{T2} showed severe muscular atrophy and myotonia (Orengo et al., 2008) while the cardiac transgenic mouse, EpA960/MCM(MerCreMer), displayed arrhythmia, cardiomyopathy and early mortality as early as two weeks after induction (Wang et al., 2009) (Wang et al., 2007). In both cases, upregulation of CUGBP1, hereafter referred to as CELF1, has been demonstrated to be an early event involved in splicing alteration and pathological phenotypes. The major function of CELF1 is to promote the production of fetal protein isoforms and phosphorylation of CELF1 by $(CUG)_n$ repeat induced protein kinase C (PKC) stabilizes and increases steady-state CELF1 levels. (Kuyumcu-Martinez et al., 2007; Wang et al., 2009) However, CELF1 overexpression causes early lethality (Ho et al., 2005; Timchenko et al., 2004). To overcome this problem, a tissue-specific tetracycline inducible system was utilized. Bitransgenic MHC-rtTA/TRECUGBP1 (MHC: α myosin heavy chain; rtTA: reverse

tetracycline transactivation) mice overexpressing CELF1 in the heart (Koshelev et al., 2010) and MDAFrtTA/TRECUGBP1 mice overexpressing CELF1 in skeletal muscle (Ward et al., 2010) were subsequently created. While dilated cardiomyopathy, AV conduction block and early mortality were observed in heart-specific CELF1 overexpressing mice (Koshelev et al., 2010), centralized nuclei and splicing mis-regulation were seen in the skeletal muscle specific CELF1 overexpression model (Ward et al., 2010).

Although the EpA960 and CELF1 overexpression models recapitulated some DM1 heart and skeletal muscle phenotypes, it is not clear if CELF1 overexpression is a cause, or a consequence, of CUG repeat expansion expression. As an alternative to the CELF1 gain-of-function model, DM pathogenesis may result from protein loss-of-function due to sequestration on repeat expansion RNAs, which are predicted to form stable RNA hairpin structures. A primary candidate for this type of sequestered factor in DM is the muscleblind-like (MBNL) proteins (Miller et al., 2000). MBNL proteins bind to dsCUG and dsCCUG RNA. This binding is proportional to repeat length and MBNL co-localizes with $(CUG)_n$ repeat expansion RNAs in ribonuclear foci in DM1 patient cells and tissues (Mankodi et al., 2003). Based on these observations, we proposed the MBNL loss-of-function (LOF) model for DM and to test this hypothesis, we generated *Mbnl1* knockout (KO) mice. In agreement with the MBNL LOF model, these KO mice recapitulate multiple features of DM1 muscle including myotonia, myopathy with centralized nuclei and split fibers, subcapsular cataracts and specific alterations in RNA splicing observed in this disease (Kanadia et al., 2003a).Further support for this model came from experiments using AAV-mediated Mbnl1 overexpression in HSA^{LR} mice

(Kanadia et al., 2006). The same homologous recombination strategy used to generate *Mbnl1* KO mouse was employed to generate *Mbnl2* KO mice, which fail to recapitulate DM muscle manifestations but do display disease-associated CNS phenotypes including abnormal rapid eye movement (REM) sleep regulation, impaired hippocampal function and increased seizure propensity (Charizanis et al., 2012). We use HITS-CLIP (High Throughput Sequencing combined with Crosslinking and Immunoprecipitation) and RNA-seq analysis for *Mbnl2* KO hippocampus and identify hundreds of mis-splicing events. Another study used a similar approach on the *Mbnl1* KO model and suggested that MBNL proteins are also required for normal RNA localization through specific binding to the 3'UTRs of its targets (Wang et al., 2012). These reports support the hypothesis that MBNL LOF is a fundamental event in DM and also imply that MBNL proteins control co/post-transcriptional regulation of RNAs.

Regulation of Gene Expression at the Co/post-transcription Level: Overview of Alternative RNA Processing

Alternative splicing (AS) is a complex process that requires a high level of precision to generate the myriad of protein isoforms necessary for different developmental stages and metabolic conditions (Blencowe, 2006). Data generated from RNA-seq of the human transcriptome suggests that >95% of human multi-exon genes produce multiple transcripts (Pan et al., 2008; Wang et al., 2008). These AS events are involved in various biological processes and are critical for different periods throughout the lifetime of the organism (Irimia and Blencowe, 2012). Alternative splicing mis-regulation has been linked to various human diseases, particularly neurological diseases and cancers (Cooper et al., 2009; Licatalosi and Darnell, 2006; Wang and Cooper, 2007). Although some individual AS events appear to be linked to certain

phenotypes, recent evidence indicates that the complex AS network impacts protein-protein interactions and signaling pathways (Buljan et al., 2012; Weatheritt and Gibson, 2012).

The accurate control of splicing is determined by both cis- and tran-acting factors. In cis, relatively conserved sequences at exon-intron junction and branch point regions of pre-mRNAs provides specific cues for recruitment of the spliceosome, an RNA-protein complex that binds to both 5' and 3' spliced sites (ss) via RNA-RNA base pairing, although protein-protein interactions are also involved (Wahl et al., 2009). However, these conserved sequences are degenerate and additional regulatory sequences in both intron and exon regions are required to facilitate spliceosome recognition and binding. These additional sequences function as splicing enhancers (exonic and intronic splicing enhancer, ESE and ISE, respectively) or silencers (exonic and intronic splicing silencer, ESS and ISS, respectively) to either promote or inhibit spliceosome recruitment (Wang and Burge, 2008). Serine-arginine rich (SR) and heterogeneous nuclear ribonucleoproteins (hnRNP) proteins are ubiquitously expressed RNPs that bind to these regulatory sequences. SR proteins often function as splicing activators and hnRNPs as repressors although these activities are switched for some splicing events (Cartegni et al., 2002). Mutations in several RNPs have been associated with human diseases (Lukong et al., 2008). In addition, tissue specific RNPs have been identified and characterized using high-throughput methods including HITS-CLIP, microarray and RNA-seq. For example, Nova (Darnell, 2006), Mbnl2 (Charizanis et al., 2012) and Rbfox proteins (Gehman et al., 2012; Gehman et al., 2011) play important splicing roles in the brain while Mbnl1 and CELF1 are more important for skeletal and

cardiac muscle splicing regulation. Using HITS-CLIP, a YGCY motif has been shown to be the principal binding site for Mbnl proteins while a YCAY motif is required for Nova proteins (Charizanis et al., 2012; Ule et al., 2006). Bayesian models also suggest interactive networks between Nova and Rbfox proteins, indicating possible functional cross-talk between RBPs (Zhang et al., 2010)

Importantly, alterations in either cis or trans-acting components of the AS machinery could result in disease. While cis- element mutations could affect splicing, such as the many mutations in the *DMD* gene in Duchenne muscular dystrophy, loss of function of a trans-acting factor, such as hnRNPA2/B1 or PURA, could cause Fragile X-associated tremor/ataxia syndrome (FXTAS) (Cooper et al., 2009). In recent years, several RBPs have been identified and alterations of these RBPs have been shown to cause neurological diseases: 1) NOVA proteins and paraneoplastic syndrome (Darnell and Posner, 2003); 2) RBFOX1 and epilepsy (Gehman et al., 2011) and RBFOX2 and cerebellar degeneration (Gehman et al., 2012) . These examples may be viewed as the tip of an iceberg since many neurological diseases do not have a known cause. Very recently, mutations in the genes encoding hnRNPA2B1 and hnRNPA1 have been reported in amyotrophic lateral sclerosis patients (Kim et al., 2013).

How do misregulated events in AS impact biological processes and human health? Alternative splicing plays a critical role in the regulation of multiple gene expression steps including transcription and the processing, turnover and translation of RNAs (de Almeida and Carmo-Fonseca, 2012) Additionally, factors that control chromatin structure and the transcriptional machinery also affect splicing and vice versa (Luco et al., 2011; Luco and Misteli, 2011; Luco et al., 2010). This dynamic, cooperative

and interactive process ensures fidelity in the control of gene expression in a highly spatial and temporal manner (Braunschweig et al., 2013)

Alternative Splicing Misregulation in DM

After the DM1 mutation was mapped to the 3' UTR of the *DMPK* gene, the CELF1 protein was shown to interact with short $(CUG)_8$ repeats (Timchenko et al., 1996a; Timchenko et al., 1996b). Increased CELF1 protein levels and insulin receptor (IR) mis-splicing were observed in DM1 patients and CELF1 overexpression studies in cell culture systems was shown to shift the splicing of IR (Savkur et al., 2001). Similarly, cTNT (Philips et al., 1998) and CLCN1 (Charlet et al., 2002) splicing events were shown to be CELF1-dependent so CELF1 was thought to play an important role in DM1 pathogenesis. The discovery that MBNL proteins specifically recognize $(CUG)_n$ repeat expansions introduced the possibility that the change in CELF protein levels was not a primary event in DM pathogenesis. The consequence of MBNL sequestration is the failure of developmental splicing transitions that disrupts the conversion of fetal to adult isoform expression during postnatal development (Kalsotra and Cooper, 2011; Lin et al., 2006). For example, the specific mis-splicing of CLCN1 exon 7a causes myotonia (Figure 1-1) (Charlet et al., 2002; Mankodi et al., 2002) Indeed, antisense oligonucleotides can be used to correct splicing pattern of the mouse Clcn1 pre-mRNA which results in the reversal of myotonia (Wheeler et al., 2007b). Therefore, DM1 is a spliceopathy and sequestration of MBNL proteins results in the specific splicing events that are mis-regulated in DM.

In fact, in the past decade, more genes have been found to be mis-spliced in DM. In the brain, mis-splicing of *MAPT* (microtubule associated protein *Tau*) (Sergeant et al., 2001), *GRIN1* (NMDAR1) and *APP* have been documented in DM1 patients (Jiang et

al., 2004). In skeletal muscle, mis-splicing of RYR1 (ryanodine receptor 1), SERCA1 (sarcoplasmic/endoplasmic reticulum calcium transporting ATPase) (Hino et al., 2007; Kimura et al., 2005), MTMR (microtubularin related 1 gene) (Buj-Bello et al., 2002), BIN1 (bridging integrator 1) (Fugier et al., 2011), CACNA1S (calcium channel, voltage dependent, L-type, alpha 1S subunit) (Tang et al., 2012) have also been reported. Many of these genes are implicated in calcium homeostasis and excitation-contraction coupling. Based on these findings, RNA GOF leading to MBNL LOF appears to be the best current model for DM (Figure 1-2). However, additional splicing factors, such as hnRNP H and hnRNP F (Jiang et al., 2004), Staufen1(Ravel-Chapuis et al., 2012) and the RNA helicase P68 (DDX5) (Laurent et al., 2012) have been implicated in DM pathogenesis. Moreover, a novel translational mechanism, repeat-associated non-ATG translation (RAN translation) has also been proposed to play a role in this disease (Zu et al., 2011). The development of effective therapies for DM1 and DM2 requires a fundamental understanding of the pathogenic events that cause this neuromuscular disease. Therefore, the objective of this thesis was to determine if the majority of DM disease manifestations can be explained by MBNL LOF.

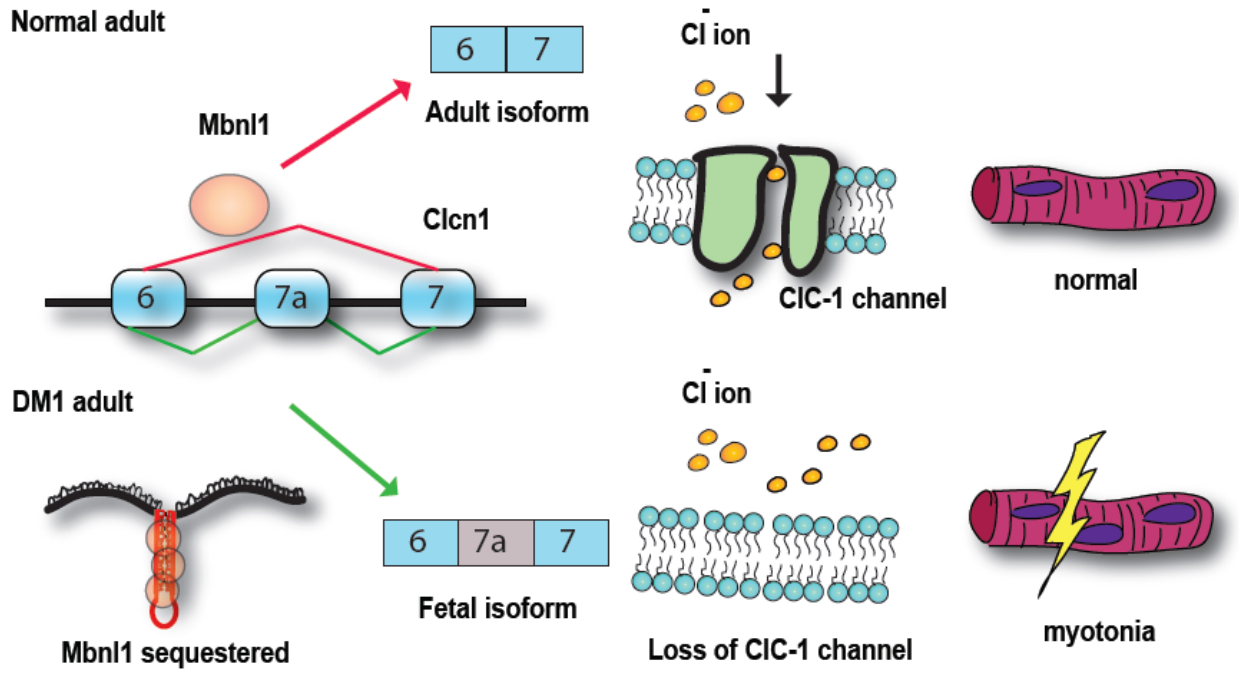

Figure 1-1. Mbnl1 regulates Clcn1 alternative splicing. In normal adults, Mbnl1 functions as a splicing regulator that promotes exon 7a skipping. The CLC-1 protein is the major chloride channel on the skeletal muscle cytoplasmic membrane or sarcolemma which regulates chloride ion transport into the cell. In DM1, $(CUG)_n$ repeat expansions sequester Mbnl1 and the fetal CLCN1 isoform, which includes exon 7a, becomes predominant in adult muscle. The inclusion of exon 7a causes a frameshift and induces degradation of Clcn1 via the NMD pathway. The consequence is loss of ClC-1 protein, impaired chloride ion flow and myotonia.

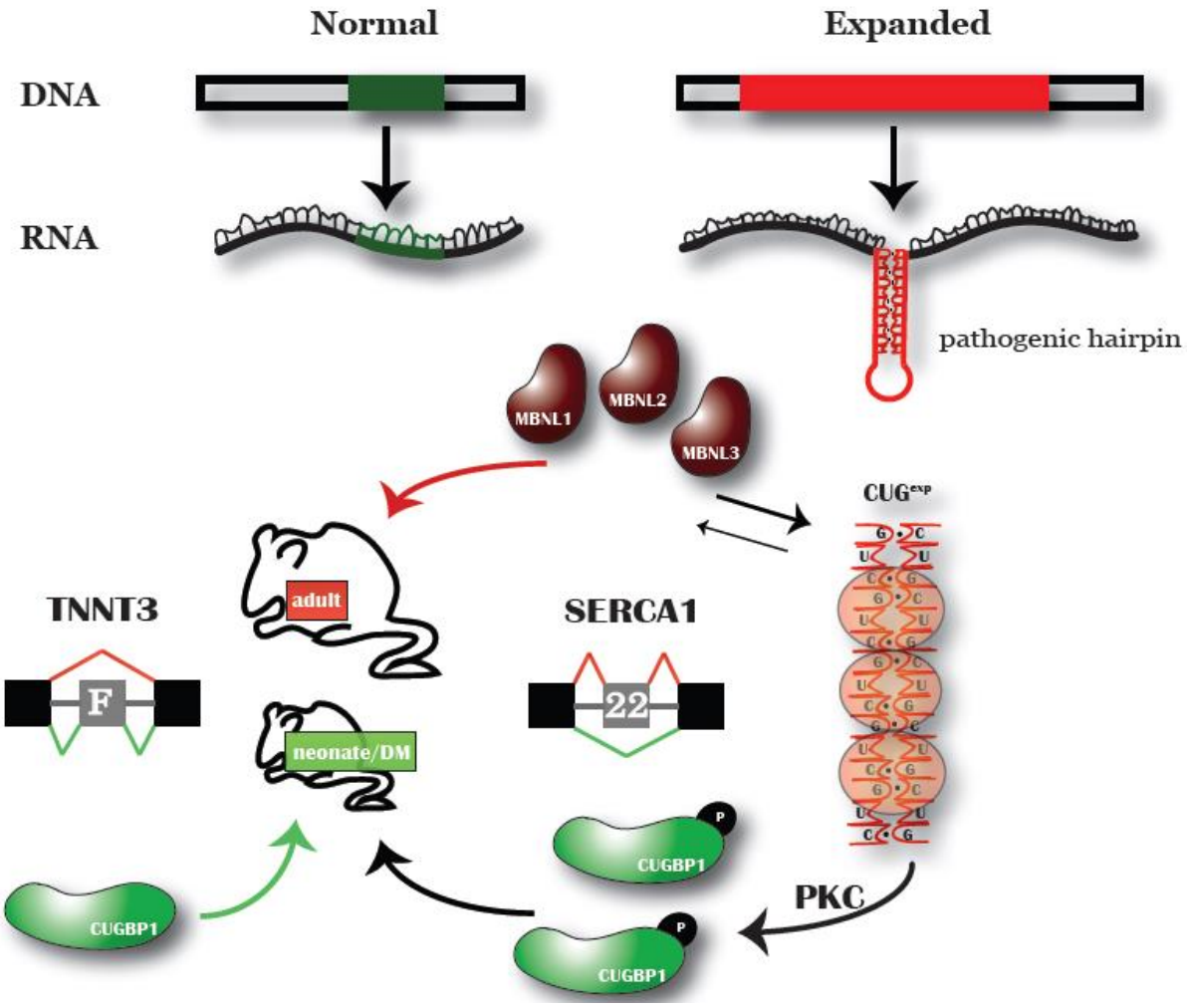

Figure 1-2. The RNA-mediated pathogenesis model for myotonic dystrophy (DM). DM is caused by $(CTG)_n$ repeat expansions in the *DMPK* 3'UTR. At the RNA level, these expanded repeats form a double-stranded hairpin which sequesters MBNL proteins. Since MBNL proteins are splicing factors that promote adult type splicing, the sequestration of MBNLs by RNA hairpins causes a splicing shift towards the fetal pattern. For example, MBNLs facilitate Serca1 exon 22 inclusion but skipping of the Tnnt3 fetal exon. By an unknown mechanism, the $(CUG)_n$ hairpin has been proposed to activate PKC leading to stabilization of CUGBP1 by hyperphosphorylation, promoting fetal pattern splicing.

CHAPTER 2
ALTERNATIVE SPLICING CHANGES IN MBNL1 KNOCKOUT AND DM1 PATIENT BRAINS

Introduction

Mbnl1 in DM Skeletal Muscle Pathogenesis

There are three paralogous proteins, Mbnl1 Mbnl2 and Mbnl3, in the Mbnl family (Pascual et al., 2006). While Mbnl1 and Mbnl2 are expressed mainly in adult tissues, Mbnl3 is expressed during embryonic stages (Kanadia et al., 2003b). *Mbnl1* knockout mice develop many symptoms of DM including skeletal muscle pathology (centralized nuclei, split fibers, myotonia), subcapsular cataracts, a low penetrant cardiovascular defect and reduced fertility (Kanadia et al., 2003a). Also, *Mbnl1* knockout mice show DM1-associated splicing changes including mis-splicing of Tnnt3 and Clcn1 in the skeletal muscle and Tnnt2 in the heart.

Mbnl1 in DM Brain Pathogenesis

Gross morphological changes in the brain did not occur in *Mbnl1* KO mice. Due to the myotonia and its effects on mobility, behavioral tests that require locomotion are unreliable. Nevertheless, *Mbnl1* behavioral analysis has been performed previously by another group and this report concluded that *Mbnl1* KOs have motivational deficits suggesting loss of Mbnl1 may contribute to certain CNS symptoms of DM patients (Matynia et al., 2010). Unfortunately, *Mbnl1* brain-specific conditional KO mice have not been generated.

Mbnl1 protein is both nuclear and cytoplasmic in neurons and the overall expression level is abundant in the brain (Daughters et al., 2009). Moreover, DM1 brain tissue shows significant splicing misregulation for specific targets, including the NMDA receptor GRIN1 and microtubule associated protein tau (MAPT). To date, no high

throughput method has been applied to any of the DM mouse models. Since we hypothesize that splicing misregulation is a fundamental event in DM, we tested the hypothesis that Mbnl1 KO brains would show a broader array of mis-splicing events compared to WT. Therefore, we collaborated with Dr. Manuel Ares (University of California at Santa Cruz) to perform splicing microarray analysis on *Mbnl1* knockout brain.

Results

Splicing Misregulation in *Mbnl1* Knockout Brain

First, we tested DM1 brain targets that were found in previous human studies (Jiang et al., 2004; Sergeant et al., 2001). However, significant splicing changes in GRIN1 exon 4 (human exon 5), MAPT exons (3,4, human exon 2,3) and exon 9 (human exon 10) as well as APP exons 7,8 were not detected (data not shown). To identify novel splicing targets, splicing events were compared between adult *Mbnl1* KOs and WT mice using splicing-sensitive microarrays. Previous studies applying the same methodology have shown that targets with sepscores (the absolute value of $\log_2$ skip/include ratio, see Materials and Methods) >0.3 are generally validated by subsequent RT-PCR (Du et al., 2010). Unexpectedly, the overall sepscores for Mbnl1 KO versus WT were <0.3 and only less than 10 genes showed a sepscore of >0.3. We validated these potential targets by RT-PCR using forward and reverse primers in the flanking exons (Table 2-1) and found 4 splicing events (Sorbs1 exon 25 , Spag9 exon 31 , Sorbs1 exon 6 and Dclk1 exon 19) that showed significant differences between WT and *Mbnl1* KOs in hippocampus and cerebellum (Figure 2-1). These differences were generally small (~10-15%) although a 40% splicing shift of Sorbs1 exon 25 was noted in *Mbnl1* KO heart. We also identified a splicing shift within an extensively spliced region

of *Camk2d*, a target identified by splicing microarray analysis. Using primers located in flanking exons, we discovered a hippocampal-specific isoform shift in *Mbnl1* KO brain. We observed that the δ9 isoform, which is not detectable in WT mice, increased in *Mbnl1* KO hippocampus but not in cerebellum. This isoform is very abundant in the early perinatal stage, as shown in P1 whole brain and P6 forebrain samples, but it decreases dramatically in P42 forebrain, indicating that δ9 is the fetal isoform (Figure 2-2).

Splicing Misregulation in DM1 Brain Autopsy Samples

To see if these splicing changes could also be detected in DM patients, we collaborated with Dr. Takashi Kimura (Hyogo University, Japan) and tested splicing patterns in human autopsy brain samples. Using primers specific for human cDNA sequences, significant differences were uncovered in SORBS1 exon 26, DCLK1 exon 19 and MPRIP exon 9 by RT-PCR. Also a significant increase of the δ9 isoform was observed in DM1 patients along with a decrease of δ1, compatible with the fetal pattern in which δ9 is the predominant isoform (Figure 2-3).

Discussion

This study reported the first splicing alterations in the brain of *Mbnl1* KO mice. Although these targets have not been analyzed by HITS-CLIP to determine if they are direct binding targets of Mbnl1, these novel targets contain multiple repeats of the MBNL binding motif YGCY. WT fetal and adult samples are used as controls in the splicing microarray so fetal isoform retention in *Mbnl1* KOs was readily detectable. Sorbs1 is a vinculin-binding protein and is ubiquitously expressed in tissues, including in the brain where it is expressed in neurons including cerebellar Purkinje cells (Lebre et al., 2001). This expression pattern is coincident with the expression of Mbnl1 in the

brain (Suenaga et al., 2012). It has been suggested that Sorbs1 is involved in macrophage function, and is also critical for insulin signaling and cytoskeletal organization (Lebre et al., 2001; Lesniewski et al., 2007; Lin et al., 2001). Interestingly, exon 25 contains a nuclear localization signal so loss of this exon could cause a change in subcellular localization (Lebre et al., 2001). Camk2 is a serine/threonine protein kinase that phosphorylates a variety of substrates, including cytoskeleton components and factors that regulate calcium homeostasis, such as the ryanodine receptor Ryr. Though the expression level of Camk2δ is lower than other isoforms, it is highly expressed in vasopressin positive neurons in the suprachiasmatic nucleus (SCN) and has been shown to play a critical role in the induction of *PER1* and *PER2* gene expression (Nomura et al., 2003; Yokota et al., 2001). The alternatively spliced exon 14b (33bp) contains a NLS and the δ9 isoform retains in the cytoplasm due to exon 14b skipping (Takeuchi et al., 1999; Xu et al., 2005). This isoform switch may be important for circadian rhythm regulation and might be a factor causing excessive daytime sleepiness in DM patients. DCLK1 is a protein kinase that could regulate microtubule polymerization (Lin et al., 2000). Since MAPT splicing dysregulation and Tau pathology have been reported in DM1 patients, the role of DCLK1 in Tau regulation deserves further investigation. Skipping of exon 19 alters autophosphorylation activity and this event may play a role in neuronal migration (Burgess and Reiner, 2002).

Mbnl1 KO skeletal muscle is characterized by >200 splicing events with a sepscore >0.3 (Du et al., 2010). Targets previously shown to have splicing shifts in DM1 brain (Grin1, MAPT, APP) were not detected by splicing microarray analysis of these mutants. These results suggest that loss of Mbnl1 alone is not enough to explain the

splicing changes seen in DM1 brains and some other splicing factor might compensate for Mbnl1 loss. Thus, splicing regulation in the *Mbnl2* KO brain was investigated.

Table 2-1. Primers for Mbnl1 brain targets validation

Gene	Gene ID	sep	exon	bp	primer fwd	primer rev
Sorbs1	20411	1.11	25	168	ccagctgattacttggagtccacagaag	gttcaccttcataccagttctggtcaatc
Bbs9	319845	0.99	2	56	gctgcttggcaggattctgtctg	ccactgttgtccacatcagccaag
Camk2d	108058	-0.90	21	89	catcgcatacattcggctcacac	cgtgtcacatgataagatgacgtgtcac
Camk2d	108058		14-16		cagccaagagtttattgaagaaaccaga	ctttcacgtcttcatcctcaatggtg
Camk2d	108058		14-16		ggaagtccagttcgagtgttcagatga	ctttcacgtcttcatcctcaatggtg
Spag9	70834	0.63	31	39	ggactggaaatggtgtcattatctccat	gggactgccacaaagaatttcacag
Mtdh	67154	-0.62	11	157	gacactagagaagagcttccagtgaatacctc	tgtcttccagcactgtgtattctgttgac
Tax1bp1	52440	0.57	10	147	ggcaacacggcaagaacttatctttc	gggtctgtatttattgaagcatcgttca
Acly	104112	0.51	14	30	ccagcacccagtaggacagcatct	cgtctcgggaacacacgtagtcaa
Fcmd	246179	-0.51	3	138	cccaagagaacaccatagaccaatgagt	gctatcaaatccaactcgattcccttt
Zmynd11	66505	0.46	4	162	gctggtattgaacaggaaggatattggt	cccatttcctgcttgttagagtgctt
Sorbs1	20411	0.38	6	90	ctgcatctgggaagactcgcct	gacttgctttcatgcttcggagattc
Mprip	26936	-0.37	9	108	gcacatggaaaccaacatgctgat	gcttggttagccagcctttcttga
Dclk1	13175	-0.37	19	74	gctgtcagtagctggcaaaatcaaga	ctcctcacatcctggttgcgtctt
Mbp	17196	0.37	5	78	cagagacacgggcatccttgact	gggagccataatgggtagttctcgt
Hnrpd	11991	0.24	7	147	ggaacagtatcagcagcagcagca	gcctggatactttcccataaccactct
Nfix	18032	-0.13	10	148	ggcaggactcgctgaaggagttt	ctgagactgctgtgggatgttcagaa
Grin1	14810		4	63	tcatcctgctggtcagcgatgac	agagccgtcacattcttggttcctg
Mapt	17762		3,4	87,87	aagaccatgctggagattacactctgc	ggtgtctccgatgcctgcttctt
Mapt	17762		9	93	cccatgccagacctaaagaatgtcag	gcttgtgatggatgttccctaacgag
App	11820		7,8	168,57	caaccaccactgagtccgtggag	gacattctctctcggtgcttggctt

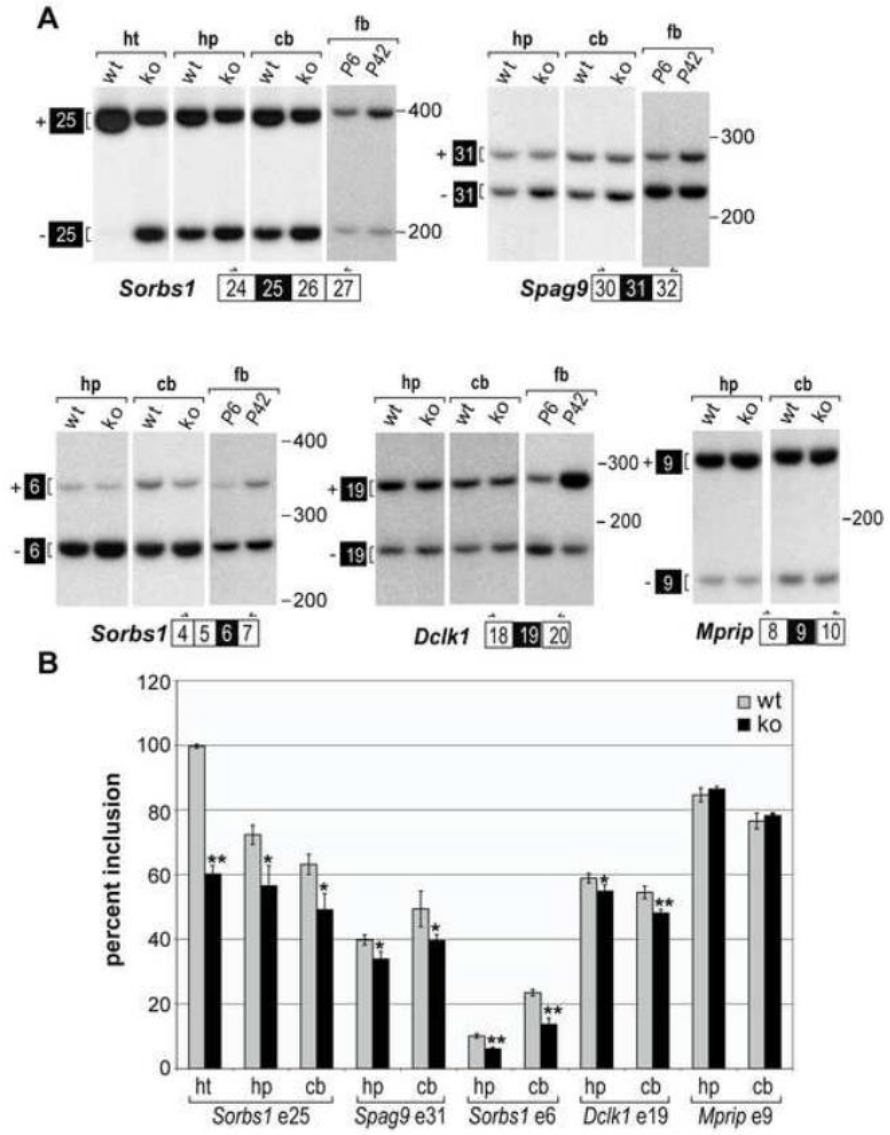

Figure 2-1. Loss of Mbnl1 causes splicing changes in brain target RNA. A) Top ranked genes acquired from splicing microarray analysis were validated by RT-PCR using WT and *Mbnl1* KO hippocampal RNAs. For Sorbs1 exon 25 splicing in the heart, loss of Mbnl1 caused a ~40% shift to the fetal isoform. However, in either hippocampus or cerebellum, the splicing shifts were only ~10-15%. Subtle, but consistent, splicing changes were also detectable for Spag9 exon 31, Sorbs1 exon 6 and Dclk1 exon 19. A splicing change in Mprip exon 9 was not detectable. Developmental assays are included on the right side of each gene to show the corresponding fetal (P6) and adult (P42) forebrain (fb) default splicing pattern. B) Statistical analysis showed significant ψ value (percent inclusion) changes except in *Mprip*. Both unpaired t-test and permutation test were used for *p* value calculation. (**p* value <0.05 and ***p* value <0.01)

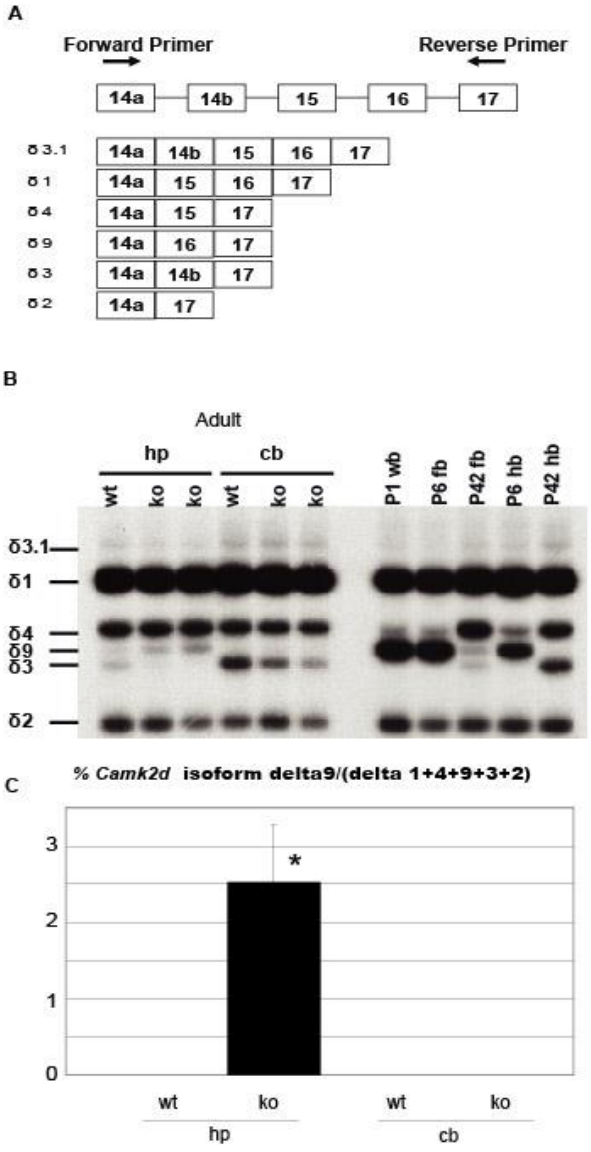

Figure 2-2. *Camk2d* splicing in *Mbnl1* KO mice and during normal development. A) Location of primers and the composition of different *Camk2d* isoforms. We designed primers within flanking exons around this region with three alternative spliced cassettes. B) Splicing assay showed a spatial and temporal specific splicing pattern for *Camk2d*. An increase of the δ9 isoform was observed in the *Mbnl1* KO. However, this change was only detectable in hippocampus and not in cerebellum. Developmental assays are shown on the right using P1 whole brain (wb), P6 forebrain (fb) and hindbrain (hb) as fetal and P42 fb and hb and adult samples. The δ9 isoform was a major isoform during the fetal stage but decreases dramatically in adults. C) Statistical analysis of *Camk2d* δ9 isoform changes. A 2.5 % shift was confirmed in the *Mbnl1* KO hippocampus (**p* value <0.05).

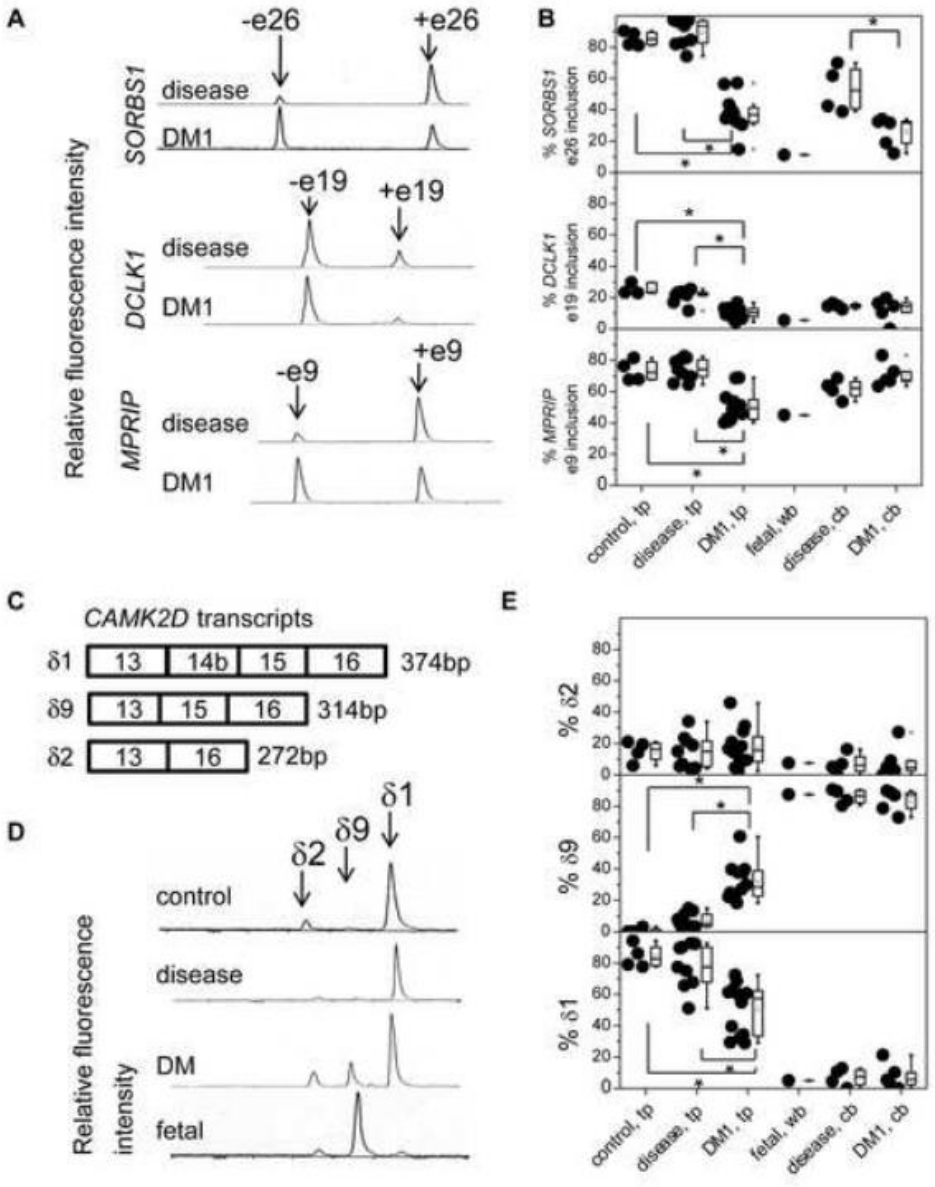

Figure 2-3. Novel targets are also mis-spliced in DM1 autopsy brains. A) Targets from the splicing microarray study were tested using DM1 patient autopsy samples. Individuals without symptoms (control) or with neurological disease (disease) and samples from fetal tissue were used as controls. B) Significant changes in SORBS1 exon 26, DCLK1 exon 19 and MPRIP exon 9 were observed and reproduced the fetal pattern. C) Composition of different *Camk2d* isoforms in human. D) Camk2d isoform analysis in different samples. Fetal type isoform δ9 increased in DM patient brain. E) Statistical analysis revealed an increase in the δ9 isoform and a decrease in the δ1 isoform in DM1 samples which is also recapitulates the fetal pattern.

CHAPTER 3
LOSS OF MBNL2 LEADS TO SPLICING DYSREGULATION IN THE BRAIN: IMPLICATIONS FOR DM1 CNS DISEASE

Introduction

Earlier Studies of *Mbnl2* Gene Trap Mouse Models

Mbnl2, one of the Mbnl family members, drew the attention of DM researchers after the successful *Mbnl1* knockout model was generated and characterized. As mentioned earlier, an *in vitro* minigene reporter study suggested that Mbnl2 may have similar effects as Mbnl1 in splicing regulation (Ho et al., 2004). Due to the possibility that loss of Mbnl2 could cause splicing changes and reproduce DM phenotypes, two different *Mbnl2* gene trap mice were created by targeting different introns. The *Mbnl2*^{GT4} line, which has a βGeo cassette insertion in intron 4 of the *Mbnl2* gene, failed to show any significant phenotypes (Lin et al., 2006). In contrast, the *Mbnl2*^{GT2} line, which contains the same gene trap cassette in intron 2, intron 2 exhibited a mild skeletal muscle phenotype and myotonia (Hao et al., 2008). These discordant results suggested that MBNL2 may have a role in DM pathogenesis but it was not clear if MBNL1 and MBNL2 possessed similar or different activities.

Additional Potential Mbnl2 Functions

An early study provided evidence that Mbnl2 plays a role in RNA localization (Adereth et al., 2005) and a recent HITS-CLIP study showed that Mbnl family members bind to the 3' UTRs of target genes (Wang et al., 2012). These results suggest that MBNL proteins may have roles beyond that as solely splicing factors, regulating many aspects of gene expression. Following a comparison of *Mbnl1* knockout and *HSA*^{LR} mice, Dr. Manuel Ares' group proposed that Mbnl2 might regulate extracellular matrix related genes by controlling mRNA levels or localization (Du et al., 2010). Interestingly,

Mbnl2 morpholino-induced knockdown in zebrafish showed some splicing changes and disruption of myofibrils and some evidence was provided for a role in regeneration (Machuca-Tzili et al., 2011). Mbnl2 expression is higher during early development in skeletal muscle and declines in adults and Mbnl2 expression increases in Duchene muscular dystrophy patient muscle (Holt et al., 2009). Interestingly, the *Mbnl2* gene also undergoes a rhythmical expression pattern in rat pineal gland suggesting a role in circadian rhythm control (Kim et al., 2009). Taken together, these results indicate that Mbnl2 plays a global role from splicing to mRNA turnover in skeletal muscle and possibly in the brain.

To address the roles of *MBNL2* in DM, we generated and characterized *Mbnl2* knockout mice using a conventional homologous recombination approach. During this study, we discovered that the expression level of Mbnl2 varies among adult tissues with high expression in various regions of the brain, moderate expression in heart and much lower expression in skeletal muscle. Mbnl2 is also expressed in hippocampal pyramidal cells and Purkinje cells in the cerebellum. In either case, the Mbnl2 localizes to the nucleus suggesting an important role in splicing regulation (Charizanis et al., 2012)

Results

Mbnl2 Regulates Hundreds of Alternative Splicing Events in the Brain

Despite the controversial results generated by the gene trap mice, we decided to create an *Mbnl2* null mouse model by a traditional gene knockout approach using homologous recombination to remove exon 2 containing the first ATG start codon. Although there is an alternative initiation codon in exon 3, this isoform knockout strategy eliminated all Mbnl2 protein expression. *Mbnl2*$^{\Delta E2/\Delta E2}$ KO mice, hereafter referred to as Mbnl2 KOs, were born small but the body weight was restored to WT levels by weaning

and these KO mice did not show any overt muscle abnormalities. However, some male mice were hyperactive prior to weaning.

Since Mbnl2 was a potential splicing factor, splicing regulation was tested in different tissues by primer pairs specifically designed for splicing assay (Table 3-1). Unexpectedly, we failed to observe significant splicing shifts in most of the Mbnl1 targets. For example, the splicing patterns of Clcn1 *and* Serca1 in skeletal muscle as well as Tnnt2 and Sorbs1 in cardiac muscle were identical to WT mice (Figure 3-1A and 1B).

Due to robust expression of *Mbnl2* in the brain, we dissected hippocampal tissue from WT and *Mbnl2* KO mice and performed splicing assays on DM1 brain targets as well as targets that were uncovered during the *Mbnl1* knockout study. RT-PCR screening of these targets (Ryr2 mis-splicing was tested based on (Takasawa et al., 2010)), uncovered five genes with significant splicing changes in *Mbnl2* KO mice, including Grin1 exon 5*,* Mapt exons 2 and 3 *,* Camk2d exon 14b-16 *,* Dclk1 exon 19 and Ryr2 exons 4 and 5. This study provided the first evidence that Mbnl2 regulates splicing in the CNS (Figure 3-2).

Splicing sensitive microarrays were employed to confirm these findings and also uncover novel *Mbnl2* brain targets. Unlike *Mbnl1*KOs, massive splicing changes were discovered and a total of 389 genes were identified with a sepscore >0.3, the threshold indicating most of them could be validated by PCR. Firstly, top twelve targets were selected for validation. These targets included Tanc2 exon 23a, Kcnma1 exon 25a, Limch1 exon E9, Spna2 exon 23, St3gal3 exon 3, Ndrg4 exon 14, Csnk1d exon 9, Ppp1r12a exon 14, Cacna1d exon 12a, Add1 exon 15, Clasp2 exon 16a,b and Mbnl1

exon 7. By comparing these mis-splicing events with the normal changes in splicing pattern during postnatal development, all the predicted Mbnl2 targets showed a shift towards the fetal pattern (Figure 3-3A). These results in the brain are similar to the effect of blocking Mbnl1 expression in skeletal muscle. Among the top 10 transcripts that showed splicing mis-regulation, Cacna1d ($Ca_v1.3$), a voltage sensitive calcium channel, showed the most dramatic shift between WT and *Mbnl2* KO mice (Figure 3-3B). For most Mbnl2 splicing targets, the default splicing pattern and the isoform switch in *Mbnl2* KOs are very similar in hippocampus and cerebellum. These results indicate that these splicing changes are universal throughout the brain, but some region-specific differences could be detected in some genes (Figure 3-4).

To confirm these targets and perform a more comprehensive survey, RNAseq was performed on WT and *Mbnl2* KO hippocampus. In collaboration with Chaolin Zhang and Robert Darnell (Rockefeller University), we found 531 alternatively spliced cassettes that showed differences between WT and mutant brain (FDR ≤0.15, Fisher's exact test with Benjamini correction). In agreement with the splicing sensitive microarray data, a top candidate was N-myc down-regulated gene 4 (*Ndrg4*), a gene associated with learning and memory (Yamamoto et al., 2011). Validation of a select set of these targets identified by RNA-seq confirmed that this experimental approach was highly reliable (e.g., see *Dgkh* exon 27 and *Slain2* exon 7 in Figure 4-13).

To determine if Mbnl2 is directly binding to these targets, HITS-CLIP was performed and this approach confirmed that the majority of the targets identified by either microarray or RNA-seq were direct binding targets. The RNA binding motif for Mbnl2 was also identified as YGCY, identical to the Mbnl1 binding motif. To test if these

novel targets found in *Mbnl2* KO mice were also mis-regulated in DM1 brain, we collaborated with Takashi Kimura's group. Among the top 12 targets, 10 out of 12 showed significant changes in DM1 temporal lobe and recapitulated the fetal splicing pattern. The gene that showed the largest difference between control and DM1 brain was *CACNA1D*, which was the same result noted in the *Mbnl2* KO study (Charizanis et al., 2012). These splicing changes were not observed in the cerebellum sample, and this difference may be due to the shorter $(CUG)_n$ repeats in DM cerebellar tissue (Lopez Castel et al., 2011).

To date, we have discovered hundreds of high confidence splicing targets and we validated >20 targets by RT-PCR. These results support the hypothesis that Mbnl2 is a critical splicing regulator during development and that loss of Mbnl2 in the brain causes a splicing shift towards fetal pattern recapitulating the mis-spliced events in DM1 brain. The next step was to determine if *Mbnl2* KO mice recapitulate DM-relevant brain phenotypes.

Enhanced Seizure Propensity in *Mbnl2* Knockout Mice

A potentially interesting phenotype that emerged from our initial KO colony was the hyperactivity phenotype in some *Mbnl2* KO males. Because of the unusual hyperactivity phenotype, these mice were referred to as pinball males. Since not all knockout mice exhibited seizures, we performed a seizure assay following low dose (40 mg/kg) intraperitoneal injections with pentylenetetrazole (PTZ), a GABA antagonist. Remarkably, both male and female *Mbnl2* KO mice tested developed tonic-clonic seizures followed by hindlimb extension and death. *Mbnl2* heterozygous knockouts also showed enhanced seizure susceptibility although with a longer latency period and less severe seizures as rated on a modified Racine Scale. Since seizures are not a routine

clinical finding in DM1 or DM2, the *DMSXL* poly(CUG) mouse model for DM1 was also tested and this transgenic model also showed higher seizure susceptibility (Figure 3-5A). To identify the specific aberrant splicing events that contributed to this phenotype eight gene targets, previously implicated in human epilepsy, were tested and Cacna1d and Ryr2 showed significant difference between WT, heterozygous and homozygous knockouts. In the case of Cacna1d, the splicing assay showed a dose effect so that Mbnl2 heterozygous KOs also showed elevated levels of the fetal splicing pattern (Figure 3-5B and Figure 3-5C).

Mbnl2 Knockout Mice Recapitulate REM Sleep Propensity Changes in DM

Excessive daytime sleepiness, or hypersomnia, is a hallmark symptom in DM1 patients. Patients suffer from an irresistible onset of short sleep events that can occur in the middle of a talk or during a meeting, resulting in problems with social interactions and preventing them from gaining employment. Previous studies have shown frequent rapid eye movement (REM) sleep propensity increases and sleep fragmentation in DM1 patients during polysomnography (PSG) (Yu et al., 2011). However, none of the existing DM mouse models recapitulated this DM1 sleep phenotype. Therefore, we collaborated with Seiji Nishino (Stanford University) in the Sleep and Circadian Neurobiology (SCN) Center to characterize Mbnl2 KO sleep physiology. Eight male WT and *Mbnl2* KO sibs (males are used to avoid estrous cycle effects on sleep) were used in this study. *Mbnl2* knockouts exhibit a normal amount of wakefulness and non-REM (NREM) sleep but increased number of REM sleep episodes during the dark cycle (the active period for mice) and successfully recapitulate the sleep phenotype seen in DM1 patients. This abnormal REM sleep phenotype could be further enhanced by sleep deprivation (Figure 3-6).This is the first time that a DM mouse model has successfully recapitulated the DM

sleep phenotype, and thus Mbnl2 KOs provide a good model for future therapeutic intervention studies.

Discussion

Mbnl2 Depletion Plays a Major Role in DM Brain Pathogenesis

The lack of phenotypes in the two previous *Mbnl2* gene trap mouse models misled the DM field into the idea that Mbnl2 function is redundant with Mbnl1. In contrast, Mbnl2 knockout mice allowed the characterization of hundreds of high confidence splicing targets and the corresponding splicing shifts occur in DM1 brain. Therefore, Mbnl2 sequestration by C(C)UG repeats RNAs appears to be an important event in the development of DM–relevant CNS pathology.

In this study, we confirmed that Mbnl2 is a critical splicing regulator during development and loss of Mbnl2 results in a splicing shift toward fetal isoforms in adult tissues. However, aberrant splicing in *Mbnl2* KOs was only seen in the brain and not in skeletal or cardiac muscle. This result highlights important differences between *in vivo* and *in vitro* studies and that spatial and temporal distribution of gene expression is critical in the evaluation of pathogenic pathways. Loss of Mbnl2 contributes to a very distinct phenotype in the CNS, which contrasts with *Mbnl1* KO mice and a skeletal muscle phenotype. Importantly, *Mbnl2* KO is the first DM1 model that recapitulates multiple DM CNS symptoms, including REM sleep propensity increases, spatial learning deficits and seizure enhancement. Of note, the REM sleep abnormality is exactly the same as a recent finding from DM1 patients and indicates a primary central sleep regulation dysfunction (Dauvilliers and Laberge, 2012; Laberge et al., 2013; Yu et al., 2011).

It has been noticed that DM1 patients are sensitive to benzodiazepines and barbiturates, two drugs that bind to $GABA_A$ receptor (Harper, 2001). Although seizures are not a common clinical symptom in DM, it is important for patients and physicians to avoid any drug that might lower the seizure threshold. For example, DM patients should avoid sleep deprivation, alcohol withdraw and caffeine use. Physicians should exercise caution when prescribing methylphenidate for treating hypersomnia (Puymirat et al., 2012), although whether this drug lowers seizure threshold is debatable (Santos et al., 2013). The new findings in this study provide answers to long-standing questions in the DM field and have additional experimental support for the MBNL LOF model for DM. Similar to other RNA binding proteins such as Nova, Rbfox and PTBP, Mbnl2 is an important splicing factor in the brain and *MBNL2* mutations could underlie some neurological diseases.

Missplicing of Mbnl2 Targets May Contribute to CNS Symptoms

During our analysis, we showed that *Mbnl2* knockout mice display *Grin1* and *Mapt* splicing abnormalities that have been documented in DM1 brain. For example, mis-splicing of GRIN1 exon 5 in human has been shown to cause age-related cognitive decline and re-direct GRIN1 localization in dendrites (Modoni et al., 2008; Pal et al., 2003). The exclusion of MAPT exon 2 could alter protein-protein interactions and promote the formation of neurofibrillary tangles. Several RNA splicing targets uncovered during this study have also been linked to learning and memory. For example, *Tanc2*, *Ndrg4* and *Cacna1d* knockout mice develop learning deficits (Han et al., 2010; McKinney et al., 2009; Yamamoto et al., 2011). Another set of genes dysregulated in *Mbnl2* KOs have been linked to epilepsy and we conclude that *Cacna1d* and *Ryr2* are the most likely candidates to account for the hyperactivity phenotype in this model.

Interestingly, *Cacna1d* mis-splicing was also found in *Rbfox1* KOs and these mice display kainic acid induced seizures (Gehman et al., 2011). Although Ryr2 mis-splicing has not been linked to seizure susceptibility, leaky Ryr2 channels caused by mutations have been found in mouse models (Lehnart et al., 2008) and in human case reports (Nagrani et al., 2011). Moreover, Cacna1d and Ryr2 colocalize and interact with each other in the hippocampus (Kim et al., 2007). These results indicate that perturbation of brain RBPs could potentially cause seizure prone effects in the brain. Of note, Ryr2, Camk2d , Csnk1d and Kcnma1 are factors that regulate circadian rhythms (Etchegaray et al., 2009; Meredith et al., 2006; Montgomery et al., 2013; Nomura et al., 2003; Pfeffer et al., 2009). Isoform switching could alter circadian cycles and potentially contribute to the hypersomnia phenotype in DM.

Based on these results, we propose that MBNL proteins promote the switch to adult isoforms during development and MBNL protein sequestration of C(C)UG RNAs leads to fetal isoform retention and DM symptoms. While loss of MBNL1 primarily causes the DM skeletal muscle phenotype, loss of Mbnl2 is the primary event leading to the DM CNS phenotype.

Table 3-1. Primers used for Mbnl2 knockout mice studies

Gene	exon	bp	forward primer	reverse primer
Tanc2	23a	30	gccatgattgagcatgttgactacagt (in exon 22: 133 bp)	cctcttccatcagcttgctcaaca (in exon 23b: 92 bp)
Kcnma1	25a	81	gattcacacctcctggaatggacagat (in exon 24: 114 bp)	gtgaggtacagctctgtgtcaggg gtcat (in exon 25b: 131 bp)
Limch1	9	36	cggaagttgccagatgtgaagaaa (in exon 8: 253 bp)	cctcctcacaccgcatgtcaaa (in exon 10: 127 bp)
Clasp2	16a,16b	27_27	gttgctgtgggaaatgccaagac (in exon 15: 102 bp)	gctccttgggatcttgcttctcttc (in exon 16c: 171 bp)
Spna2	23	60	gattggtggaaagtggaagtgaatgac (in exon 22: 149 bp)	tgatccactgctgtaactcgtttg ct (in exon 24: 199 bp)
St3gal3	3	48	gcctcttcctggtcctgggattt (in exon 2: 145 bp)	caggaggaagcccagcctatc atact (in exon 4: 43 bp)
Ndrg4	14	39	cttcctgcaaggcatgggctaca (in exon 13: 52 bp)	gggcttcagcaggacacctcca t (in exon 15: 1942 bp)
Csnk1d	9	63	gatacctctcgcatgtccacctcaca (in exon 8: 140 bp)	gcattgtctgcccttcacagcaa a (in exon 10: 2166 bp)
Ppp1r12a	14	171	caagcaccacatcaacaccaacagtt (in exon 13: 168 bp)	cttcgtccctaacaggagtgag gtatga (in exon 15: 91 bp)
Cacna1d	12a	60	catgcccaccagcgagactgaa (in exon 11: 88 bp)	caccaggacaatcaccagcca gtaaa (in exon 13: 161 bp)
Add1	15	37	ggatgagacaagagagcagaaaga gaaga (in exon 14: 99 bp)	ctgggaaggcaagtgcttctga a (in exon 16: 1836 bp)
Mbnl1	7	54	ggctgcccaataccaggtcaac (in exon 6: 258 bp)	gggagaaatgctgtatgctgctg taa (in exon 8: 154 bp)
Grin1	4	63	tcatcctgctggtcagcgatgac (in exon 3:177 bp)	agagccgtcacattcttggttcct g (in exon 5: 101 bp)
Camk2d	14b-16	33_60_42	cagccaagagtttattgaagaaaccag a (in exon 14a: 38 bp)	ctttcacgtcttcatcctcaatggt g (in exon 17: 49 bp)
Mapt	3,4	87_87	aagaccatgctggagattacactctgc (in exon 2: 113 bp)	ggtgtctccgatgcctgcttctt (in exon 5: 66 bp)
Ryr2	4,5	21_15	cggacctgtctatctgcacctttgt (in exon 3: 105 bp)	cataccactgtaggaatggcgt agca (in exon 6: 75 bp)
Dlg2	17b	42	ccattctacaagaacaaggagcagag tga (in exon 17a: 100 bp)	gcctcgtgacaggttcatagga aaga (in exon 18: 51 bp)

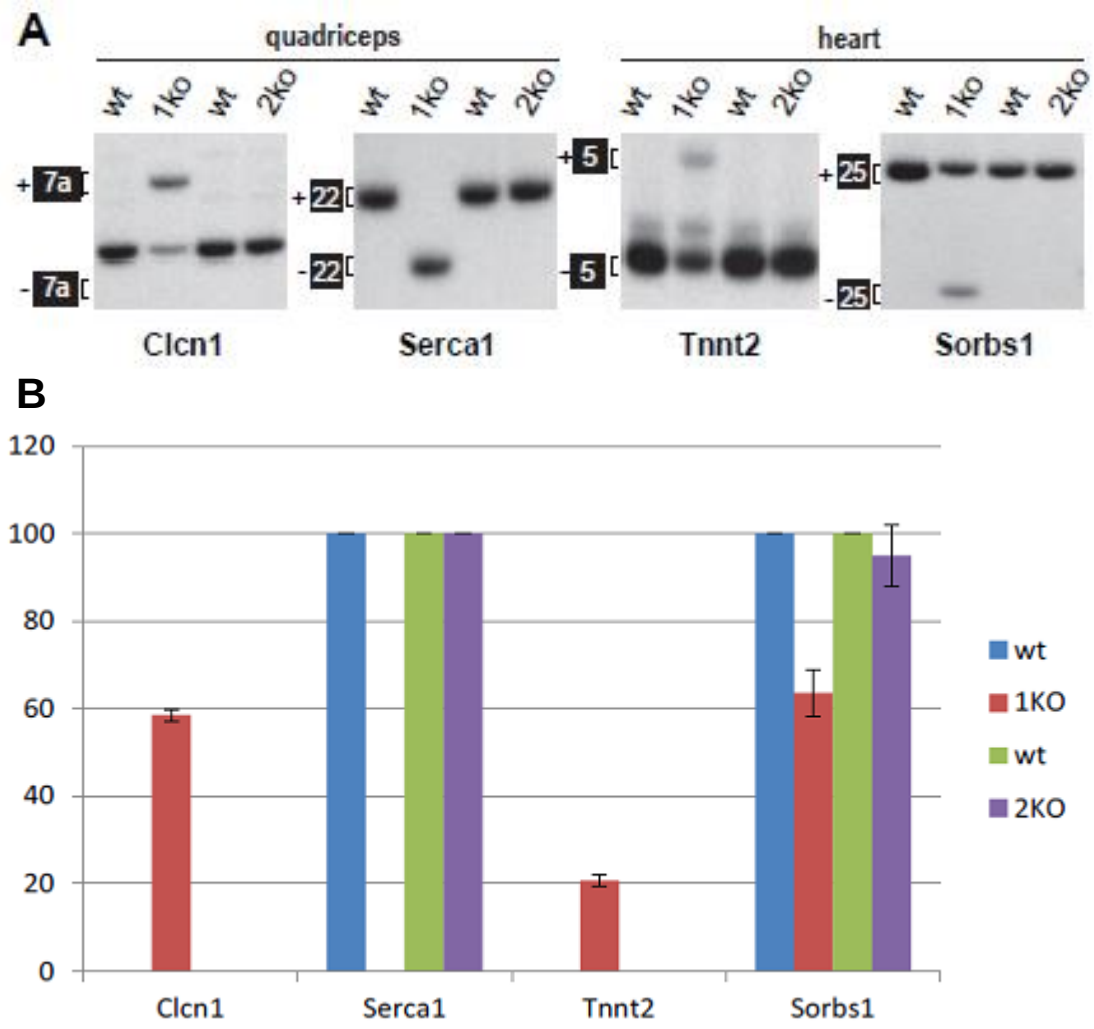

Figure 3-1. No splicing changes in *Mbnl2* knockout skeletal and cardiac muscles. A) Splicing patterns of DM1 skeletal muscle targets Clcn1 and Serca1 and heart targets Tnnt2 and Sorbs1 are shown. In contrast to *Mbnl1* knockouts, *Mbnl2* KOs showed the same splicing pattern as WT controls. B) Bar graph showing that only *Mbnl1* KOs showed significant splicing changes compared with WT.

A

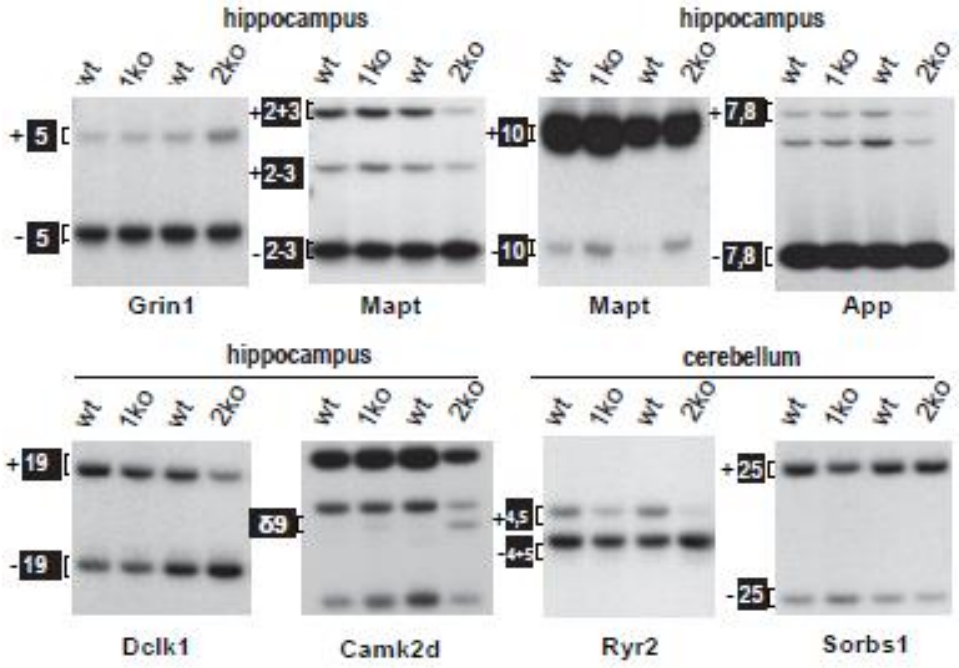

B

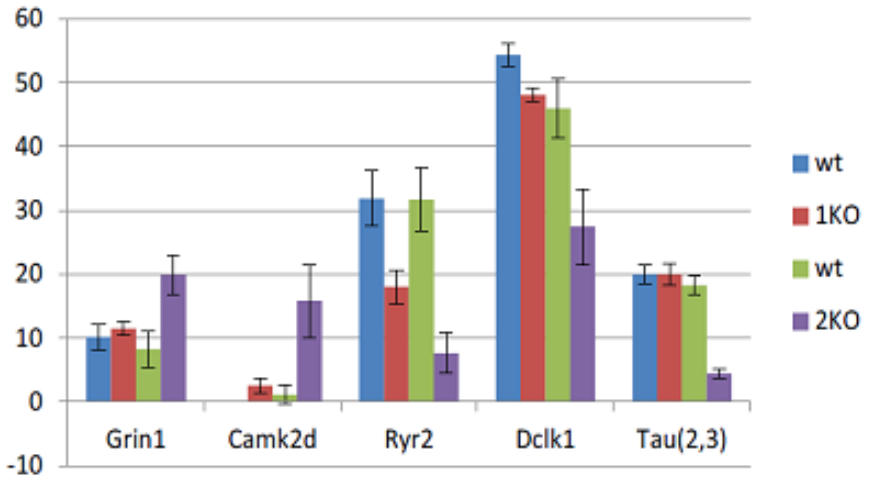

Figure 3-2. *Mbnl2* knockout mice showed significant splicing misregulation in the brain. A) RT-PCR analysis of *Mbnl2* knockout hippocampal and cerebellar tissues. Screened targets included DM1 CNS targets (Grin1, Mapt, App, Camk2d), Mbnl1 targets (Sorbs1, Dclk1, Camk2d, Spag9) and the alternatively spliced cassette of Ryr family members (Ryr1,Ryr2, Ryr3). B) Statistical analysis of hippocampal samples confirmed that splicing changes were significant between *Mbnl2* KOs and WT sibs for five targets.

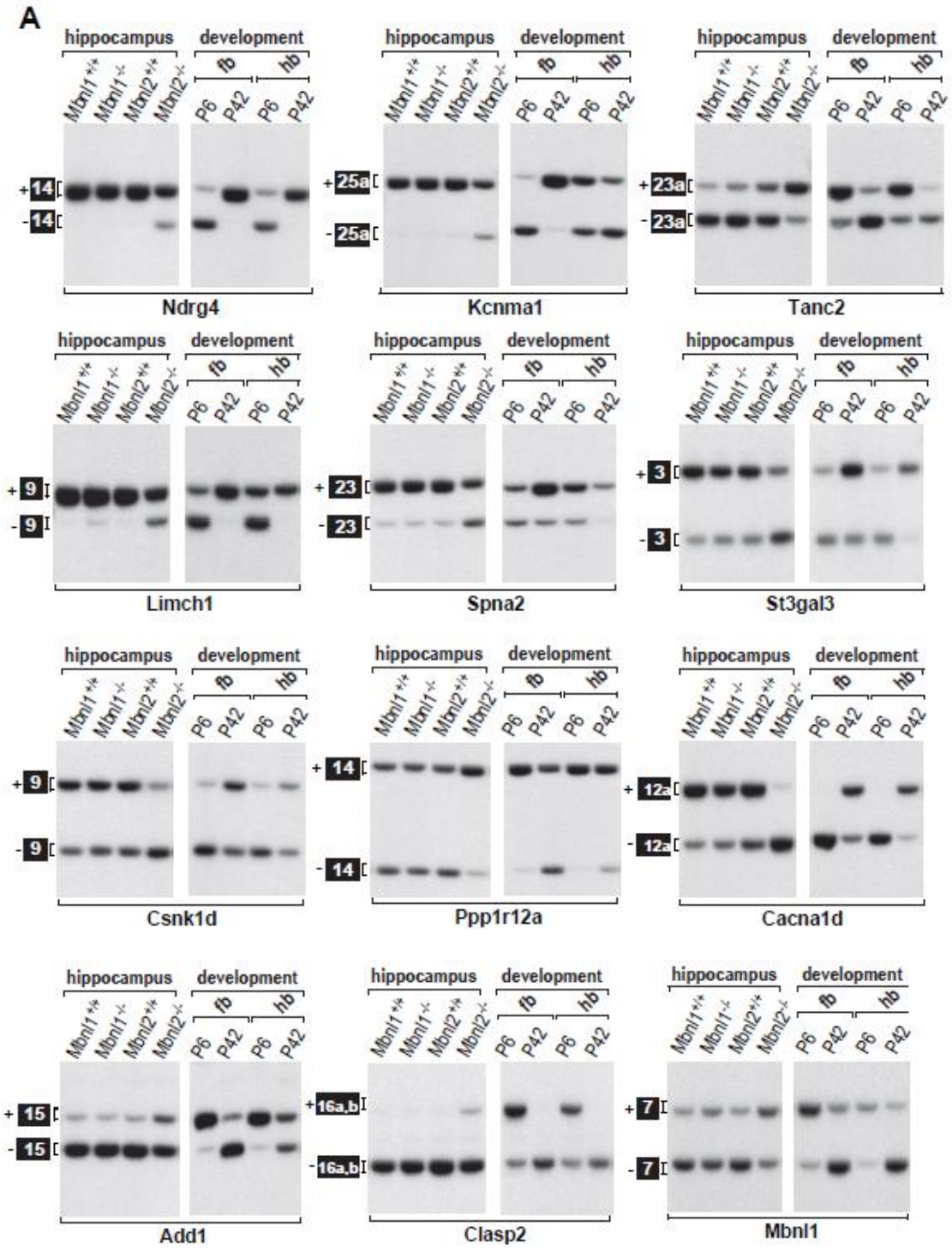

Figure 3-3. RT- PCR validation of novel targets discovered by splicing sensitive microarrays. A) Using hippocampal RNA from WT, *Mbnl1* KO and *Mbnl2* KO mice, 12 mis-splicing events were confirmed. B) Bar graph showing that all *Mbnl2* KO samples showed significant differences compared with WT ($n \geq 3$ in each group, $p \leq 0.01$ using unpaired t-test).

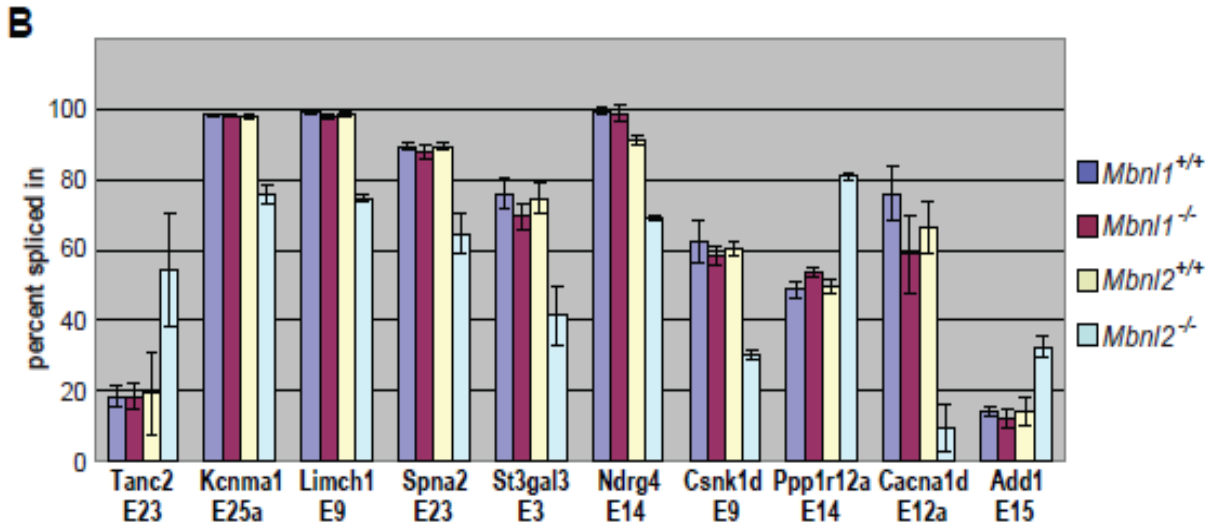

Figure 3-3. Continued

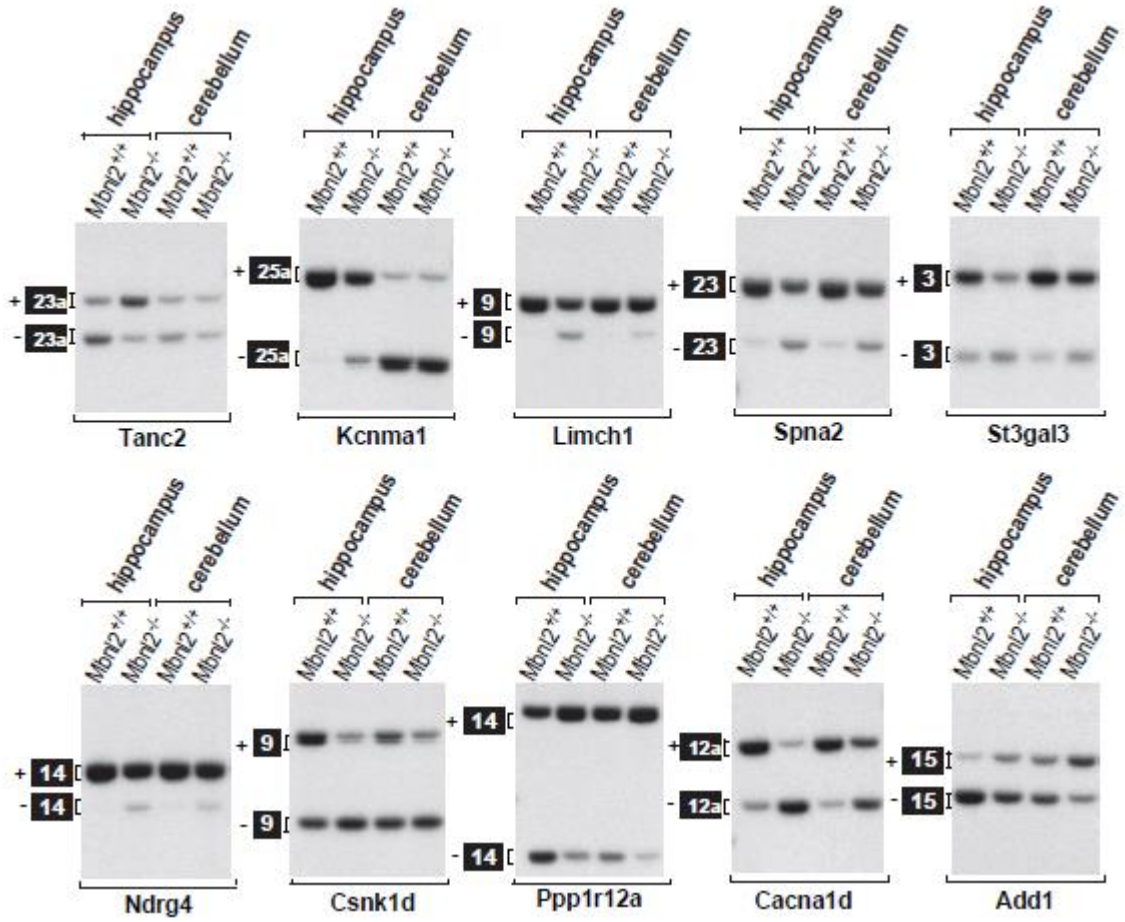

Figure 3-4. Gel images of splicing patterns between hippocampal and cerebellar tissues. In most of the targets tested, a similar default splicing pattern was observed between hippocampi and cerebella. The only exception was Kcnma1 in which the default splicing pattern is quite different between these two brain regions. In most cases, hippocampal samples showed larger splicing shifts compared to cerebellum, which may indicate that loss of Mbnl2 has a larger impact on hippocampal splicing regulation.

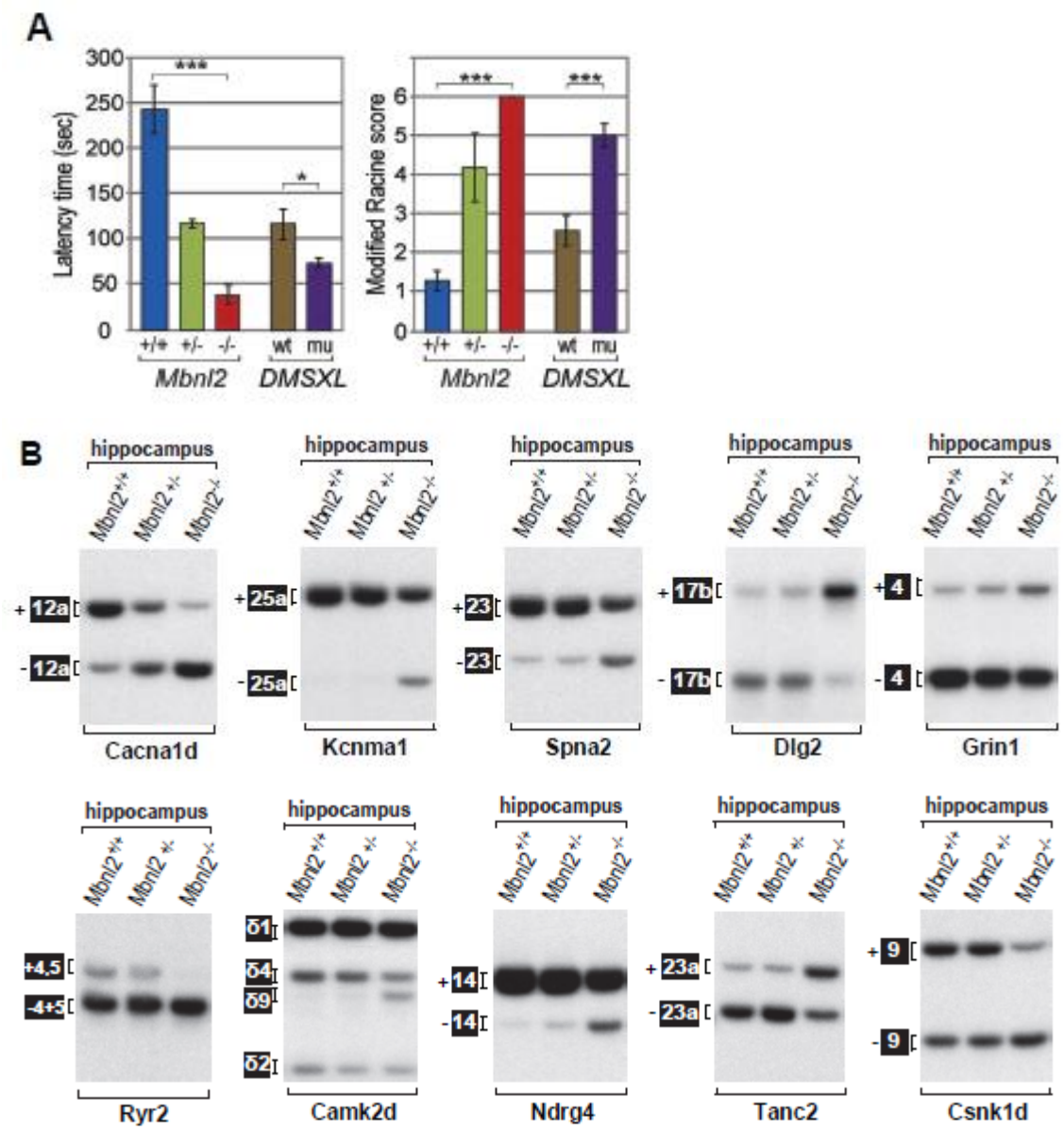

Figure 3-5. Enhanced seizure phenotype in *Mbnl2* knockouts. A) PTZ tests were performed on *Mbnl2* knockouts and *DMSXL* mice and the latency between PTZ injection and seizure activity were recorded. Decreased latencies were observed in *Mbnl2* heterozygous KOs and *Mbnl2* null KO mice and a difference between *DMSXL* mutants and WT controls was also seen (left). Bar graph of Modified Racine Score showed a significant increase in seizure severity in *Mbnl2* heterozygous, homozygous KOs and *DMSXL* mutants. B) The top *Mbnl2* targets previously linked to human seizure syndromes were also assayed. C) Bar graph showing that only Cacna1d and Ryr2 showed a significant difference between WT and *Mbnl2* heterozygous KOs.

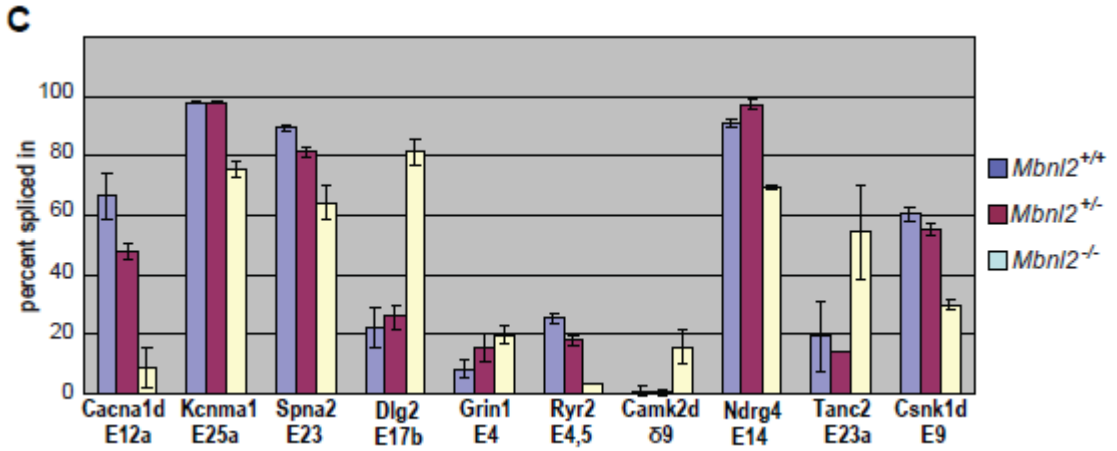

Figure 3-5. Continued.

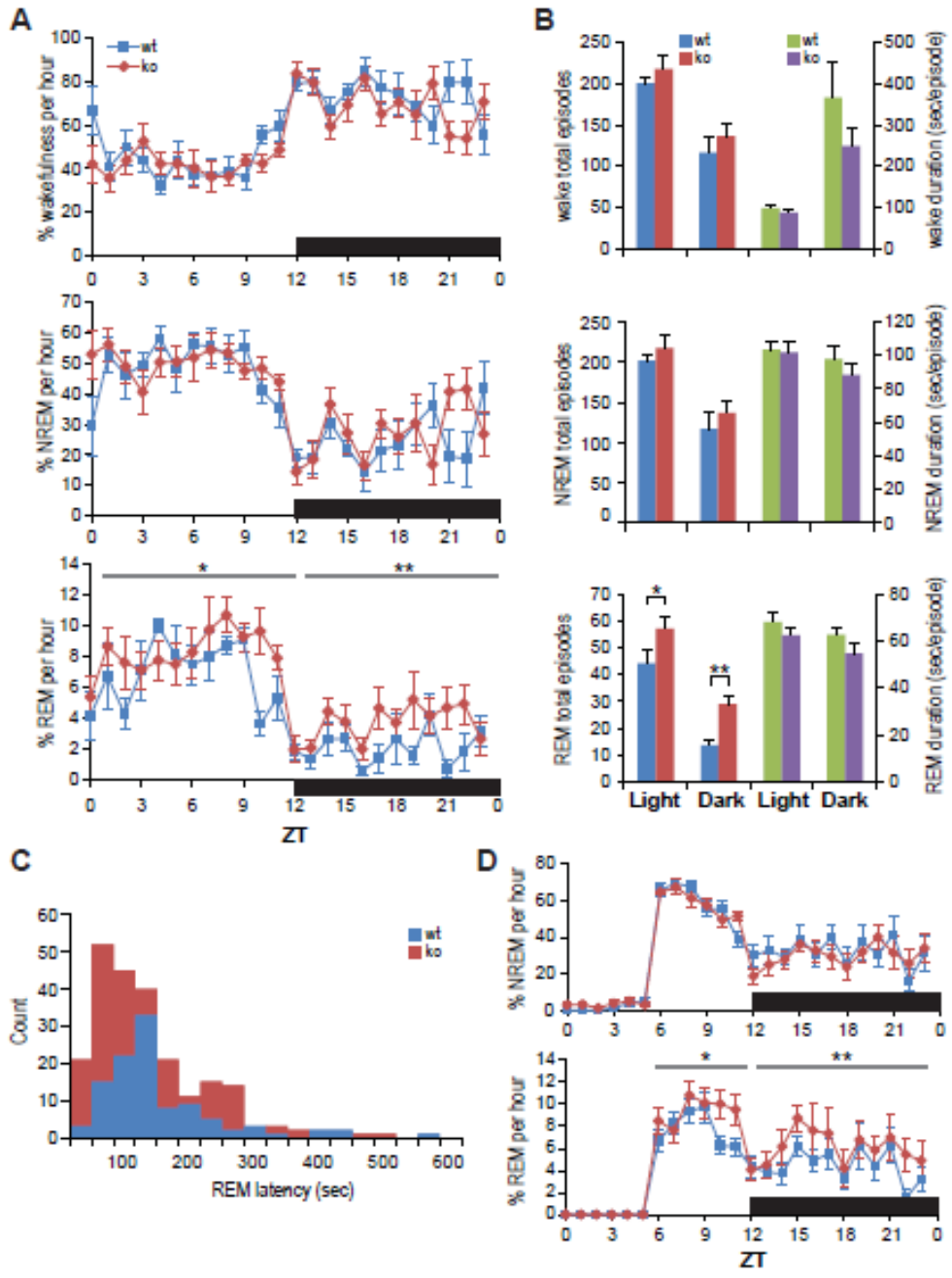

Figure 3-6. *Mbnl2* knockout mice recapitulate abnormal sleep pattern of DM1 patients. A) Total wakefulness and NREM sleep remained similar to WT, while REM sleep increased significantly in *Mbnl2* KOs particularly during the dark (awake) period. B) REM sleep total episodes increased in *Mbnl2* KOs. C) REM latency is shorter in *Mbnl2* KOs. D) REM sleep percentage increases were enhanced by sleep deprivation.

CHAPTER 4
COMPOUND *Mbnl* KNOCKOUT MICE AS A DM DISEASE MODEL

DM is a Disease Characterized by Compound Loss of *Mbnl* Gene Expression

The *Mbnl1* knockout project provided strong support for the hypothesis that DM is an RNA-mediated disease caused by loss of MBNL activity. Importantly, loss of Mbnl1 recapitulated DM-associated skeletal muscle pathogenesis while the *Mbnl2* knockout project indicated that Mbnl2 is not redundant with Mbnl1 but, instead, Mbnl2 is a key player in DM brain pathogenesis. However, DM is a multi-systemic disease and loss of Mbnl1 or Mbnl2 alone failed to fully explain the array of symptoms seen in DM1 patients. For example, adult DM1 patients suffer from skeletal muscle weakness and atrophy and have cardiac conduction block and arrhythmia resulting in sudden death. In addition, congenital DM (CDM) is characterized by a severe phenotype including muscle hypotonia (floppy infant), club feet and cognitive dysfunction while juvenile-onset DM manifests with devastating symptoms and shortened lifespan. During our studies on *Mbnl1* and *Mbnl2* single KOs, muscle weakness and atrophy was not a routine finding in either model. Although a low penetrant cardiac defect was observed for *Mbnl1* KO mice, the effects on heart function were both mild and inconsistent (data not shown). To test the hypothesis that compound depletion of Mbnl activity explains the missing DM1 phenotypes in single KO models, we generated *Mbnl1*; *Mbnl2* double KOs (DKOs).

Results

Mbnl1 and Mbnl2 Double Knockouts Are Embryonic Lethal

To obtain $Mbnl1^{\Delta E3/\Delta E3}$; $Mbnl2^{\Delta E2/\Delta E2}$ DKO mice, we set up mating using mixed BL6; 129 background $Mbnl1^{+/\Delta E3}$; $Mbnl2^{+/\Delta E2}$ mice. The reason to choose a heterozygous, instead of homozygous, mating protocol was due to the fact that

Mbnl1$^{\Delta E3/\Delta E3}$ KO mice are poor breeders. After generating >200 pups, we did not obtain any DKO mice. The results of this mating scheme indicated that *Mbnl1*$^{\Delta E3/\Delta E3}$; *Mbnl2* $^{\Delta E2/\Delta E2}$ DKO mice were embryonic lethal. Although we have not performed a comprehensive study of embryos at different time gestational stages, *Mbnl1*; *Mbnl2* MEFs were obtained from overtly normal E13.5 embryos so lethality occurs sometime between this stage and birth. Therefore, it is possible that *Mbnl1*; *Mbnl2* DKOs are a good model for CDM and this possibility is being pursued.

As a byproduct of this mating scheme, we generated *Mbnl1*$^{\Delta E3/\Delta E3}$; *Mbnl2* $^{+/\Delta E2}$ (1KO; 2HET) and *Mbnl1*$^{+/\Delta E3}$; *Mbnl2* $^{\Delta E2/\Delta E2}$ (2KO; 1HET) mice although the number of progeny obtained was lower than expected for Mendelian ratios (Figure 4-1). The number of viable 2KO; 1HET mice was extremely low so adequate numbers were not available for further study.

Characterization of 1KO; 2HET Mice Showed Enhanced Skeletal Muscle Phenotypes

Although we failed to obtain viable *Mbnl1*; *Mbnl2* DKO mice from heterozygous matings, the 1KO2HET mice were ~30% smaller in body weight compared with *Mbnl1* KO mice from weaning to 3 months of age (Figure 4-2A). These 1KO2HET mice had shorter lifespans compared with *Mbnl1* KO mice and all died by ~22 weeks of age (Figure 4-2B). Rotarod analysis showed decreased latencies to fall for 1KO2HET mice compared with WT and *Mbnl1* KO controls at 8 weeks of age, indicating impaired motor activity (Figure 4-3A). To evaluate if this rotarod deficit reflected elevated muscle weakness, grip strength was also assessed at different time points. Significantly reduced muscle power was observed for 1KO2HET mice (1-3 months of age) compared with control mice (WT and *Mbnl1* KO). After 10 weeks of age, grip strength dropped to

~50% of control mice (Figure 4-3B). Since *Mbnl2* knockout mice did not show muscle abnormalities, 1KO2HET mouse model was the first *Mbnl* knockout that developed skeletal muscle weakness.

Another interesting phenotype of 1KO2HET mice was the elevated degree of myotonia. To quantify the severity of myotonia, electromyography (EMG) was performed on *Mbnl1* KO and 1KO2HET mice on both gastrocnemius (GA) and tibialis anterior (TA) muscles. While *Mbnl1* KO mice are characterized by robust myotonia, the 1KO2HET showed a significant enhancement in myotonia duration and amplitude (Figure 4-4A). Almost every insertion of the EMG needle electrode elicited myotonia in 1KO2HET muscle and most myotonic runs (repetitive series of action potentials) lasted longer >30 sec. The durations of myotonic discharges in 1KO2HET muscles were about 2.5 to ~4-fold compared to *Mbnl1* KOs while amplitudes increased ~3-fold (Figure 4-4B). Importantly, this increased myotonia was the result of an almost complete splicing shift towards fetal pattern for Clcn1 (Figure 4-4C) (Table 4-1) and a loss of Clcn1 protein from the muscle sarcolemma (Figure 4-4D).

Although *Mbnl1* KO mice develop DM-like skeletal muscle pathologic features, the 1KO2HET mice exhibited an increase in pathological muscle features including numerous centralized nuclei and split fibers as well as evidence of muscle fiber degeneration (Figure 4-5A). To determine if 1KO2HET mice reproduced of the splicing changes previously observed in DM1 skeletal muscle, RT-PCR assays were performed on a number of Mbnl1 splicing targets including Ryr1 (exon 70) , Serca1 (exon 22), Cacna1s (exon 29) which have been previously implicated in calcium homeostasis and excitation-contraction (EC) coupling (Tang et al., 2012). Alternative splicing of Bin1 exon

11, which has been suggested to cause DM1 muscle weakness, (Fugier et al., 2011), Tnnt3 F exon and Nfix exon 8, which have shown splicing changes in the *Mbnl1* KO model, were also tested (Du et al., 2010). For most of these genes, 1KO2HET mice showed statistically significant enhanced splicing changes while several, Serca1 and Tnnt3, were equivalent to *Mbnl1* KO muscle (Figure 4-5B). Collectively, these results indicated that 1KO2HET mice have higher percentage of fetal isoform retention in adult skeletal muscle and these changes may account for the elevated levels of myotonia and muscle weakness in this compound mutant line.

Neuromuscular Junction Deficits in 1KO2HET mice

Since marked deterioration of motor activity was noted in 1KO2HET mice, the effect of compound loss of Mbnl1 and Mbnl2 on the neuromuscular junction (NMJ) was examined. Severe alterations in NMJ morphology were present in 1KO2HET TA muscle with fragmented and blunted innervating nerve branching as well as aberrant endplate structures, which were quite distinct from normal neurofilament staining and pretzel-shaped endplate structures seen in WT mice (Figure 4-6A). Multiple (n=>100) NMJs on each muscle were categorized into four morphological groups. The 1KO2HET mice showed a significant decrease of mature NMJs and an increase in fragmented structures (Figure 4-6B). These morphological changes were accompanied by alternative splicing changes of cold shock domain protein A (Csda) exon 6, a repressive transcription factor which binds to the myogenin promoter and represses *AchR* gene expression, in both *Mbnl1* KO and 1KO2HET mutant muscles (Figure 4-6C).

Compound Mbnl Knockout Mice Exhibit Abnormal Heart Phenotypes

Under normal husbandry conditions, several 1KO2HET mice died unexpectedly without showing signs of dyspnea or lethargy the day before death. Therefore, the

possibility that death resulted from cardiac dysfunction was pursued. Although these mice are vulnerable to anesthesia, electrocardiography (ECG) studies revealed the heart rate under anesthesia in WT, *Mbnl1* KO and 1KO2HET mice was not significantly different (Figure 4-7A). However, consistent increases in PR interval and QRS prolongation were observed in 1KO2HET mice (Figure 4-7B). A >50% PR interval increase was noted between WT and 1KO2HET mice (Figure 4-7C) accompanied by a ~30% increase in QRS interval (Figure 4-7D). Heart to body weight ratios by also indicated a 61% increase in 1KO2HET compared with WT mice (Figure 4-8A). A notable feature of the 1KO2HET heart was an enlarged right atrium as shown by magnetic resonance imaging (MRI) (Figure 4-8 B to F). The 1KO2HET mice also exhibited an end diastolic volume (EDV) decrease (Figure 4-8 B) and an increase in whole volume (WV)/EDV ratio (Figure 4-8E). MRI also highlighted enlargement of the right atrium during both systolic and diastolic phases. An increase ventricular wall thickness was also present and especially prominent in the left ventricle indicating myocardial hypertrophy (Figure 4-8G). Although ejection fraction (EF) rate, which indicates heart failure, was not significantly different between 1KO2HET and WT hearts myocardial hypertrophy might be a compensatory mechanism that retains EF within the normal range for anesthetized animals and a telemetry heart assessment is required to determine if this is a possibility. Diffuse fibrosis in valvular areas as well as ventricular base and papillary muscles was also observed in 1KO2HET heart sections (Figure 4-9A). In some cases, fibrosis could also be seen in the dilated right atrium (data not shown). Splicing assays on Mbnl1 heart targets showed that Tnnt2 splicing was dramatically shifted toward the fetal isoform with elevated exon 5 inclusion in 1KO2HET

mice. The same trend of enhanced splicing shifts to fetal isoforms was seen for *Ryr2* exons 4,5 of, a candidate gene for arrhythmia, and Cacna1s exon 29 , a DM1 heart target (Tang et al., 2012). In addition, top ranked targets from the *Mbnl1* KO heart splicing sensitive microarray analysis, such as Sorbs1 exon 25, Tmem63b exon 4, Spag9 exon 31, Mbnl1 exon 7 and Arhgef7 exon 16, showed a consistent augmentation of fetal splicing changes in 1KO2HET heart compared to *Mbnl1* KOs strain (Figure 4-9B) although only *Arhgef7* did not reached statistical significance (Figure 4-9C).

Upregulation of Mbnl2 Expression and Relocalization into Nuclei in the Absence of Mbnl1

Previously, we have provided evidence that splicing of Mbnl1 and Mbnl2 pre-mRNAs is auto- and cross- regulated (Charizanis et al, 2012, Zhang et al, 2013). Interestingly, immunoblot analysis of Mbnl2 demonstrated a remarkable up-regulation of Mbnl2 protein in *Mbnl1* KO mice, particularly in skeletal muscle (Figure 4-10A), but could also be seen in heart and brain. This upregulation of Mbnl2 protein level was due to either increased *Mbnl2* transcription or decreased RNA turnover since qRT-PCR showed a 4.6-fold increase of Mbnl2 mRNA (Figure 4-10B)(Table 4-1). In support of our previous studies of auto- and cross-regulation in the *Mbnl* gene family, both Mbnl1 exon 7 and the corresponding Mbnl2 exon 6 contain a nuclear localization signal (NLS) and in *Mbnl1* KO and 1KO2HET quadriceps, more exon 6 containing Mbnl2 isoforms were produced (Figure 4-10C), which suggested that Mbnl2 protein relocalization into nuclei was increased following *Mbnl1* loss. Following subcellular fractionation, immunoblot analysis confirmed that Mbnl2 upregulation coincided with a predominant nuclear localization pattern in the absence of Mbnl1 (Figure 4-10D). In addition to Mbnl2 exon 6,

three other alternative spliced cassettes were also affected in the absence of Mbnl1 and these cassettes were further shifted in 1KO2HET mice. The most evident change after Mbnl1 ablation was the splicing of Mbnl1 exon 7 (54 nt) in skeletal muscle while the most significant change after alteration of Mbnl2 levels was the corresponding Mbnl2 exon 6 (54 nt) in the heart (Figure 4-11A). Compared to WT and *Mbnl1* KOs, all four alternatively spliced cassette exons in the two organs (quadriceps and heart) showed significant differences (Figure 4-11B).

Mbnl2 is Re-Targeted to Mbnl1 Targets in *Mbnl1* Knockout Muscle

During the analysis of *Mbnl2* KO mice, skeletal muscle abnormalities, including myotonia, splicing changes or loss of Clcn1, were not detected. However, an enhancement of the Clcn1 exon 7a splicing shift was observed in 1KO2HET mice. What RNA targets does Mbnl2 bind and does this interaction lead to alternative splicing changes for these targets? Is the splicing of these RNA targets different in the presence or absence of Mbnl1? Our hypothesis was, in the absence of Mbnl1, Mbnl2 would prioritize its binding to those targets co-regulated by Mbnl1 due to the critical role of Mbnl1 in skeletal muscle splicing. On the other hand, the binding of Mbnl2 on Mbnl2 targets might decrease when Mbnl1 is depleted. To address these possibilities, Mbnl2 HITS-CLIP was performed on WT and *Mbnl1* KO muscles.

The HITS-CLIP data showed an ~40% increase of the number of unique Mbnl2 tags likely due to up-regulation of Mbnl2 in the absence of Mbnl1. For alternatively spliced cassettes, the CLIP tag peak heights increase dramatically in *Mbnl1* KO muscle. For example, for Ldb3, the number of Mbnl2 CLIP tags was 39 in WT and 218 in *Mbnl1* KO, an increase of 5.6-fold. For Ttn, the numbers were 36 in WT and 165 in *Mbnl1* KO,

an increase of 4.6-fold while for Atp2a1, 53 tags were sequenced in WT but 130 in *Mbnl1* KO muscle, an increase of 2.5-fold (Figure 4-12).

Mbnl1+/ΔE3; Mbnl2 ΔE2/ΔE2 Knockout Mice Show Complementary Splicing Changes in the Brain

Although the number of *Mbnl1*$^{+/\Delta E3}$; *Mbnl2* $^{\Delta E2/\Delta E2}$ (1HET2KO) mice was significantly lower (Table 1), mice that survived until weaning were indistinguishable from their littermates. All 1HET2KO mice (n=5) survived >6 months of age. However, RT-PCR analysis of Mbnl2 brain RNA targets showed a splicing shift enhancement in 1HET2KO mice (Figure 4-13). These results indicate that Mbnl2 is primarily responsible for alternative splicing regulation during postnatal development in the brain and Mbnl1 compensated for Mbnl2 loss in *Mbnl2* KOs. Conditional brain-specific *Mbnl1*; Mbnl2 DKO mice are required to confirm these findings.

Discussion

Compensatory Functions for MBNL2 in Skeletal Muscle

Previous studies have shown that Mbnl2 is expressed at a very low level in skeletal muscle compared with other tissues and no splicing changes for Mbnl1 skeletal muscle targets were reported in *Mbnl2* knockout mice (Charizanis et al., 2012; Holt et al., 2009). Therefore, loss of Mbnl2 alone did not result in a skeletal muscle phenotype while Mbnl1 was expressed. However, further loss of Mbnl2 in muscle causes enhanced physiological and splicing phenotypes. The 1KO2HET mouse model provides the first evidence that Mbnl2 is critical for normal skeletal muscle and heart functions.

In DM1 patients, muscle weakness and atrophy and myotonia are characteristic manifestations of disease. These 1KO2HET mice appear to be a good model for DM1 muscle pathology since there are signs of degeneration and regeneration, grip strength

weakness and NMJ deficits. NMJ defects have been previously reported in DM1 patients (Allen et al., 1969; Coers et al., 1973). Muscle biopsy studies on DM1 patients also indicate that ribonuclear foci are detected in subjunctional nuclei and Mbnl1 is sequestered at high levels in these foci (Wheeler et al., 2007a). Our studies show that NMJ structure is severely affected in 1KO2HET mice, particularly maturation defects and signs of early degenerative changes (Kummer et al., 2004; Sahashi et al., 2012; Valdez et al., 2010). We also discovered that the splicing of Csda, a repressive transcription factor bound to the myogenin promoter, was abnormal in 1KO2HET mice, and this mis-splicing event might promote this phenotype (Berghella et al., 2008; Ferraro et al., 2012).

Mbnl2 Functions and the DM Heart

In the heart of 1KO2HET mice, we characterized a conduction block and structural changes. Various types of arrhythmia have been reported in DM1, however, first degree AV block is the most common abnormal cardiac finding in DM1. Conduction block and sudden death due to arrhythmia have been widely recognized as important pathological features of this disease and recent studies suggest that preventive cardiac pacemaker implantation is important (Groh et al., 2008; Wahbi and Duboc, 2012; Wahbi et al., 2012). Fibrosis and fatty infiltrations have also been found in the conduction system and cardiac regions in DM1 patients and chamber dilatation and myocardia hypertrophy in the ventricle are also reported features (Ashizawa and Sarkar, 2011; Motta et al., 1979; Nguyen et al., 1988). In our study, we successfully characterized first degree AV block and abnormal cardiac morphology in 1KO2HET mice, although physiological evaluation revealed that the ejection fraction (EF) rate was not changed. However, EF rate decreases reflecting left ventricular dysfunction is not observed in

DM1 patients <40 year of age. Analysis of the literature reveals that DM1 echocardiogram analysis has shown that lower EF (<50%) is observed. NMJ defects have been reported in DM1 patients (Allen et al., 1969; Coers et al., 1973) although a different study suggested less severe involvement in DM1 patients. (Bhakta et al., 2010). Another study also concluded that structural defects appeared earlier than EF decreases (De Ambroggi et al., 1995). In summary, our cardiac results on 1KO2HET mice are compatible with previous studies on DM1 patients.

We know in other RBP families, it is not uncommon that more than one family member is involved in similar, but not identical, functions. For example, both Rbfox1 and 2 are CNS-specific RBPs and loss of each protein resulted in distinctly different phenotypes (Gehman et al., 2012; Gehman et al., 2011). When one Rbfox protein is knocked out, the other protein is upregulated putatively to compensate for loss of the paralog. We observed a similar phenomenon in the Mbnl family with upregulation of Mbnl2 in the absence of Mbnl1. However, Mbnls are broadly expressed in tissues, and Mbnl1 and Mbnl2 have functions that appear to be specialized for different tissues. In the brain, Mbnl2 is highly expressed in the nuclei of hippocampal pyramidal neurons and cerebellar Purkinje cells while Mbnl1 is expressed in both the nucleus and cytoplasm (Charizanis et al., 2012). In skeletal muscle, Mbnl1 is highly expressed and localized predominantly in the nucleus while Mbnl2 is primarily cytoplasmic. These differences in distribution patterns imply their primary functions vary in different organ systems. However, when one protein is depleted by C(C)UG RNA sequestration, the other compensates by overexpression and re-localization to the nucleus. These results

do not conflict with prior suggestions that Mbnl proteins also possess functions other than splicing (Adereth et al., 2005; Wang et al., 2012).

Table 4-1. Primers for RT-PCR in 1KO2HET studies

Gene	Exon	Bp	Forward primer	Reverse primer
Clcn1	7a	79	ggaatacctcacactcaaggcc	cacggaacacaaaggcactgaatgt
Ryr1	70	15	gcgtgaagaacagaacttcgtggtc	cttggtgcgttcctgatctgagc
Cacna1s	29	57	gagatccttggaatgtgtttgacttcct	ggttcagcagcttgaccagtctcat
Serca1	22	41	gctcatggtcctcaagatctcac	gggtcagtgcctcagctttg
Bin1	11a	45	cagaacctcaatgatgtcctggtca	ctctggctcatggttcactctgatct
Ryr1	83	18	cttcgagaggcagaacaaggcag	aacaggtcctgtgtgaactcgtcatc
Tnnt3	9	39	tctgacgaggaaactgaacaag	tgtcaatgagggcttggag
Nfix	8	123	ggagagtccagtagatgatgtgttctatcct	ggatgatggacgtggaagggaa
Tnnt2	4,5,6,	11_12_30	gccgaggaggtggtggaggagta	gtctcagcctcaccctcaggctca
Ryr2	4,5	21_15	cggacctgtctatctgcacctttgt	cataccactgtaggaatggcgtagca
Sorbs1	25	168	ccagctgattacttggagtccacagaag	gttcaccttcataccagttctggtcaatc
Tmem63b	4	39	ctggctctggacttcatgtgctttc	gagacggaggtgagacgctcatacc
Spag9	31	39	ggactggaaatggtgtcattatctccat	gggactgccacaaagaatttcacag
Mbnl1	7	54	ggctgcccaataccaggtcaac	gggagaaatgctgtatgctgctgtaa
Afhgef7	16	225	gcagacgaaggtcacatctgtgagc	cacagcgaactcctcgtccgaag
Mbnl2	6	54	tcaccctcctgcacacttgcag	ctctttggtaagggatgaagagcacc
Mbnl1	9	95	tattgtgcatgacacccgctacaagt	tgtgacgacagctctacatctgggtaa
Mbnl2	8	95	cgtcttgcactaccagcaggctc	gacatagcagaactagccttaggttgtg
Csnk1d	9	63	gatacctctcgcatgtccacctcaca	gcattgtctgcccttcacagcaaa
Cacna1d	12a	60	catgcccaccagcgagactgaa	caccaggacaatcaccagccagtaaa
Mapt	3,4	87_87_	aagaccatgctggagattacactctgc	ggtgtctccgatgcctgcttctt
Dgkh	30	131	gcacagtctttcgcatagtgccaaa	gggagggttccgttcaagctcttt
Slain2	7	78	cagtcttccaaacctatcccgaacat	ggtggtttgtgtgaactgggtagttc

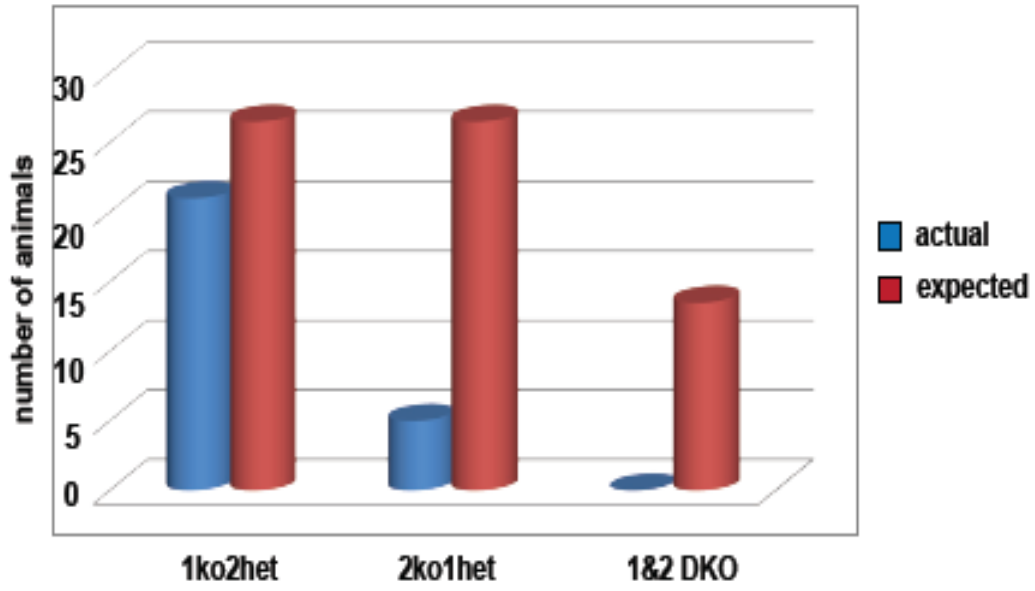

	1ko2het	2ko1het	1&2 DKO
Actual no.(%)	21(10%)	5(2.38%)	0 (0%)
Expected no.(%)	26.25(12.5%)	26.25(12.5%)	13.125(6.25%)

Figure 4-1. *Mbnl1* and *Mbnl2* double knockouts are embryonic lethal. Expected and actual numbers of mice obtained with each genotype are shown. The exact numbers and percentages are shown below. These results indicate compound knockouts are prone to embryonic lethality.

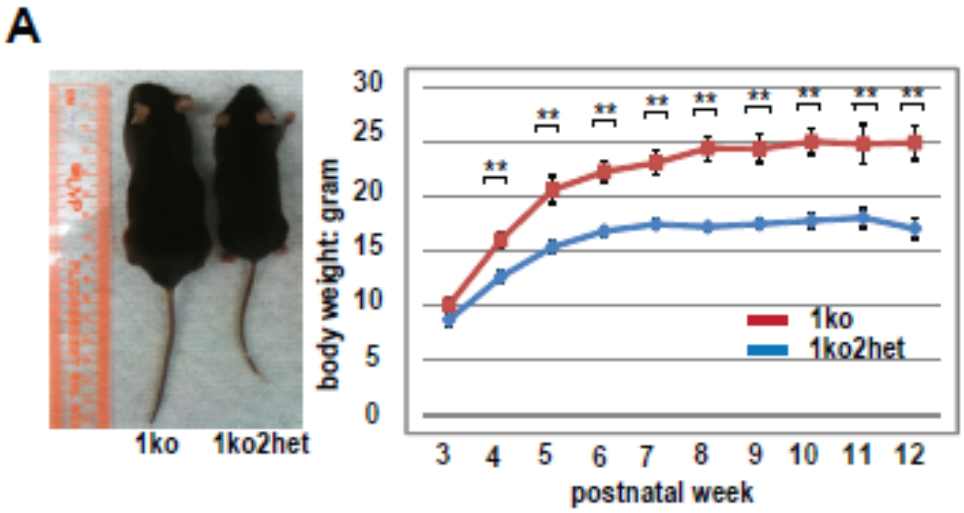

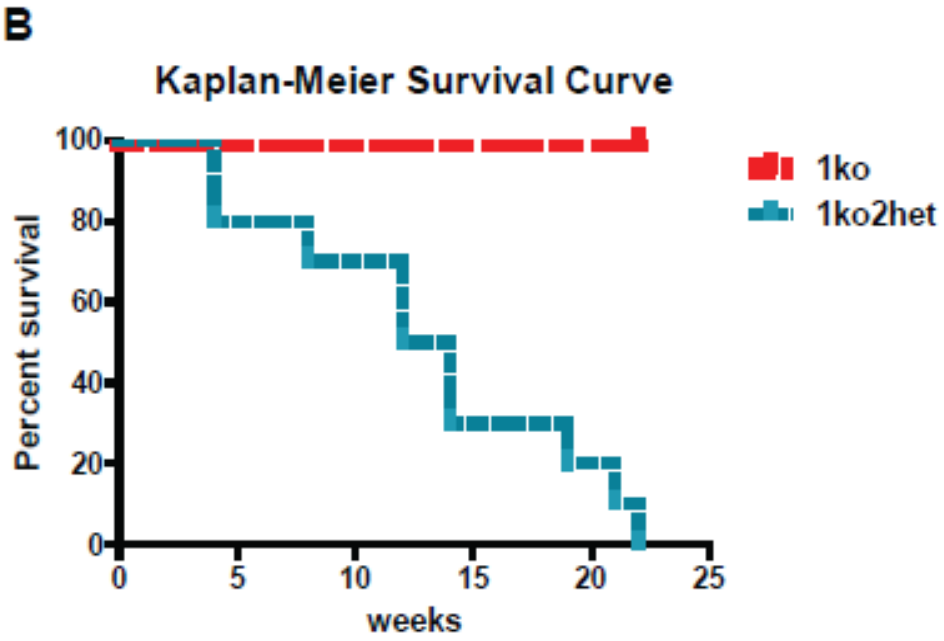

Figure 4-2. The Mbnl1 KO; Mbnl2 HET (1KO2HET) mice were smaller and had a shorter lifespan. A) The body weight of 1KO2HET was about ~30% less than *Mbnl1* KOs. B) Kaplan-Meier curve for *Mbnl1* KO versus 1KO2HET.

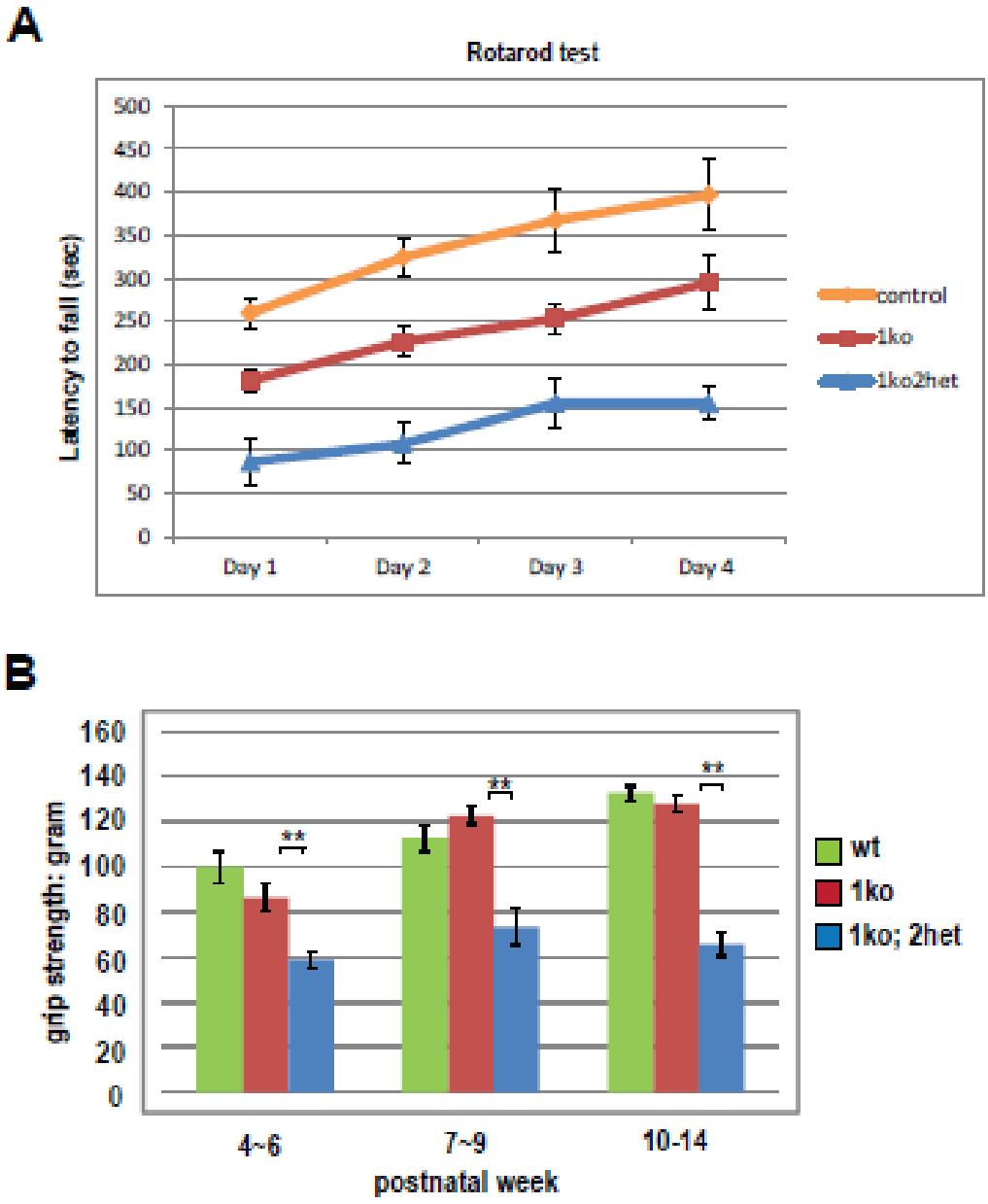

Figure 4-3. 1KO2HET mice exhibit motor deficits. A) The rotarod test was performed on mice 8 weeks of age. *Mbnl1* KOs showed decreased latency to fall while 1KO2HET mice showed further decline. B) Grip strength test at different developmental stages.

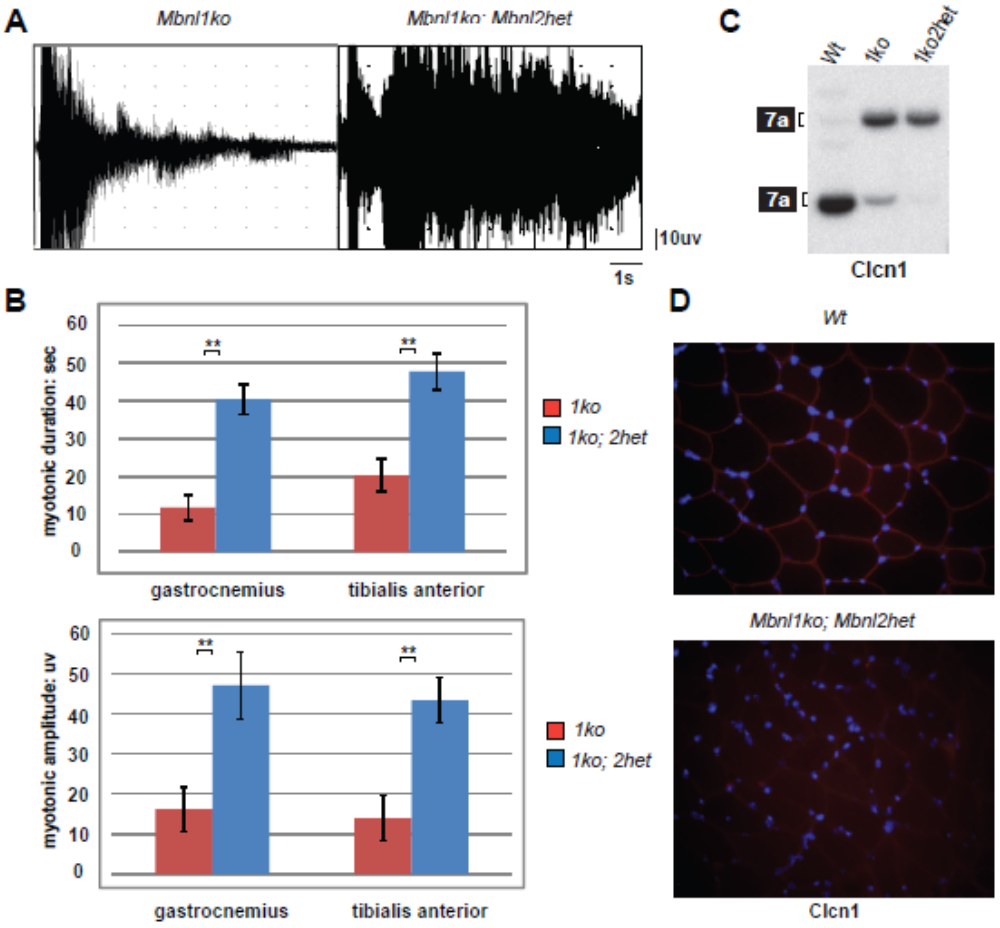

Figure 4-4. 1KO2HET mice showed enhanced myotonia. A) Representative figures of myotonic discharges recorded during electromyography. Mbnl1 KO (left) showed a fast tapering of myotonic discharges in 10 sec, however, the 1KO2HET showed prolonged, consistent and robust myotonia. B) Bar graph showing features of myotonic discharges. In two different muscles (gastrocnemius and tibialis anterior) the 1KO2HET mice showed a 2.5 to 4-fold increase in myotonic discharge duration and amplitude compared with Mbnl1 KOs. C) Enhanced myotonia in 1KO2HET mice correlated with increased mis-splicing change of Clcn1. In 1KO2HET mice, splicing was shifted almost completely to the fetal isoform which includes exon 7a. The inclusion Clcn1 exon 7a induces nonsense mediated decay D) Loss of Clcn1 protein in 1KO2HET muscle compared with WT (red, Clcn1 staining; blue, DAPI staining).

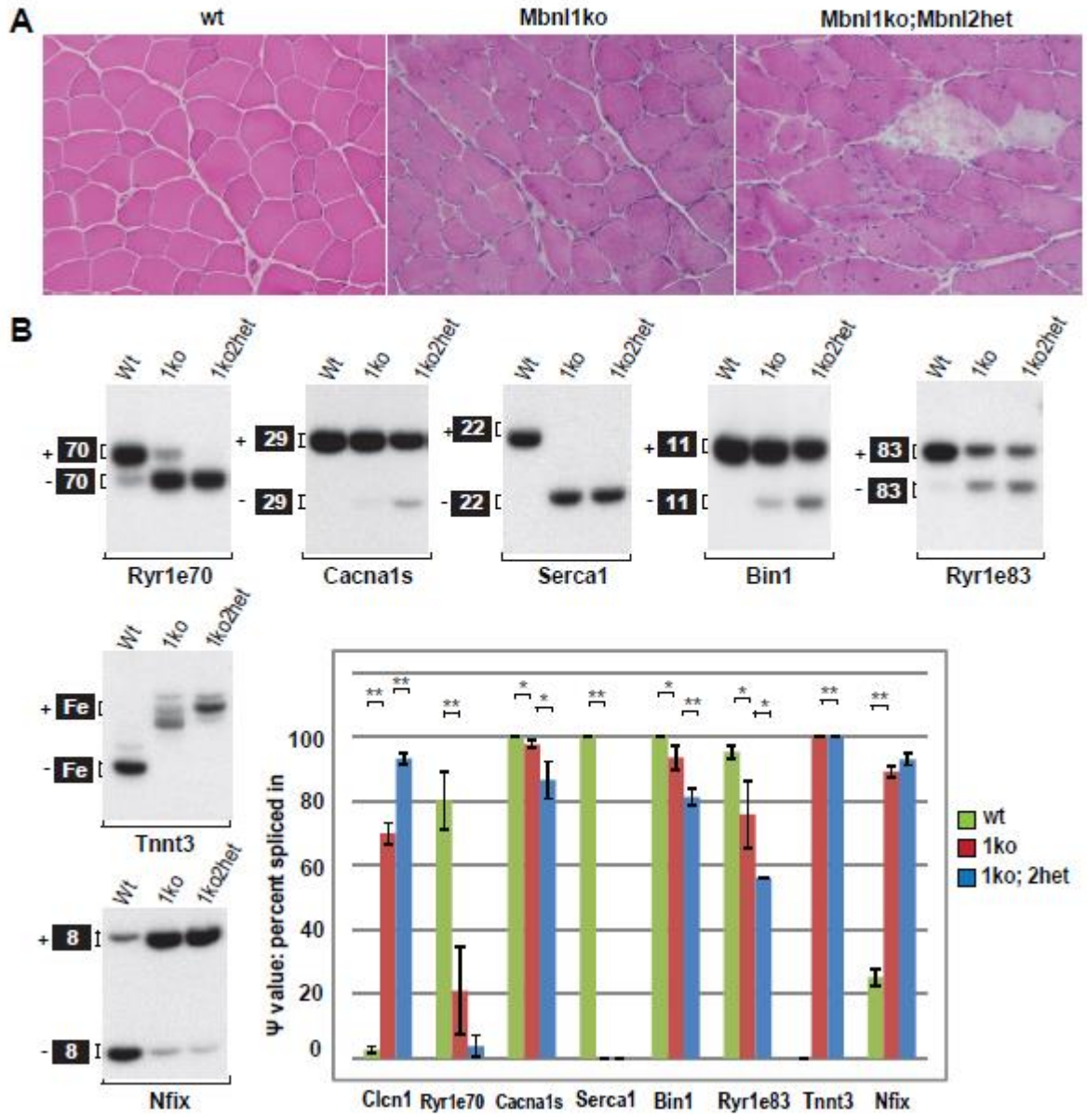

Figure 4-5. 1KO2HET mice showed enhanced skeletal muscle pathology. A) H&E staining of cross-sections from tibialis anterior muscles. The *Mbnl1* KO showed some centralized nuclei and split fibers (middle panel) compared with WT (left panel). The 1KO2HET showed an increase in muscle abnormalities accompanied with signs of fiber degeneration. B) Splicing assay on known DM1 skeletal muscle targets. A consistent increase (or at least the same in the case of Serca1) in mis-splicing towards fetal isoform patterns was seen. Gene transcripts showed significant changes (except Nfix) between *Mbnl1* KO and 1KO2HET mice.

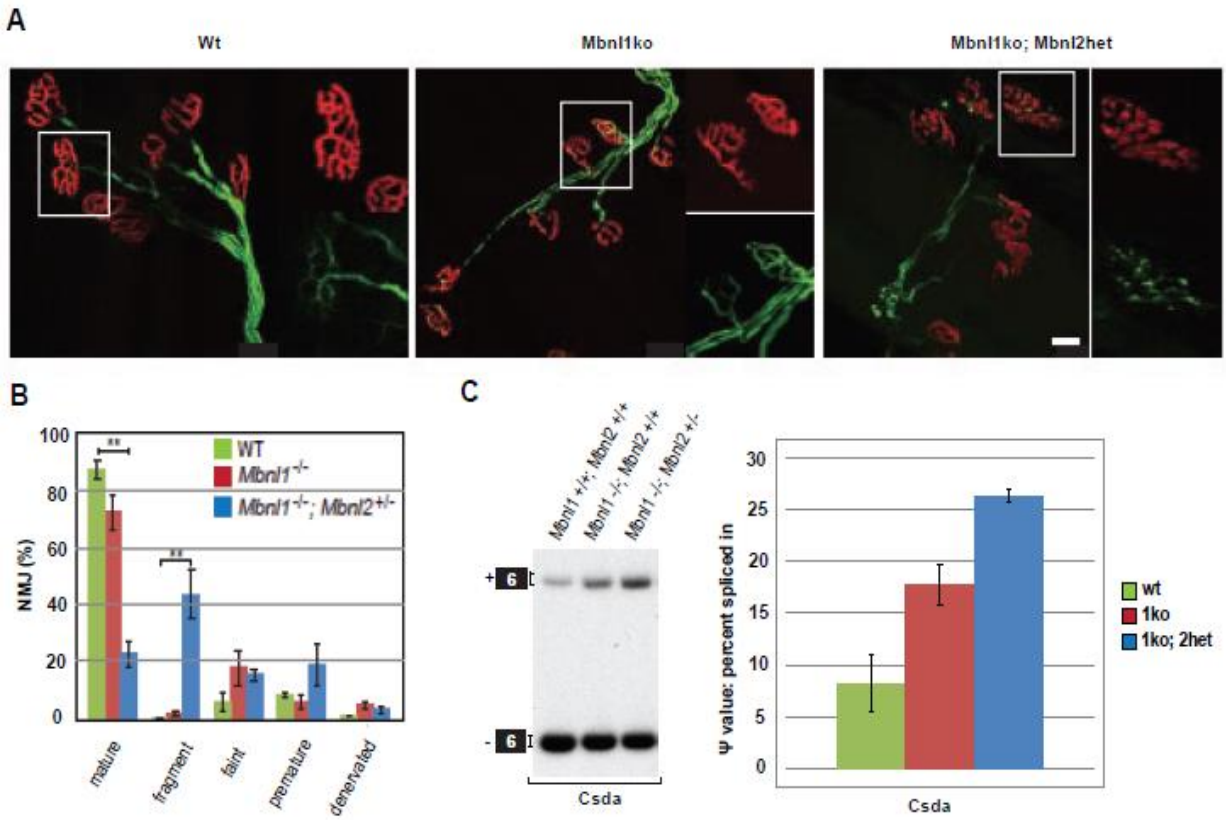

Figure 4-6. 1KO2HET mice showed a consistent defect in NMJ structure. A) NMJ staining of WT, *Mbnl1* KO and 1KO2HET are shown from top to bottom. While WT and *Mbnl1* KO muscles showed pretzel-shaped end plates and distinct terminal axonal branches, 1KO2HET exhibits signs of NMJ degeneration (fragmentation of endplates, sprouting of synapses and decreased number of mature innervated NMJs). B) Bar graph of various NMJ morphological defects. C) Csda splicing misregulation with bar graph showing a significant difference between these three groups of mice (n=3 in each group, $p<0.01$)

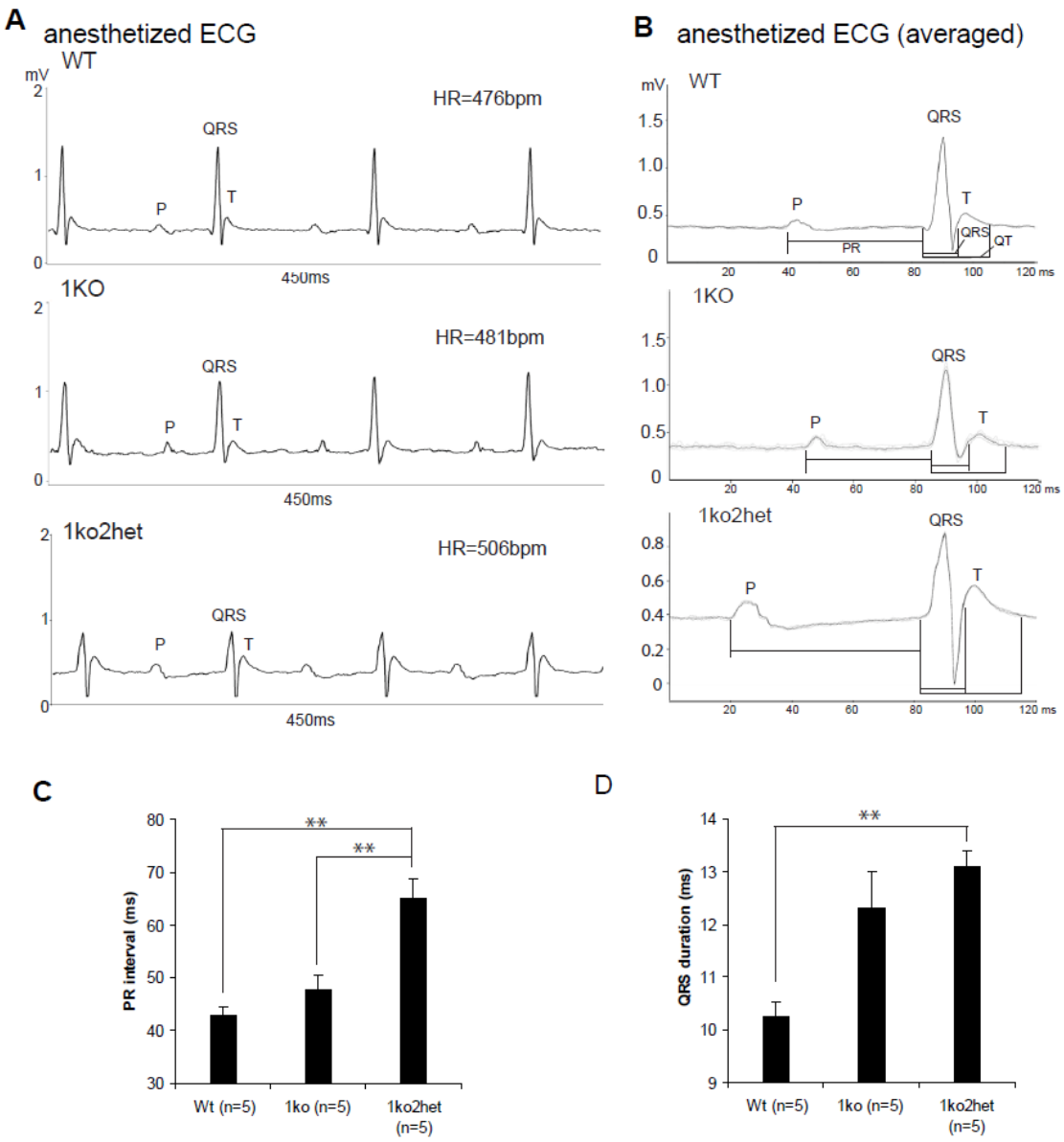

Figure 4-7. Cardiac conduction block in 1KO2HET mice. A) Baseline ECG recordings on WT, *Mbnl1* KO and 1KO2HET hearts. B) Prolonged PR and QRS intervals in 1KO2HET mice. C) Bar graph showing the PR interval difference between three groups. The 1KO2HET showed a significant PR interval prolongation compared with the other groups. D) Significant QRS interval prolongation was also seen in 1KO2HET mice. (n=5 in each group).

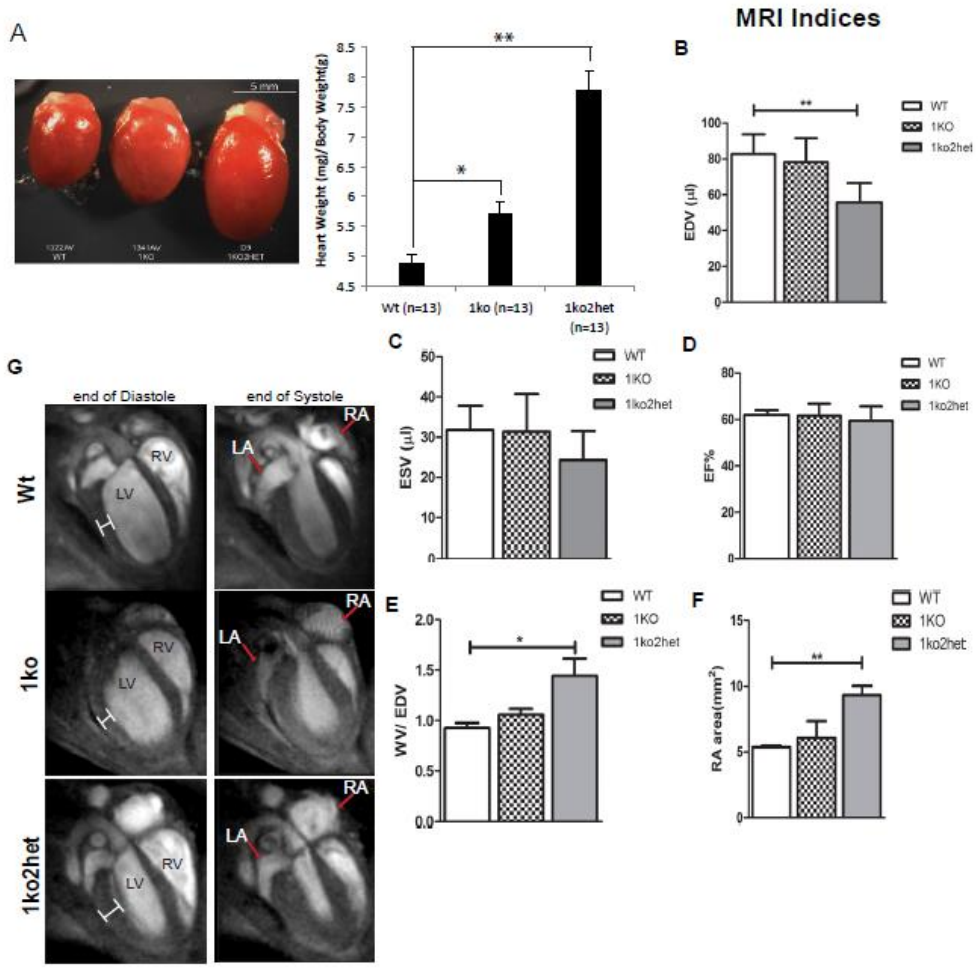

Figure 4-8. The heart of 1KO2HET mice showed structural and physiological abnormalities. A) Heart enlargement 1KO2HET mice (right) compared with WT (left) and *Mbnl1* KO (middle) (left panel). After normalizing for body weight, 1KO2HET mice showed significant increases in heart weight/body weight ratio (right panel). B to F) Bar graphs of MRI results showing that 1KO2HET hearts develop decreased end diastolic volume (EDV), increased WV/EDV and increased RA areas. G) MRI four chamber view showing increased thickness of LV wall and increased size of RA (ESV, end systolic volume; WV, whole volume; EDV, end diastolic volume; EF, ejection fraction; RA, right atrium; LA, left atrium; RV, right ventricle; LV, left ventricle).

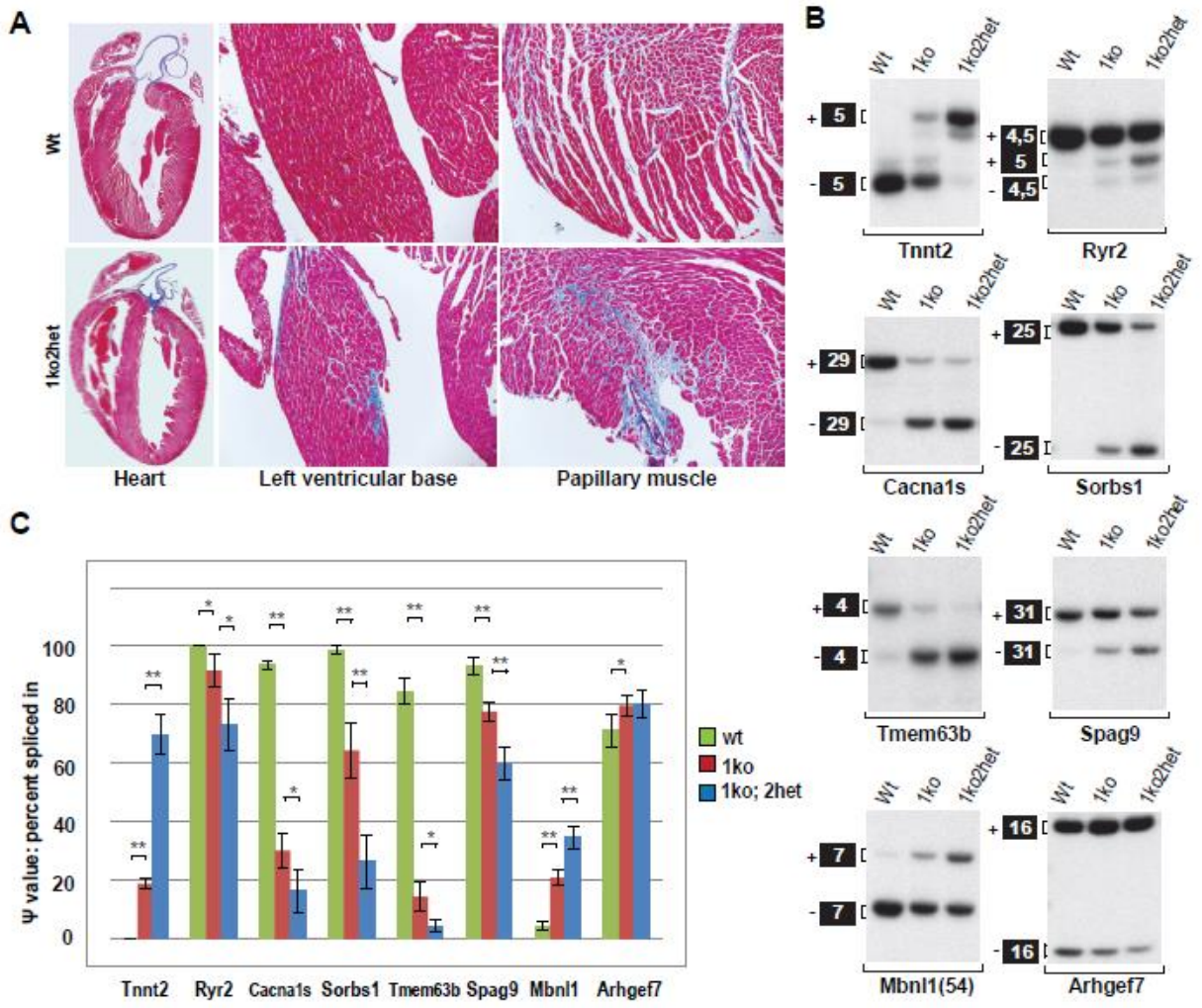

Figure 4-9. 1KO2HET hearts showed fibrosis and enhanced splicing perturbation. A) Trichrome staining of WT and 1KO2HET heart sections. Fibrosis (blue) was detectable around the aortic valve area, at the left ventricular base and in papillary muscle of the left ventricle. B) Splicing assay on Mbnl1 heart targets. A dramatic change was seen for Tnnt2 exon 5 between *Mbnl1* KO and 1KO2HET. Enhanced splicing changes were also evident for other targets. C) Bar graph showing transcripts that with significant splicing changes (except Arhgef7) between *Mbnl1* KO and 1KO2HET.

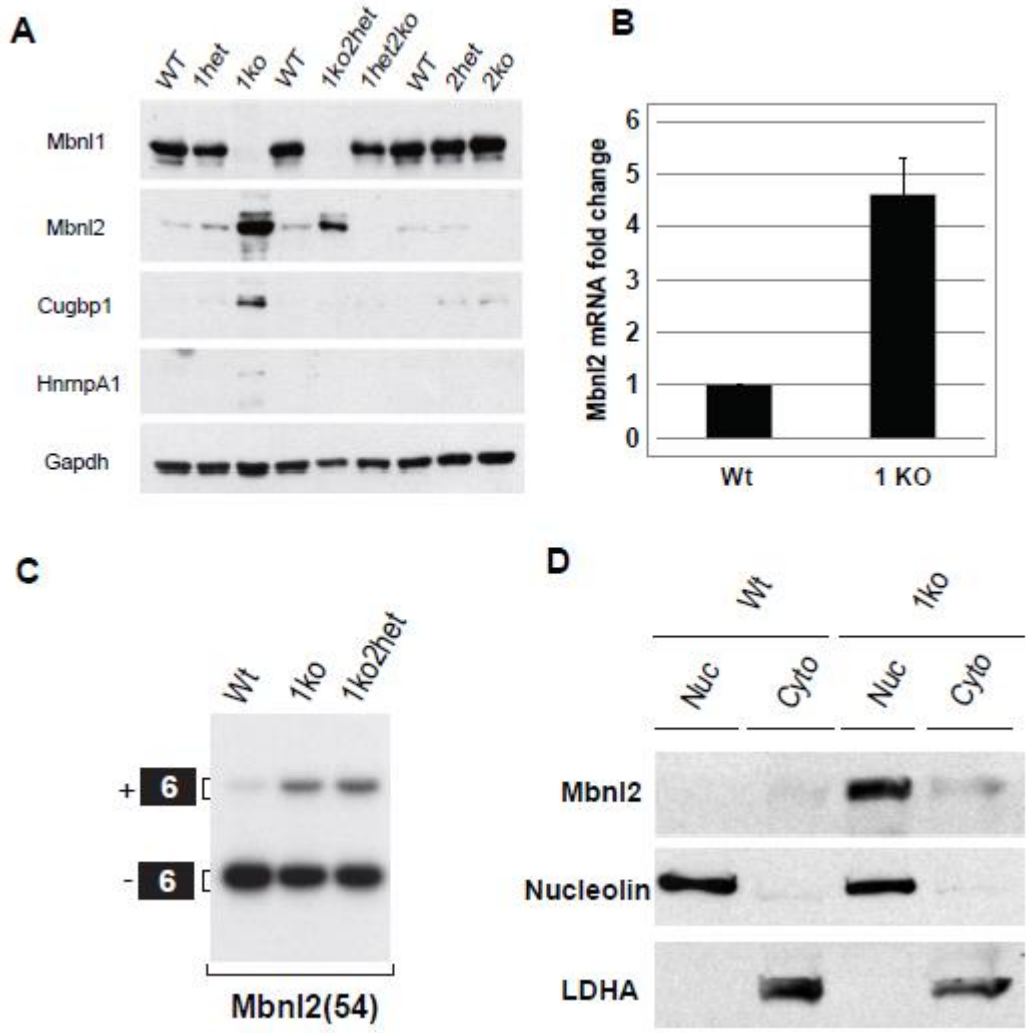

Figure 4-10. Up-regulation and relocalization of Mbnl2 in *Mbnl1* knockout mice. A) Immunoblots showing Mbnl2 protein expression in quadriceps. Mbnl2 was highly upregulated in *Mbnl1* KOs. B) Bar graph of qRT-PCR showing that Mbnl2 mRNA levels increased 4.6-fold in *Mbnl1* KO quadriceps. C) Relocation of Mbnl2 and splicing regulation. Elevated Mbnl2 exon 6 splicing occurred in *Mbnl1* knockout mice. D) Immunoblot of subcellular fractionations from WT and *Mbnl1* KO mice quadriceps with Mbnl2 (top), nucleolin (nuclear marker, middle) and LDHA (cytoplasmic marker, bottom) shown.

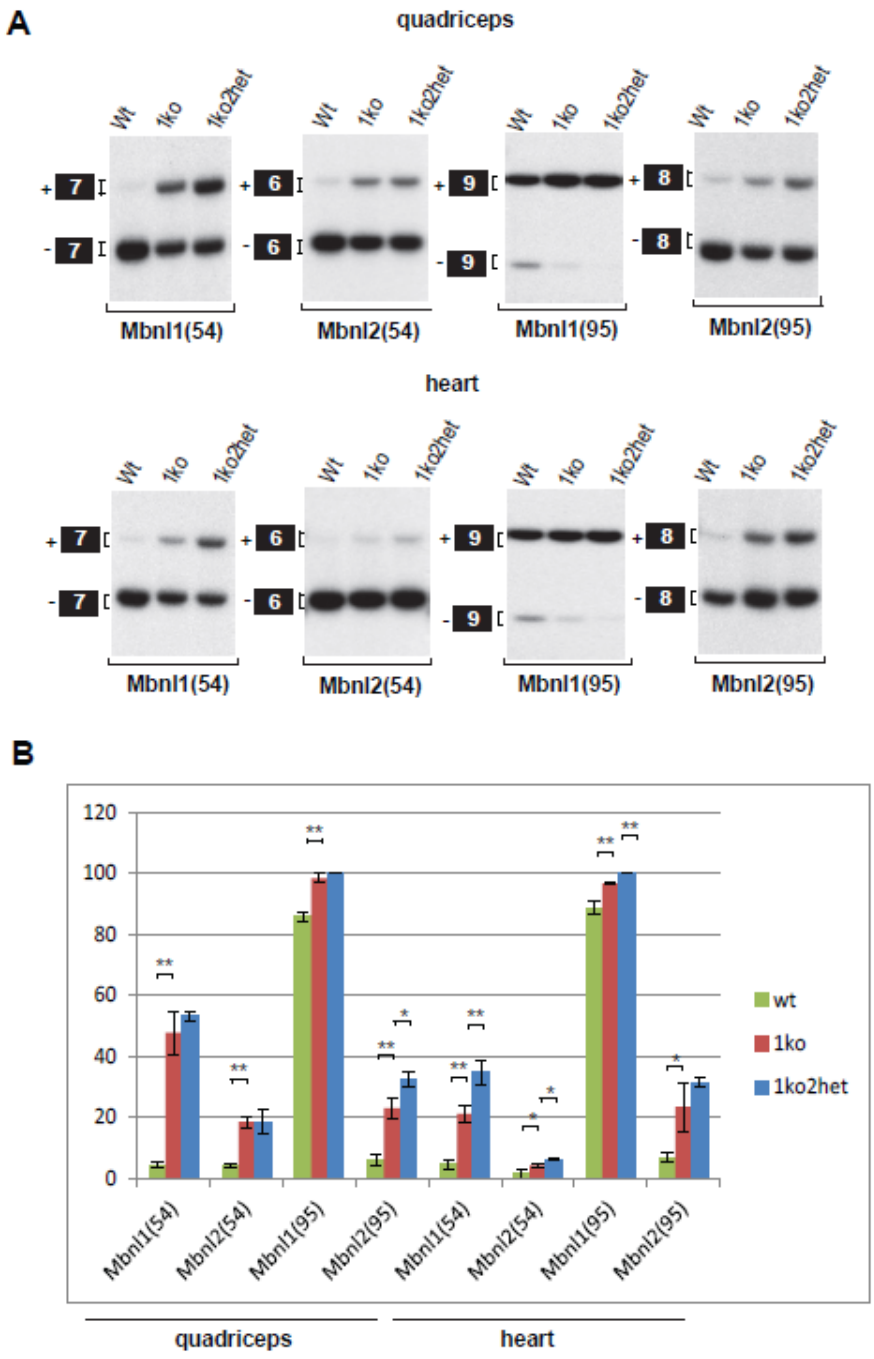

Figure 4-11. Auto- and cross-regulation of Mbnl1 and Mbnl2. A) Splicing assay showed Mbnl1 exon 7 and 9 and Mbnl2 exon 6 and 8 in WT, *Mbnl1* KO and 1KO2HET heart. Loss of Mbnl1 caused a significant increase in the inclusion of all alternative exons. B) Increased exon inclusions were seen in 1KO and 1KO2HET compared with Wt, although some of them did not reach statistical significance between 1KO and 1KO2HET.

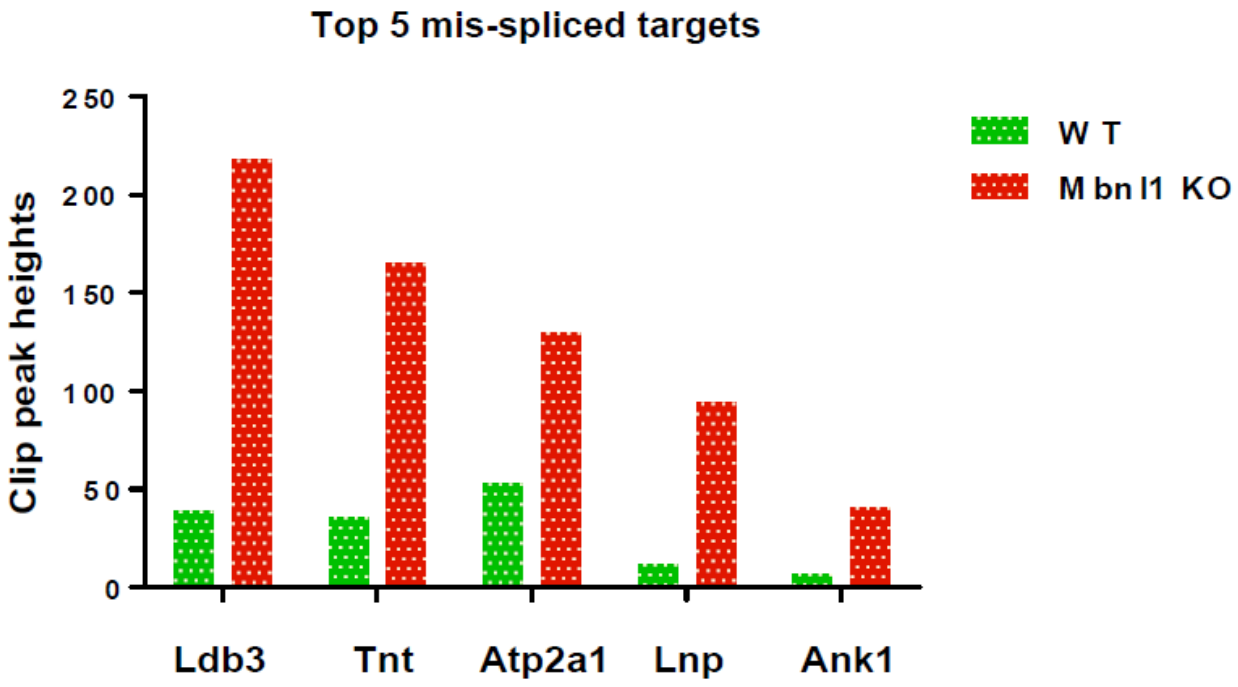

	WT	Mbnl1 KO	1KO/wt	1KO-wt
Ldb3	39	218	5.589744	179
Ttn	36	165	4.583333	129
Atp2a1	53	130	2.45283	77
Lnp	12	94	7.833333	82
Ank1	7	41	5.857143	34

Figure 4-12. Mbnl2 HITS-CLIP on WT and *Mbnl1* KO quadriceps. The top five targets showing the largest Mbnl2 CLIP peak heights in *Mbnl1* KO mice were selected. A 2.5 - 7.8-fold increase was observed for these targets.

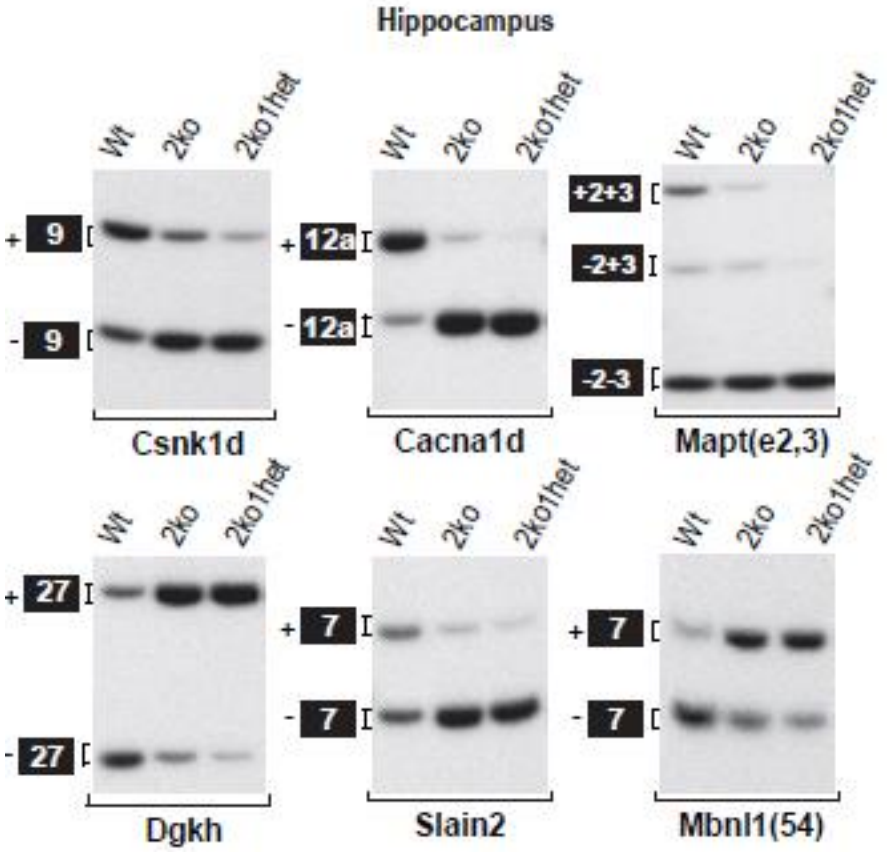

Figure 4-13. RT-PCR analysis of splicing in 2KO1HET mice for Mbnl2 targets. Due to limited mouse available, we only tested one 2KO1HET mouse for these assays. The results showed subtle but consistent enhancements of splicing alteration in 2KO1HET mice.

CHAPTER 5
MBNL COMPOUND CONDITIONAL KNOCKOUT MICE AS DM DISEASE MODELS

Introduction

To overcome the embryonic lethality of *Mbnl1*; *Mbnl2* constitutive DKOs, a conditional knockout strategy was used. The *Mbnl1* conditional KO model has not been created yet but we do have mice carrying *Mbnl2* conditional allele. So a tissue-specific knockout for *Mbnl2*, using Nestin-cre mice from JAX lab was applied. Nestin-cre mediated recombination occurs primarily in neurons in the brain and expression begins at E10.5 to 11.5 and is complete by E14.5 to 15.5. Nestin is also expressed at a much lower level in heart, somite-derived tissues and kidneys. Previous studies have shown the recombination occurs in different genetic backgrounds (Dubois et al., 2006).

Results

Reduced Body Size, Life Span and Motor Deficits in *Mbnl1*$^{\Delta E3/\Delta E3}$; *Mbnl2* $^{cond/cond}$; *Nestin*$^{+/-}$ mice

Crosses between *Mbnl1*$^{+/\Delta E3}$, *Mbnl2* $^{cond/cond}$; *Nestin* $^{+/-}$ and *Mbnl1*$^{+/\Delta E3}$, *Mbnl2*$^{cond/cond}$; *Nestin* $^{-/-}$ generated *Mbnl1*$^{\Delta E3/\Delta E3}$, *Mbnl2*$^{cond/cond}$; *Nestin* $^{+/-}$ (Nestin DKO) mice. These mice were ~40% smaller at the age of weaning (Figure 5-1A). These mice either died, or had to be euthanized, by 22 weeks of age although many survived <15 weeks of age (Figure 5-1B). Motor functions were severely affected (Figure 5-2A) and leg contractures were noted (Figure 5-2B). All the mice of other genotypes generated from this mating did not show similar phenotypes. To make our data more convincing, we chose mice of seven other genotypes to serve as control. These mice are *Mbnl1*$^{+/+}$, *Mbnl2*$^{+/+}$; *Nestin* $^{-/-}$; *Mbnl1*$^{+/+}$, *Mbnl2*$^{+/+}$; *Nestin* $^{+/-}$; *Mbnl1*$^{\Delta E3/\Delta E3}$, *Mbnl2*$^{+/+}$; *Nestin* $^{-/-}$; *Mbnl1*$^{\Delta E3/\Delta E3}$, *Mbnl2*$^{+/+}$; *Nestin*$^{+/-}$; *Mbnl1*$^{+/+}$, *Mbnl2*$^{cond/cond}$; *Nestin* $^{-/-}$; *Mbnl1*$^{+/+}$, *Mbnl2*$^{cond/cond}$; *Nestin* $^{+/-}$; *Mbnl1*$^{\Delta E3/\Delta E3}$, *Mbnl2*$^{cond/cond}$; *Nestin* $^{-/-}$. The Nestin DKO mice

and seven other control mice were tested on Rotarod. Rotarod analysis at 5 weeks of age demonstrated that Nestin DKO mice showed a significant decline in motor performance and while control mice improved during the consecutive 4 day trial, Nestin DKO failed to show a significant improvement (Figure 5-2C). At the age of 9 weeks, Nestin DKO showed further declines. However, control mice with the *Mbnl1*$^{\Delta E3/\Delta E3}$ allele also started to show a decline (data not shown), compatible with the Rotarod results in a previous constitutive compound knockout study. Grip strength testing was also performed at 6 weeks and 12 weeks of age and Nestin DKO mice showed less strength compared with control mice (Figure 5-2D). Due to facial muscle weakness, malocclusion was also evident so teeth had to be trimmed frequently. Facial weakness is a common clinical feature in DM1 (Harper, 2001).

Aberrant Splicing in the *Mbnl1*$^{\Delta E3/\Delta E3}$; *Mbnl2* $^{cond/cond}$; *Nestin*$^{+/-}$ Brain

To test if in Nestin DKO mice display enhanced mis-splicing, validated targets were selected from the previous microarray studies for *Mbnl1* and *Mbnl2* single knockout mice (Table 5-1). We selected three different genotypes as controls for the splicing assay including *Mbnl1*$^{+/+}$; *Mbnl2*$^{+/+}$; *Nestin*$^{+/-}$, *Mbnl1*$^{E3/\Delta E3}$; *Mbnl2*$^{cond/cond}$; *Nestin*$^{-/-}$ *and Mbnl1*$^{+/+}$; *Mbnl2*$^{cond/cond}$; *Nestin* $^{+/-}$ mice representing WT, *Mbnl1* KO and *Mbnl2* KO phenotypes, respectively.

Since mis-splicing of GRIN1 (NMDAR1) and MAPT (Tau) have been reported in DM1 patients, these two targets were tested initially. *Mbnl1*$^{+/+}$; *Mbnl2*$^{cond/cond}$; *Nestin* $^{+/-}$ mice reproduced the splicing shifts seen in *Mbnl2* constitutive KOs but the ψ value (percent spliced-in) for Nestin DKO mice was ~7-fold greater compared with WT. For Mapt splicing, Mbnl2 Nestin DKO showed a reduction of isoforms containing exon 2 (top two bands, +/- exon 3), however, Nestin DKO mice showed a complete loss of adult

isoforms. Indeed, Nestin DKO mice fully recapitulated the P6 fetal splicing pattern (Figure 5-3).

Cacna1d and Csnk1d, two of the top ten ranked targets in the *Mbnl2* KO splicing microarray study, were also evaluated. The splicing of Cacna1d shifted to the fetal isoform, which excludes alternative exon 12a. In Nestin DKO, the Cacna1d adult isoform was totally eliminated. For Csnk1d, *Mbnl2* conditional KOs shifted splicing towards the isoform excluding exon 9 and the ψ value was further reduced in Nestin DKOs. Again, the splicing pattern in Nestin DKOs was identical to the P6 fetal pattern (Figure 5-3).

We noticed during our *Mbnl2* knockout studies that some targets shifted towards the fetal isoform but still this shift was partial and not similar to the default fetal pattern. We selected four genes (*Add1*, *Clasp2*, *Ndrg4* and *Kcnma1*) in this category and splicing analysis showed a dramatic switch from the default adult to fetal pattern in Nestin DKOs. The most dramatic splicing shift was seen for Kcnma1, which showed a modest shift in *Mbnl2* Nestin conditional KOs (similar to *Mbnl2* null mice). In Nestin DKO mice, this splicing shifted to the fetal isoform, which excludes exon 25a, and the ψ value changed from 100 to 7, the largest shift of all brain targets tested to date (Figure 5-4). We also tested the top Mbnl1 targets. Sorbs1 and Camk2d were mis-regulated in the brain of *Mbnl1* KOs as well as DM1 patients. While *Mbnl1* KOs showed subtle splicing changes in Sorbs1, *Mbnl2* Nestin conditional KOs showed no changes and Nestin DKOs showed a 40% shift towards the fetal isoform excluding exon 25. On the other hand, the δ9 isoform of Camk2d has been identified in both mice and human as the fetal isoform and also the predominant isoform in DM1 patients. In agreement with prior

reports, *Mbnl1* KOs show a small increase in the δ9 isoform and *Mbnl2* Nestin conditional KOs show a 15% increase of the δ9 isoform among four major isoforms. In Nestin DKO mice, the δ9 isoform increased dramatically, or up to 50%, and became the most abundant isoform which recapitulated the fetal splicing pattern (Figure 5-5).

Previously, some lower ranked targets on the Mbnl2 splicing microarray list were not significant so two of these targets, Camkk2 and Slitrk4, were evaluated in the Nestin DKO. In the case of Slitrk4, shifting towards fetal splicing occurred with a 15-20% change between WT and Nestin DKOs but the splicing pattern did not switch completely to fetal pattern (Figure 5-5). For the twelve targets tested, Nestin DKOs showed significant differences compared with *Mbnl1*$^{+/+}$; *Mbnl2*$^{cond/cond}$; *Nestin* $^{+/-}$ (Figure 5-6) (Grin 1 $p<0.05$; all other genes $p<0.01$ in unpaired t test for two groups).

Reduced NMDA-Mediated Excitatory Post-Synaptic Potential (EPSP) in *Mbnl1*$^{\Delta E3/\Delta E3}$; *Mbnl2*$^{cond/cond}$; *Nestin* $^{+/-}$ mice

In the *Mbnl2* constitutive KOs, loss of Mbnl2 led to learning and memory deficits by the Morris Water Maze test as well as electrophysiological changes including LTP deficits. Therefore, we also tested Nestin DKOs together with three control lines. A significant difference in NMDA-mediated EPSP between Nestin DKO and the controls was observed indicating that Nestin DKOs have abnormal hippocampal function in synaptic transmission (Figure 5-7).

Discussion

Potential Involvement of Mbnl1 in Learning and Memory

Although our previous studies on *Mbnl1* KO brain revealed subtle splicing and behavioral changes, Mbnl1 did not appear to possess essential functions in the CNS. However, Nestin DKO mice provided evidence that Mbnl1 may play significant role

when Mbnl2 is depleted. For many of the Mbnl2 targets in which *Mbnl2* KO mice did not show a complete switch to the fetal splicing pattern, Nestin DKOs did. Interestingly, many of these targets have been linked to learning and memory. For example, Grin1, Mapt (Sergeant et al., 2001), Add1 (Vukojevic et al., 2012), Ndrg4 (Yamamoto et al., 2011), Clasp2 (Beffert et al., 2012), Kcnma1 (Bell et al., 2008) and Camkk2 (Mairet-Coello et al., 2013; Peters et al., 2003) were all reported to contribute to learning deficits. In a *C.elegans* study, the C-terminal sequence of α-adducin (Add1) includes a lysine-rich region that is important for binding with spectrin and actin. Spliced isoforms containing that region could rescue the Add1 mutant (tm3760) memory defects while other isoforms could not (Vukojevic et al., 2012). Our EPSP study showed a significant difference between Nestin DKO and controls, which is consistent with our prediction. One of the targets, Slitrk4, was interesting because whole-genome DNA chip analysis of DM1 embryonic stem cells showed downregulation of Slitrk4 and Slitrk4 mis-expression accounts for neurite growth and synaptogenesis (Marteyn et al., 2011). Although current understanding of Slitrk4 function is relatively limited, the six Slitrk family members are highly expressed in the CNS and many of them have been linked to neuropsychiatric disorders (Aruga and Mikoshiba, 2003; Proenca et al., 2011). We detected a significant splicing change in Nestin DKOs towards the fetal pattern.

Table 5-1. Primers for RT-PCR in *Mbnl* compound conditional knockout mice studies.

Gene	Exon	Bp	Forward primer	Reverse primer
Grin1	4	63	tcatcctgctggtcagcgatgac	agagccgtcacattcttggttcctg
Mapt	3,4	87,87	aagaccatgctggagattacactc tgc	ggtgtctccgatgcctgcttctt
Cacna1d	12a	60	catgcccaccagcgagactgaa	caccaggacaatcaccagccag taaa
Csnk1d	9	63	gatacctctcgcatgtccacctcac a	gcattgtctgcccttcacagcaaa
Add1	15	37	ggatgagacaagagagcagaaa gagaaga	ctgggaaggcaagtgcttctgaa
Clasp2	16a, 16b	27_27	gttgctgtgggaaatgccaagac	gctccttgggatcttgcttctcttc
Ndrg4	14	39	cttcctgcaaggcatgggctaca	gggcttcagcaggacacctccat
Kcnma1	25a	81	gattcacacctcctggaatggaca gat	gtgaggtacagctctgtgtcaggg tcat
Sorbs1	25	168	ccagctgattacttggagtccacag aag	gttcaccttcataccagttctggtca atc
Camk2d	14b, 15,16	33_60_42	cagccaagagtttattgaagaaac caga	ctttcacgtcttcatcctcaatggtg
Camkk2	16	43	ggtgaccgaagaggaggtcgag aa	agggaccacctttcacaagagc actt
Slitrk4	2	72	gctccctctctctgcttggacatga	ccactgatatgtcagaatctgcatt tgtagaa
Csda	6	207	atggagttcctgtagaagggagtc gctat	aacctcgggcggtaagtcggat
Dag1	2b	57	gaacacctgctgctgctcccttt	caagccaccagttgctaaggaa gaaa

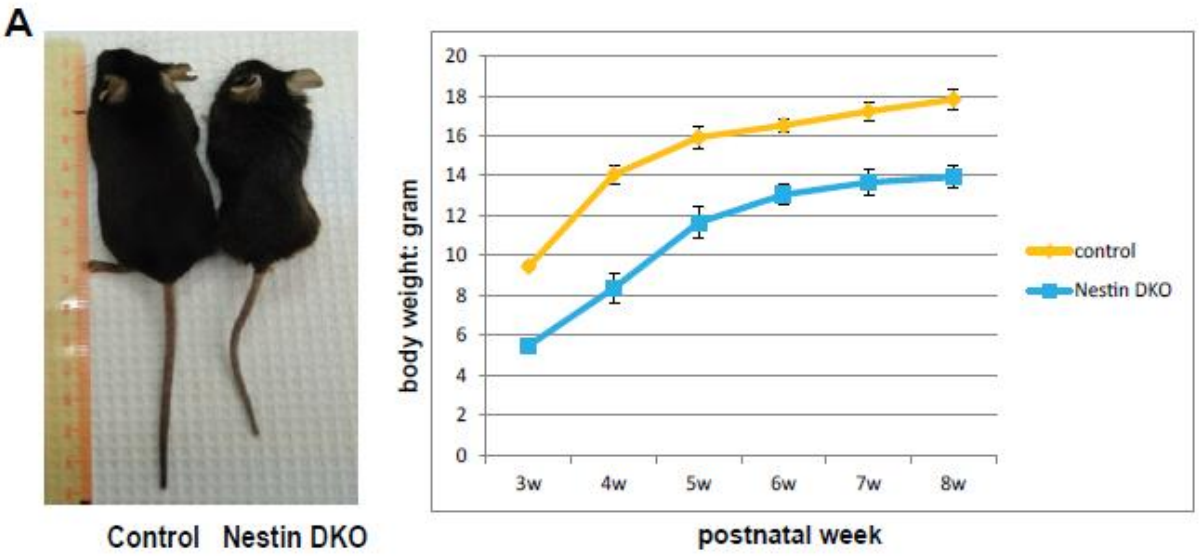

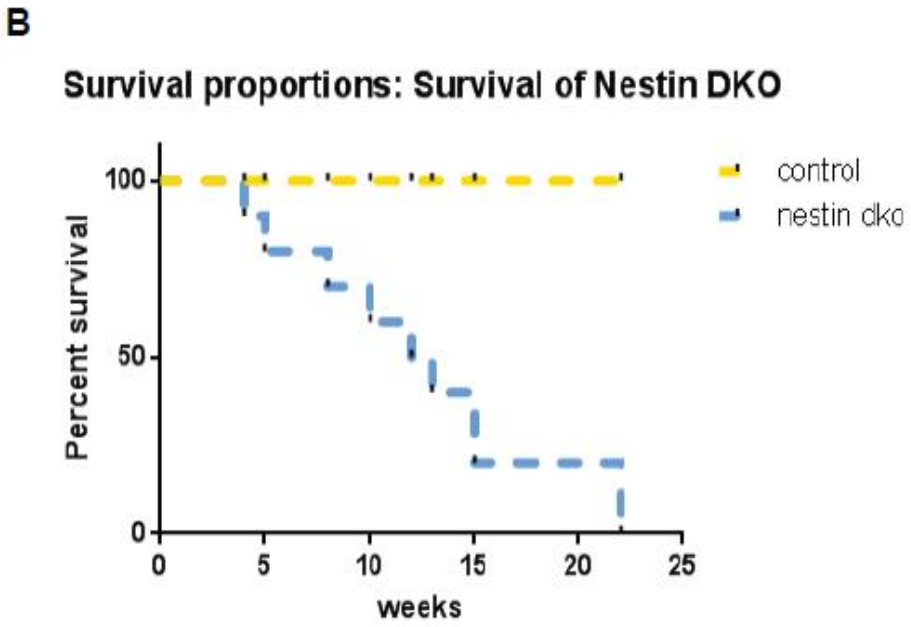

Figure 5-1. Nestin DKO mice were smaller and showed reduced lifespan. A) Nestin DKO mice with a control mouse (left). Average body weight of Nestin DKO mice was ~40% less than controls at P21 and this difference dropped to 20-25% by 8 weeks of age. B) Kaplan-Meier curve of control versus Nestin DKO mice. The genotypes of seven other control mice were mentioned in the main section.

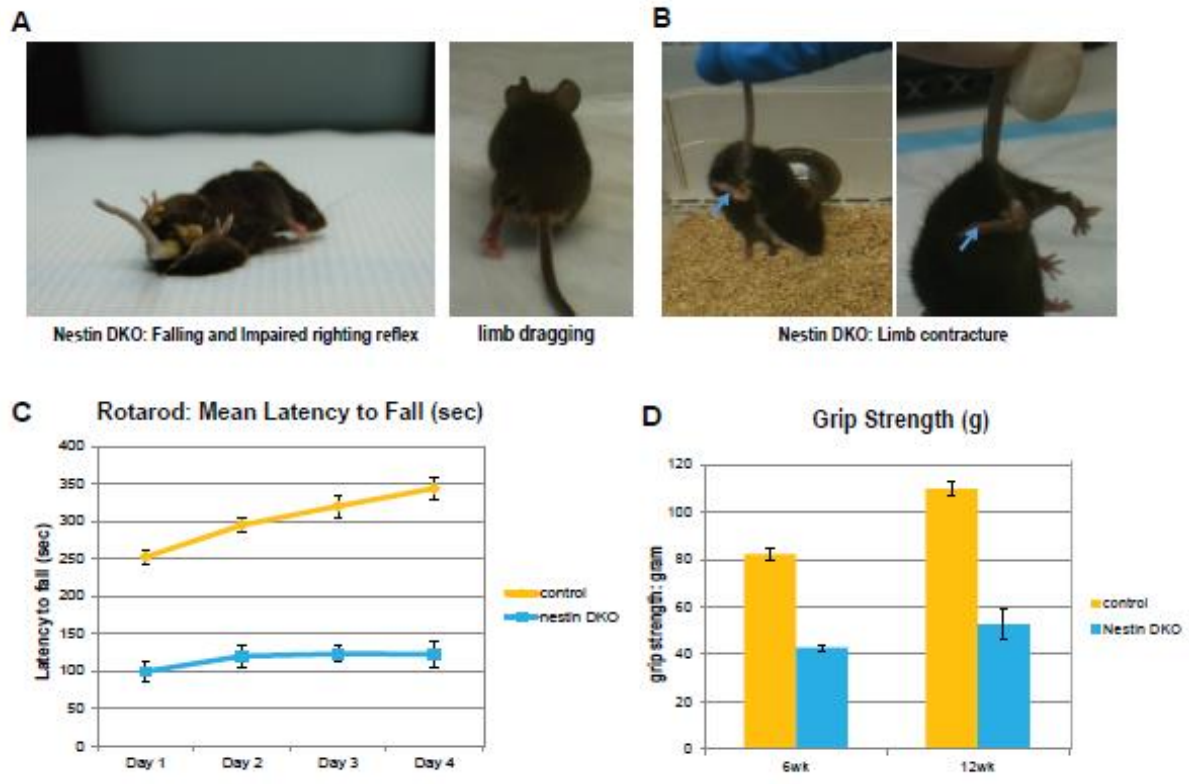

Figure 5-2. Nestin DKO mice display an array of motor defects. A) Nestin DKO showed a tendency to fall, poor righting reflex (left) and limb weakness during locomotion (right). B) Nestin DKO mice showed limb contracture at ~3 months of age (left). C) Nestin DKO showed motor deficits by the rotarod assay. D) Grip strength test showing that Nestin DKOs had decreased grip strength compared with controls at two time points.

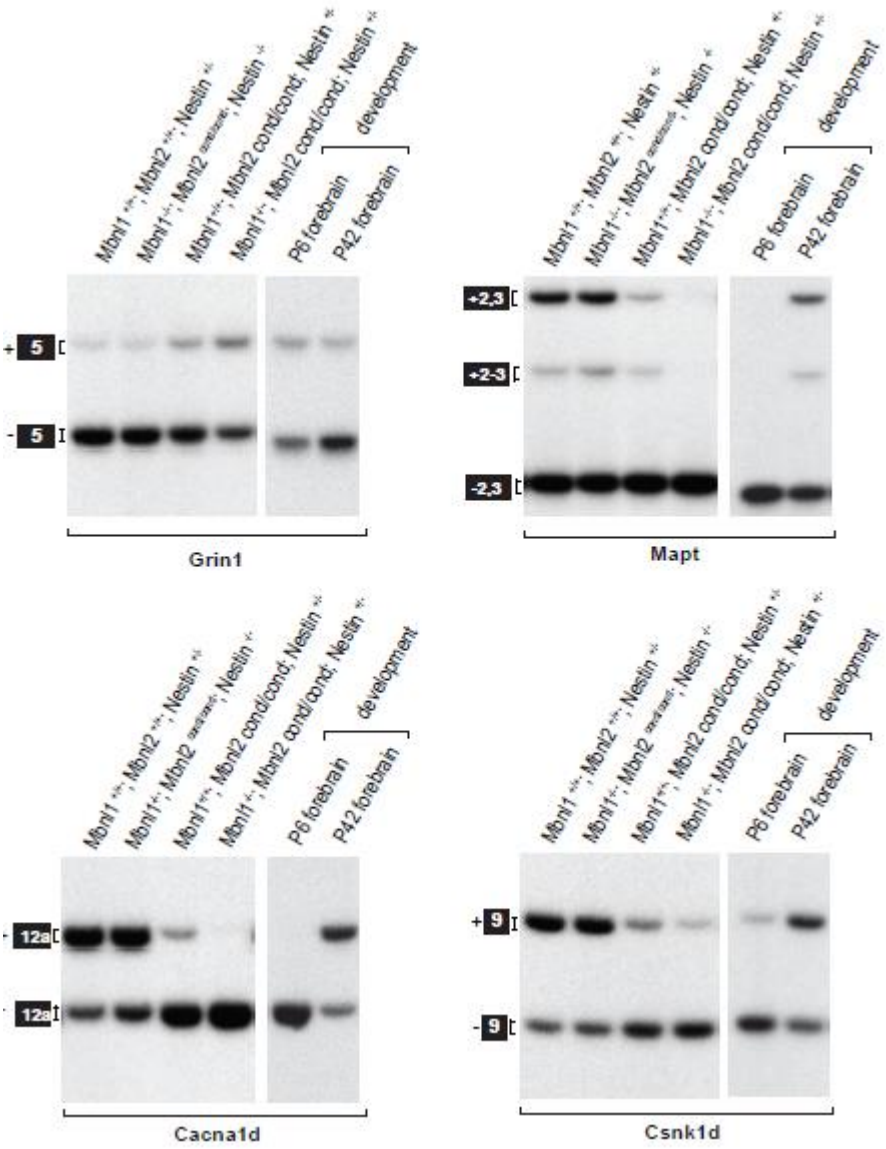

Figure 5-3. Nestin DKO mice hippocampal samples showed enhanced splicing anomalies on DM1 brain targets. For Grin1, exon 5 inclusion increased in Nestin DKO. For Mapt, exon 2 inclusive isoforms were reduced in Nestin DKOs. For Cacna1d, the exon 12a inclusive isoform was decreased and Csnk1d also showed a reduction of exon 9 inclusion in Nestin DKO mice.

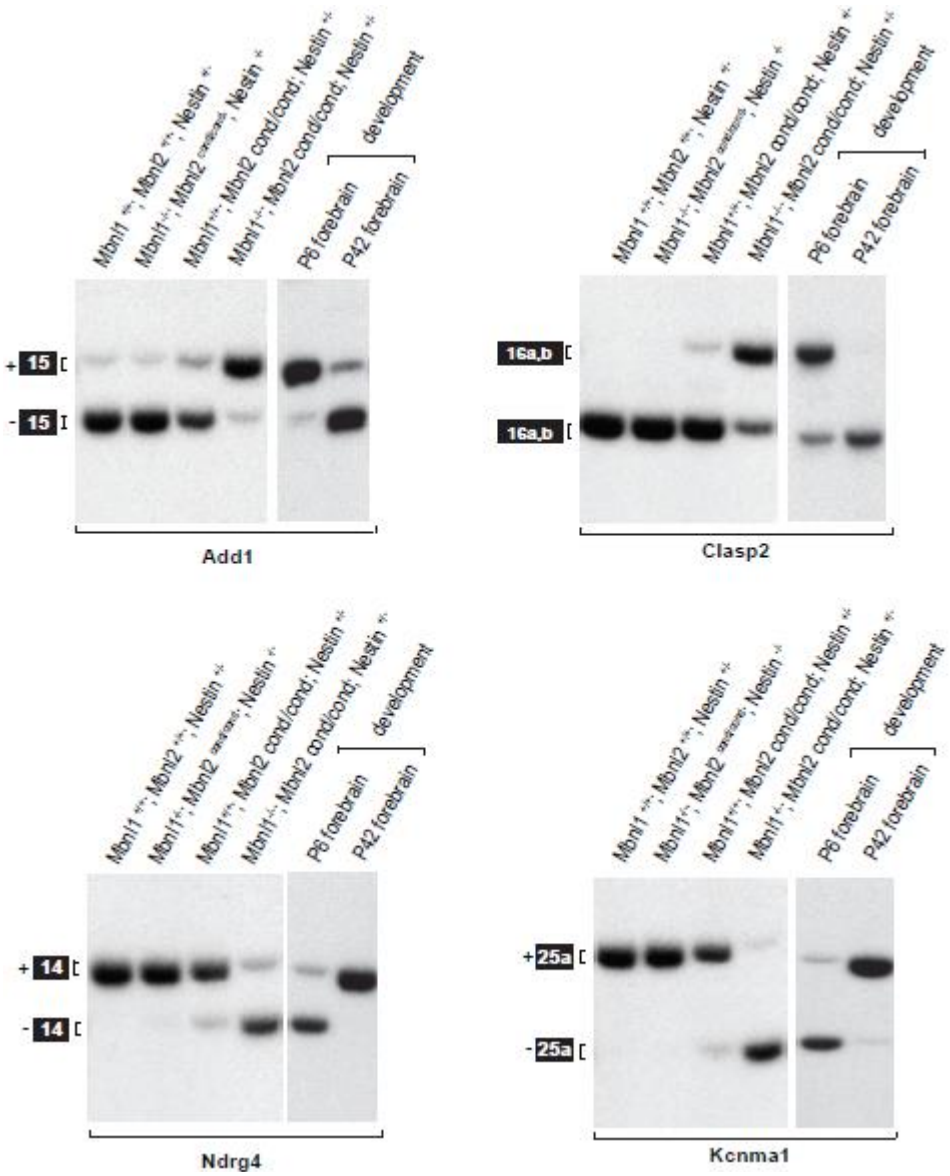

Figure 5-4. Nestin DKO mice showed enhanced splicing deficits in Mbnl2 brain targets. In *Mbnl2* KOs, splicing shifted towards the fetal pattern although adult isoforms were still predominant. In Nestin DKO,a the splicing pattern became indistinguishable from the fetal pattern (P6 forebrain).

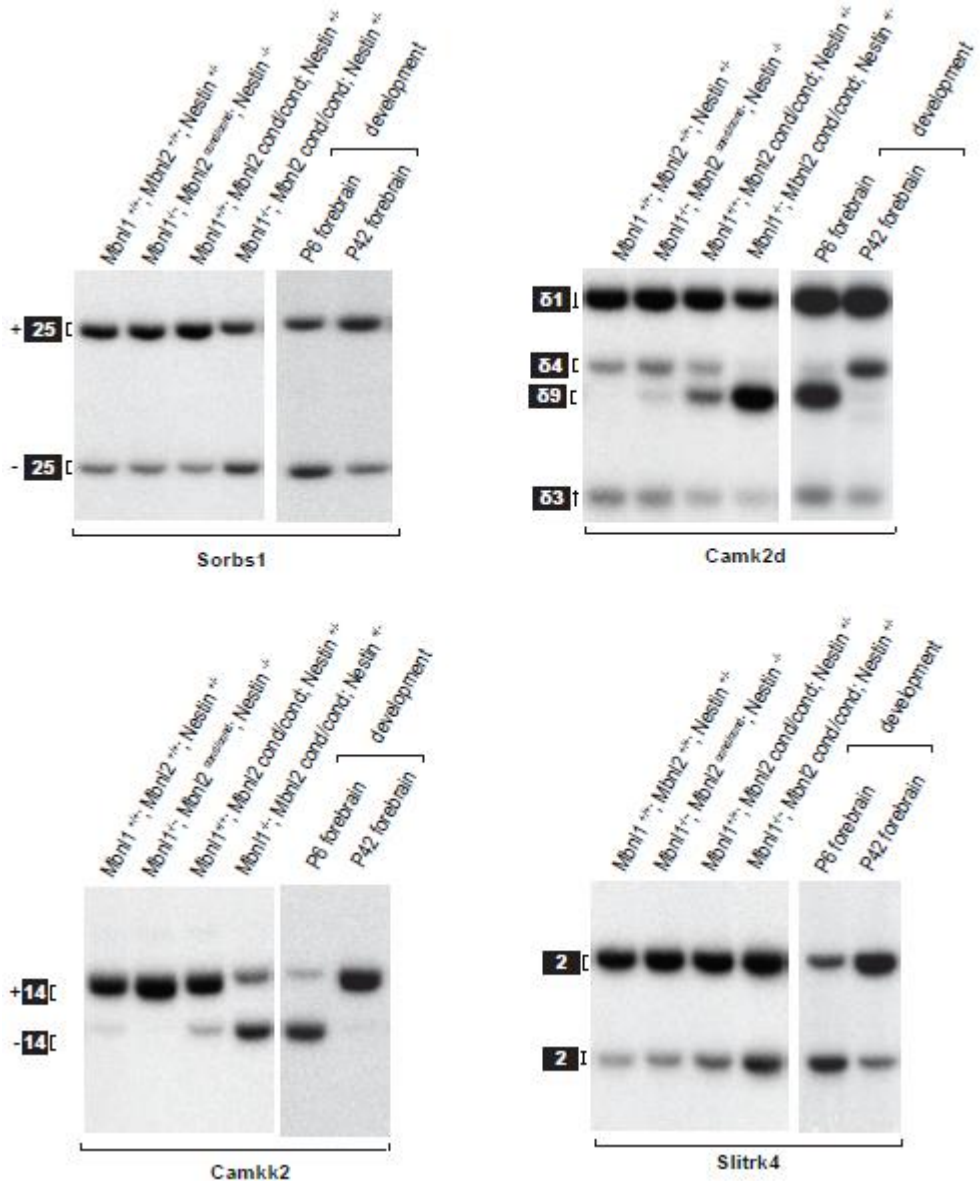

Figure 5-5. Nestin DKO mice hippocampal samples showed enhanced splicing alterations. Nestin DKOs showed effects on the splicing of Sorbs1 and Camk2d. For Camkk2 and Slitrk4, Nestin DKO showed splicing switches that were close, but not identical to, P6 fetal forebrain.

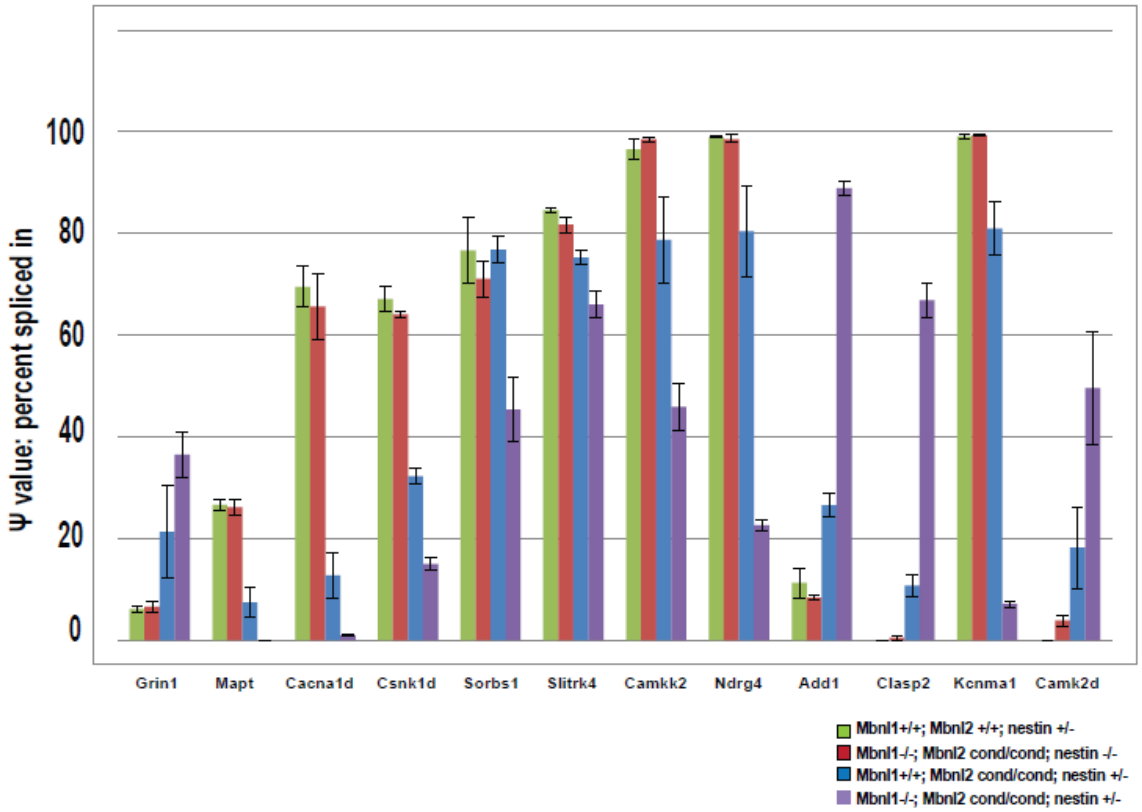

Figure 5-6. Bar graph of splicing assay results. Nestin DKO exhibited significant splicing differences compared to the other groups, especially for the six gene transcripts shown (right). All the targets show significant differences between Mbnl2 Nestin conditional KOs and Nestin DKOs (Grin1 $p<0.05$, all others $p<0.01$ in unpaired t test for two groups; $p<0.01$ using One way Anova test for four groups).

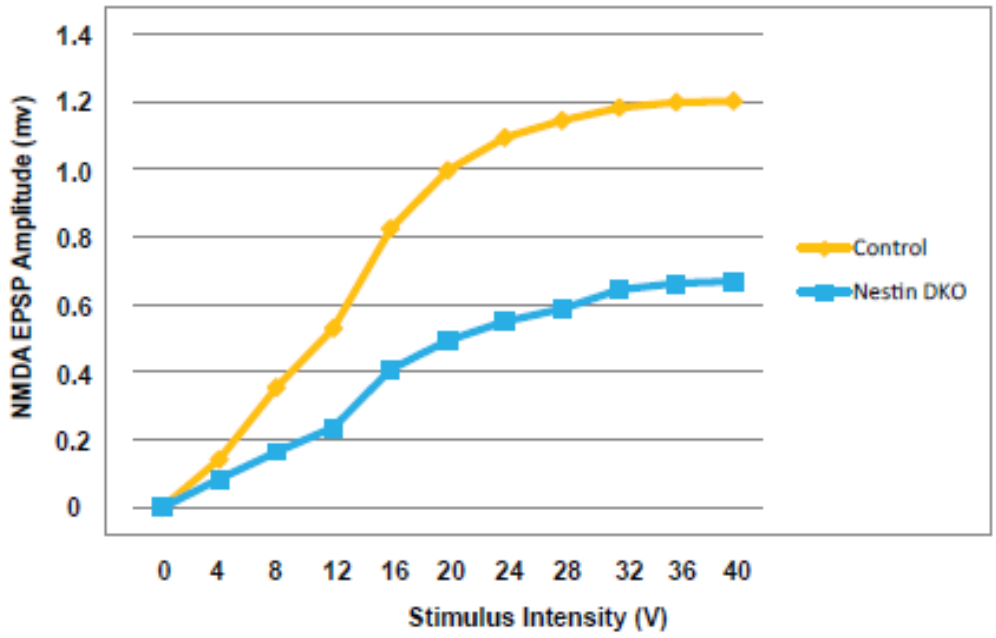

Figure 5-7. Deterioration of hippocampal functions in Nestin DKO mice. Nestin DKO mice showed decreased NMDA-mediated EPSP. The input-output curve was not significantly different (data not shown, n=3 in each group).

CHAPTER 6
CONCLUDING REMARKS AND FUTURE DIRECTIONS

Summary of the Projects

To date, a handful of DM mouse models have provided insights into the disease mechanism. However, most of these mice are transgenic models, which randomly integrate transgenes into genomic loci and may be expressed at a high level. High level expression of a transgene may be toxic and therefore some models show overt phenotypes more severe than observed in DM1. Although we have shown distinct phenotypes in *Mbnl1* and *Mbnl2* single knockout mice, they did not fully recapitulate DM1 symptoms. For example, muscle weakness/wasting and robust cardiac phenotypes are absent in these two models. Here, we demonstrate that *Mbnl1* and *Mbnl2* DKO mice are not viable. Also, we report two *Mbnl1* and *Mbnl2* compound KO models. In the 1KO2HET model, Mbnl2 levels increase and in the Nestin DKO model, Mbnl2 is deleted only in neurons. In both cases, we saw disease-relevant phenotypes and enhanced splicing changes. Previously, we determined that Mbnl1 is specific for splicing regulation in muscle systems while Mbnl2 functions primarily in the brain. Both of these Mbnl proteins serve as backup splicing regulators during the postnatal developmental transition in specific tissues (Figure 6-1). While one Mbnl is ablated, the other Mbnl is upregulated and shifts into the nucleus (Figure 6-2). Overall, these results provide novel support for the Mbnl loss of function hypothesis and further strengthen the RNA gain of function model in DM.

Future Experimental Directions and Therapeutic Implications

Mbnl1 and Mbnl2 DKOs recapitulate adult DM1 phenotypes but failed to model CDM disease. *Mbnl1*; *Mbnl2* constitutive DKOs can be identified at E13.5 without overt

defects but a detailed study is required to determine when these pups fail to survive during late, or early perinatal, stages. The next step is to generate *Mbnl1*; *Mbnl2*; *Mbnl3* conditional knockouts.

Currently, a comprehensive analysis of Nestin DKO mice remains to be done. For electrophysiology, discrepancies between our current data and the *Mbnl2* null experiments require further investigation. Although we observed a difference between Nestin DKO and controls, the value of NMDA-mediated EPSP is similar to previous results in *Mbnl2* null mice (Charizanis et al., 2012). Also, we must complete the LTP study to evaluate synaptic plasticity in these mice. Because Mapt mis-splicing was uncovered in the Nestin DKO brain, we expect to see pathological findings indicating a tauopathy (e.g., neurofibrillary tangles) in Nestin DKO brains. For the motor deficit, we anticipate pathological changes in motor neurons, either in anterior horn cells or pyramidal neurons in the brain. Cerebellar Purkinje cells may also show morphological and/or physiological changes since Mbnl1 and Mbnl2 were highly expressed in these neurons.

For the conditional KO projects, Myogenin-cre DKO mice have been generated by mating with Myogenin(Myog)-cre mice (Li et al., 2005). The preliminary data of this skeletal muscle-specific *Mbnl1*; *Mbnl2* DKOs, showed severe muscle pathology with centralized nuclei in nearly every muscle fiber and prominent muscle fiber degeneration. Severe NMJ defects and splicing alterations were also discovered and these abnormalities were apparently more profound than in 1KO2HET mice (data not shown). This model would recapitulate late stage DM1 muscle pathology and would be a valuable model in elucidating DM molecular pathogenesis and novel therapies and also

could serve as a complementary model for determining the functions of Mbnl1 and Mbnl2 in muscles and nerves. For example, the 1KO2HET showed NMJ defects but it is not clear if this results from muscle or neuronal dysfunction (or both). Currently *Mbnl1* and *Mbnl3* conditional whole locus knockouts are being generated. Once these models are available, triple Myog conditional knockouts will also be an option. Our current studies provided valuable information for DM treatment in the future and emphasized the importance of total MBNL protein replacement therapies. Recently, antisense oligonucleotide (AON) therapies have shown promise in early trials. Using gapmers design to introduce DNA sequences in an RNA-based AON, RNase H was activated and the *DMPK* mutant transcript could be effectively cleaved (Wheeler et al., 2012). Phosphorodiamidate morpholino oligomer (PMOs) based $(CAG)_n$ repeats, which redistribute Mbnl1 and force expansion RNAs into the cytoplasm, is another strategy (Wheeler et al., 2009). However, whether these blocked RNA hairpins would undergo RAN translation remains to be determined. Although the function of DMPK is not fully understood, *Dmpk* knockout mouse models have suggested that Dmpk may be important for maintaining the integrity of skeletal muscle and the nuclear envelope (Harmon et al., 2011; Kaliman and Llagostera, 2008). Therefore, degradation of DMPK transcripts might not be a safe strategy. Since AAV-mediated overexpression of Mbnl1 has proven effective in rescuing the abnormal muscle phenotype in the poly(CUG) mouse model (Kanadia et al., 2006) and overexpression of Mbnl1 is tolerable in a transgenic mouse model (Chamberlain and Ranum, 2012), we anticipate MBNL replacement therapy will be an alternative therapeutic strategy once the technological hurdles have been overcome.

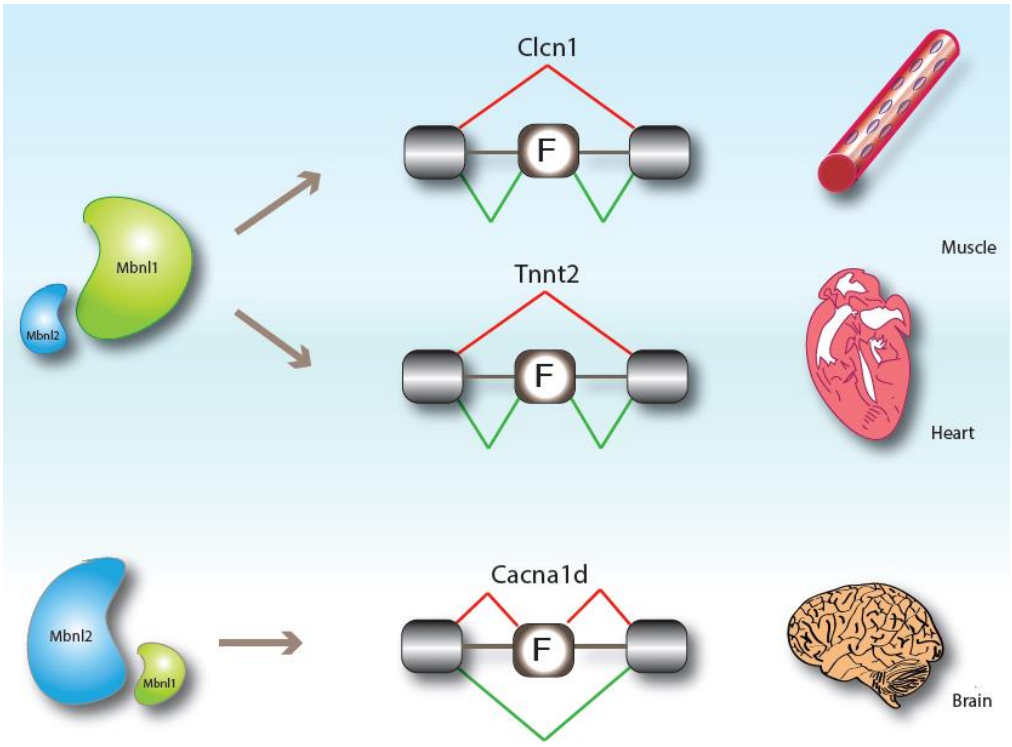

Figure 6-1. A proposed model for Mbnl splicing regulation. Mbnl1 regulates major developmental splicing events in skeletal muscle and heart while Mbnl2 controls alternative splicing of specific targets in the brain. The Mbnl proteins promote adult isoform formation.

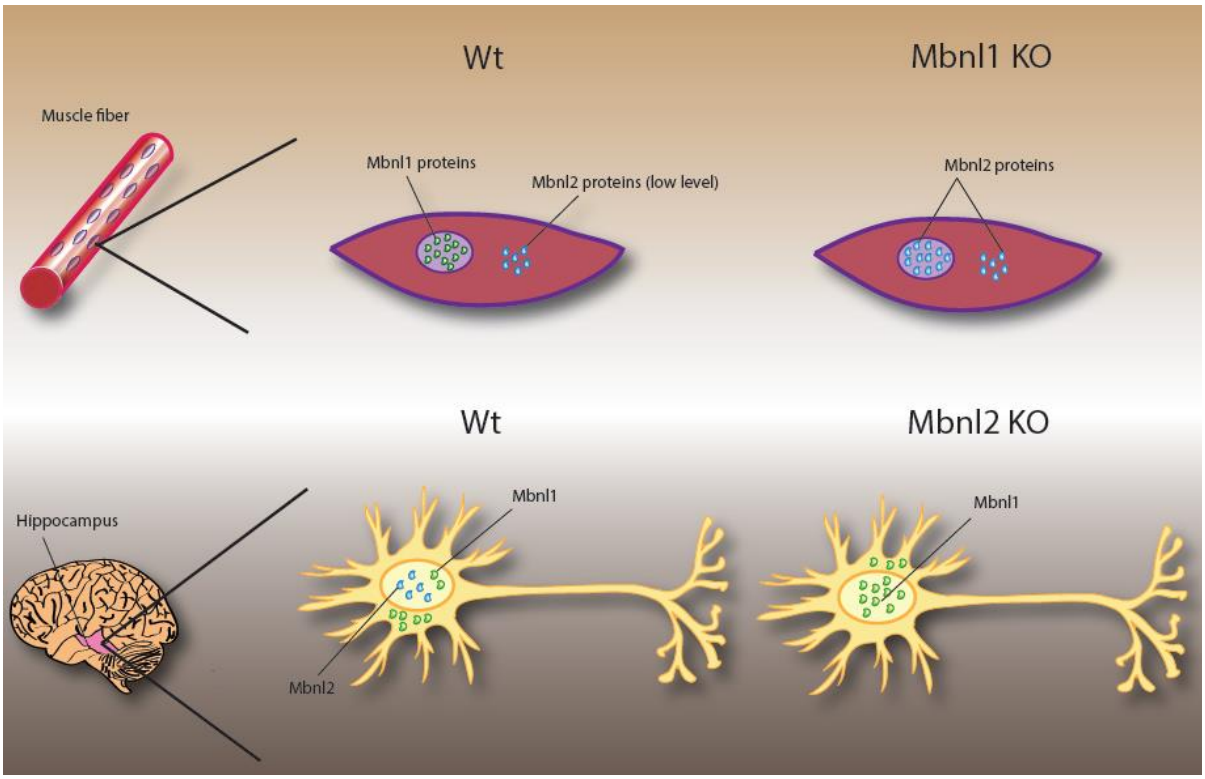

Figure 6-2. Upregulation and relocation of Mbnl proteins in the absence of their partner. In normal skeletal muscle, Mbnl1 regulates splicing in the nucleus and Mbnl2 remains in the cytoplasm. In the absence of Mbnl1, Mbnl2 is upregulated and enters the nucleus to control splicing. On the contrary, Mbnl2 is normally in the nucleus and regulates splicing in the brain while Mbnl1 is cytoplasmic. When Mbnl2 is ablated, Mbnl1 shuffles into the nucleus to regulate splicing.

CHAPTER 7
MATERIALS AND METHODS

Mice Mbnl Knockout Models

Detailed information on the generation of *Mbnl1* and *Mbnl2* knockout mice have been published mentioned previously (Charizanis et al., 2012; Kanadia et al., 2003a) Constitutive compound double knockouts were generated on a mixed BL6/129 background by crossing *Mbnl1*$^{+/DE3}$ *and Mbnl2*$^{+/DE2}$ males and females together. *Mbnl1*$^{DE3/DE3}$ *; Mbnl2*$^{cond/cond}$; Nestin +/- mice were generated by crossing male *Mbnl1*$^{+/DE3}$ *; Mbnl2*$^{cond/cond}$ *; Nestin* +/- with female *Mbnl1*$^{+/DE3}$ *; Mbnl2*$^{cond/cond}$ *; Nestin -/-* mice All animal procedures were reviewed and approved by IACUC at University of Florida.

Splicing Assay and Quantitative PCR

Mouse RNA from quadriceps muscle, heart and brain (hippocampi and cerebelli) were extracted by Tri-reagent (Sigma, St. Louis) and cDNA was obtained by using 5 µg of RNA and reverse transcription with SuperScript III (Invitrogen). For each PCR reaction, 2.5 µCi of [α^{32}P]-dCTP (PerkinElmer Life Sciences) were used followed by autoradiography and phosphorimaging detected by typhoon phosphoimager (9200 GE healthcare life science) and quantified with ImageQuant software (GE healthcare life science) to calculate the Ψ value (percent spliced in).

Quantitative RT-PCR to determine Mbnl2 RNA levels was performed using Wt and *Mbnl1* knockout quadriceps muscle and MyiQ single color real-time PCR detection system (Biorad, CA). First-strand cDNA was prepared as described above and Mbnl2 transcripts containing exon 2 were amplified using 2XiQ SYBR Green Supermix (Biorad, CA) and 250 nM of primer pairs for Mbnl2 or Gapdh. Real-time PCR reaction conditions

were 95.0°C for 10 min, 45 cycles of 95.0°C for 15 sec, 55.0°C for 30 sec and 72.0°C for 30 sec followed by 7 min at 72ºC.

Human RNA and RT-PCR Analysis

Autopsy was performed from temporal lobe and cerebellum of donated DM1 and disease control brains. Normal adult and fetal control samples were purchased from different venders. RNA was isolated using ISOGEN procedure (Nippon Gene) and 1-3 ug of RNA was used for cDNA synthesis. We used capillary electrophoresis (Hitachi Electronics) to analyze RNA quality and PCR products and Mann-Whitney U test for the statistical analysis.

PTZ Tests

To test the seizure susceptibility in *Mbnl2* knockout (heterozygous and homozygous) and DMSXL mice, we injected low dose of PTZ (pentylenetetrazol; 40 mg/kg) into control and mutant mice peritoneum and recorded their behavioral activities in the following 60 minutes. The onset of seizure was noted and scores were determined by a modified Racine Scale.

Sleep Analysis

Eight mice of 6 months old Wt and *Mbnl2* knockout mice each were implanted with electrodes in the brain and EEG/EMG were recorded simultaneously. Wakefulness, NREM and REM sleep were determined based on EEG/EMG criteria which have been described in detail elsewhere. In short, low amplitude and mixed frequency (>4 Hz) EEG combined with large EMG fluctuation indicates wakefulness; High amplitude/low frequency (0.5-4 Hz) EEG with EMG fluctuation indicates NREM sleep; Low amplitude/high frequency EEG accompanied theta waves (7-9 Hz) and low amplitude

EMG indicate REM sleep. These experiments were performed at the Sleep and Circadian Neurobiology (SCN) lab at Stanford University.

Rotarod Test

Mice (8 weeks for constitutive knockout mice and controls, n=5; 5 weeks for conditional knockout mice and controls, n≥8) were tested four times a day for consecutive four days using an accelerating rotarod (AccuScan Instruments). These mice were allowed to acclimate to the behavioral test room for 30 minutes before they were placed on the rotarod. In between each test, mice were allowed to rest 10 minutes in their cages. A constant acceleration program which started at the speed of 4 rpm, increased to 40 rpm in the first 5 minutes and continued at 40 rpm for another 5 minutes was used for all mice and latency to fall from the rotating bar was recorded.

Grip Strength Test

Mice (n=6 for each genotype and time point) were assessed for forelimb grip strength using a grip strength meter (Columbia Instruments). Mice were tested five times and the numbers were averaged.

Electromyography

Electromyography (EMG) was performed on *Mbnl1* knockout and 1KO2HET mice (2-3 months of age, n=4 each genotype) skeletal muscles (tibialis anterior and gastrocnemius) under general anesthesia (intraperitoneal injection of ketamine, 100 mg/kg and xylazine, 10 mg/kg). Mice were placed on a thermostatic heating pad and 30G concentric needle electrodes (CareFusion Teca Elite, n=4-5 insertions/muscle) were used with the TECASynergy EMG system (VIASYS Healthcare). Myotonic amplitudes were measured 8 sec post-insertion.

Histology and Immunofluorescent Study

Frozen transverse sections of 10 um thickness were made from tibialis anterior muscle at Leica Cryostat. Sections were incubated in hematoxylin and eosin (H&E) to determine the extent of DM related muscle pathology. For Clcn1 staining, fixed cross sections were detected by Clcn1 antibody (Alpha Diagnostic, Tx) For cardiac analysis, heart sections (5 um) were made and fibrosis was detected by Masson's trichrome stain.

Surface ECG

A detailed procedure of ECG acquisition has been described elsewhere (Gehrmann and Berul, 2000; Kasahara et al., 2001). Briefly, mice were anesthetized with1.5% isoflurane and cardiac electrical activities were recorded by six surface leads. These ECG recordings were acquired by a multichannel amplifier and converted to digital signals for analysis. (MAClab system; AD Instruments. Milford, Massachusetts)

ECG-gated Cine Cardiac MRI

Detailed materials and methods for cardiac MRI have been described previously (Slawson et al., 1998). In short, mice were anesthetized with 1.5% isofluorane and a warm air fan (SA Instruments, Stony Brook, NY) was used to maintain stable body temperature. MRI images were acquired from a 4.7 Tesla, bore size 33cm horizontal scanner (Agilent, Palo Alto, CA) This system includes a 12 cm inner diameter active-shield gradient coil and has a 40G/cm gradient strength and rise-time of 135 μs. A home-made quadrature saddle-shaped transceiver surface coil of 20x30 mm in size was used. Mice were positioned with the heart in the magnet iso-center, and for the long- and short-axis orientation of the heart was scouted using a gradient-echo sequence. Shimming and pulse calibration were performed automatically prior to each

experiment. Cine-FLASH was used to acquire temporally resolved dynamic short-axis and long-axis images of the heart with the following parameters: TReff = RR-interval, TE = 1.8 ms , flip angle = 30° , field of view 25×25 mm^2; acquisition matrix 128×128 pixels; and slice thickness 1 mm. The number of frames per cardiac cycle was adapted to the heart rate of each mouse to cover the whole cardiac cycle.

Western Blot for Protein Analysis

Dissected tissue from quadriceps, heart and brain were homogenized with lysis buffer (20 mM HEPES-KOH, pH 8.0, 100 mM KCl, 0.1% Igepal CA-630 (Sigma), 0.5 mM phenylmethysulfonyl fluoride, 5 mg/ml pepstain A, 1 mg/ml chymostatin, 1 mM e-aminocaproic acid, 1 mM *p*-aminobenzamidine, 1 mg/ml leupeptin, 2 mg/ml aprotinin) on ice, followed by sonication and centrifugation (16,100*g*, 15 min, 4°C) as reported previously (Charizanis et al., 2012). Proteins were detected by immunoblotting (50 µg lysate/lane) using rabbit polyclonal anti-Mbnl1 antibody A2764 (gift of C. Thornton, University of Rochester), mouse monoclonal (mAb) anti-Mbnl2 3B4 (Santa Cruz Biotechnology, CA), mouse anti-Gapdh mAb 6C5 (Abcam, MA), rabbit polyclonal anti-nucleolin (Abcam, MA), rabbit polyclonal anti-Ldha (Cell Signaling Technology, MA) and HRP-conjugated anti-mouse or anti-rabbit secondary antibody followed by ECL (GE Healthcare). Subcellular fractionations were performed using NE-PER Nuclear and Cytoplasmic Extraction Reagents (Thermo Scientific).

NMJ Staining

Tibialis anterior (TA) muscles were dissected from Wt, *Mbnl1* knockout and 1KO2HET mice and fixed overnight in 1% formaldehyde. After PBS wash, TA was teased into 5-10 smaller muscle bundles. Accetylcholine receptors were stained with 1µg/ml α-bungarotoxin (α-BTX) conjugated with Alexa Fluor 594 (Invitrogen). Axons and

synaptic detection were performed by incubating with chicken polyclonal anti-neurofilaments (NFH-1) antibody (Encor Biotechnology, Gainesville, FL) followed by Alexa 488 goat anti-chicken IgG (Invitrogen)

HITS-CLIP

Quadriceps muscle was dissected from Wt, *Mbnl1* and *Mbnl2* knockout mice (15-16 weeks of age, n=3), snap frozen in liquid nitrogen, powdered in liquid N_2 and crosslinked with UV-light using a UV Stratalinker 1800 (Stratagene). Immunoprecipitation was performed using anti-Mbnl2 mAb 3B4 (7.5 µg/2 mg lysate)(Santa Cruz Biotechnology, CA) and RNA tags were generated using RNase A concentrations of 38.6 U/ml and 0.0386 U/ml for high and low RNase, respectively. cDNA libraries were generated and sequenced and raw reads were filtered and aligned to the reference genome sequence using Burrow-Wheeler Aligner (BWA). Unique CLIP tags were identified after removing PCR duplicates computationally.

Electrophysiology

Details for electrophysiology have been noted elsewhere (Charizanis et al., 2012). In short, hippocampal slices were made using fresh brain tissue and incubated in standard artificial cerebrospinal fluid (ACSF) within a holding chamber under room temperature. The recording chamber was (Harvard Apparatus) perfused with oxygenated ACSF under proper flow rate, PH level, humidity and temperature. Slices were transferred to the recording chamber 30-60 minutes before recording. Extracellular synaptic field potential were recorded with glass micropipettes. A single diphasic stimulus pulse was generated from a stimulator (Grass Instrument Co.) to the Shaffer collateral commissural pathway and signals were filtered and recorded followed by computational analysis. For N-methyl-D-aspartate receptor (NMDAR) mediated EPSP,

slices were incubated in ACSF containing low magnesium, picrotoxin (PTX) and 6,7-dinitroquinoxaline-2,3-dione (DNQX).

LIST OF REFERENCES

Adereth, Y., Dammai, V., Kose, N., Li, R., and Hsu, T. (2005). RNA-dependent integrin alpha3 protein localization regulated by the Muscleblind-like protein MLP1. Nature cell biology *7*, 1240-1247
.

Allen, D.E., Johnson, A.G., and Woolf, A.L. (1969). The intramuscular nerve endings in dystrophia myotonica--a biopsy study by vital staining and electron microscopy. Journal of anatomy *105*, 1-26.

Aruga, J., and Mikoshiba, K. (2003). Identification and characterization of Slitrk, a novel neuronal transmembrane protein family controlling neurite outgrowth. Mol Cell Neurosci *24*, 117-129.

Ashizawa, T. (1998). Myotonic dystrophy as a brain disorder. Archives of neurology *55*, 291-293.

Ashizawa, T., and Sarkar, P.S. (2011). Myotonic dystrophy types 1 and 2. Handb Clin Neurol *101*, 193-237.

Barroso, F.A., and Nogues, M.A. (2009). Images in clinical medicine. Percussion myotonia. N Engl J Med *360*, e13.

Batra, R., Charizanis, K., and Swanson, M.S. (2010). Partners in crime: bidirectional transcription in unstable microsatellite disease. Human molecular genetics *19*, R77-82.

Beffert, U., Dillon, G.M., Sullivan, J.M., Stuart, C.E., Gilbert, J.P., Kambouris, J.A., and Ho, A. (2012). Microtubule plus-end tracking protein CLASP2 regulates neuronal polarity and synaptic function. J Neurosci *32*, 13906-13916.

Bell, T.J., Miyashiro, K.Y., Sul, J.Y., McCullough, R., Buckley, P.T., Jochems, J., Meaney, D.F., Haydon, P., Cantor, C., Parsons, T.D.*, et al.* (2008). Cytoplasmic BK(Ca) channel intron-containing mRNAs contribute to the intrinsic excitability of hippocampal neurons. Proc Natl Acad Sci U S A *105*, 1901-1906.

Berghella, L., De Angelis, L., De Buysscher, T., Mortazavi, A., Biressi, S., Forcales, S.V., Sirabella, D., Cossu, G., and Wold, B.J. (2008). A highly conserved molecular switch binds MSY-3 to regulate myogenin repression in postnatal muscle. Genes Dev *22*, 2125-2138.

Bhakta, D., Groh, M.R., Shen, C., Pascuzzi, R.M., and Groh, W.J. (2010). Increased mortality with left ventricular systolic dysfunction and heart failure in adults with myotonic dystrophy type 1. American heart journal *160*, 1137-1141, 1141 e1131.

Blencowe, B.J. (2006). Alternative splicing: new insights from global analyses. Cell *126*, 37-47.

Braunschweig, U., Gueroussov, S., Plocik, A.M., Graveley, B.R., and Blencowe, B.J. (2013). Dynamic integration of splicing within gene regulatory pathways. Cell *152*, 1252-1269.

Brook, J.D., McCurrach, M.E., Harley, H.G., Buckler, A.J., Church, D., Aburatani, H., Hunter, K., Stanton, V.P., Thirion, J.P., Hudson, T.*, et al.* (1992). Molecular basis of myotonic dystrophy: expansion of a trinucleotide (CTG) repeat at the 3' end of a transcript encoding a protein kinase family member. Cell *68*, 799-808.

Buj-Bello, A., Furling, D., Tronchere, H., Laporte, J., Lerouge, T., Butler-Browne, G.S., and Mandel, J.L. (2002). Muscle-specific alternative splicing of myotubularin-related 1 gene is impaired in DM1 muscle cells. Human molecular genetics *11*, 2297-2307.

Buljan, M., Chalancon, G., Eustermann, S., Wagner, G.P., Fuxreiter, M., Bateman, A., and Babu, M.M. (2012). Tissue-specific splicing of disordered segments that embed binding motifs rewires protein interaction networks. Mol Cell *46*, 871-883.

Burgess, H.A., and Reiner, O. (2002). Alternative splice variants of doublecortin-like kinase are differentially expressed and have different kinase activities. J Biol Chem *277*, 17696-17705.

Buxton, J., Shelbourne, P., Davies, J., Jones, C., Van Tongeren, T., Aslanidis, C., de Jong, P., Jansen, G., Anvret, M., Riley, B.*, et al.* (1992). Detection of an unstable fragment of DNA specific to individuals with myotonic dystrophy. Nature *355*, 547-548.

Campbell, C., Sherlock, R., Jacob, P., and Blayney, M. (2004). Congenital myotonic dystrophy: assisted ventilation duration and outcome. Pediatrics *113*, 811-816.

Cartegni, L., Chew, S.L., and Krainer, A.R. (2002). Listening to silence and understanding nonsense: exonic mutations that affect splicing. Nature reviews Genetics *3*, 285-298
.
Chamberlain, C.M., and Ranum, L.P. (2012). Mouse model of muscleblind-like 1 overexpression: skeletal muscle effects and therapeutic promise. Human molecular genetics.

Charizanis, K., Lee, K.-Y., Batra, R., Goodwin, M., Zhang, C., Yuan, Y., Shiue, L., Cline, M., Scotti, M.M., Xia, G.*, et al.* (2012). Muscleblind-like 2-Mediated Alternative Splicing in the Developing Brain and Dysregulation in Myotonic Dystrophy. Neuron *75*, 437-450.

Charlet, B.N., Savkur, R.S., Singh, G., Philips, A.V., Grice, E.A., and Cooper, T.A. (2002). Loss of the muscle-specific chloride channel in type 1 myotonic dystrophy due to misregulated alternative splicing. Mol Cell *10*, 45-53.

Coers, C., Telerman-Toppet, N., and Gerard, J.M. (1973). Terminal innervation ratio in neuromuscular disease. II. Disorders of lower motor neuron, peripheral nerve, and muscle. Archives of neurology *29*, 215-222.

Cooper, T.A., Wan, L., and Dreyfuss, G. (2009). RNA and disease. Cell *136*, 777-793.

Darnell, R.B. (2006). Developing global insight into RNA regulation. Cold Spring Harbor symposia on quantitative biology *71*, 321-327.

Darnell, R.B., and Posner, J.B. (2003). Paraneoplastic syndromes involving the nervous system. N Engl J Med *349*, 1543-1554.

Daughters, R.S., Tuttle, D.L., Gao, W., Ikeda, Y., Moseley, M.L., Ebner, T.J., Swanson, M.S., and Ranum, L.P. (2009). RNA gain-of-function in spinocerebellar ataxia type 8. PLoS genetics *5*, e1000600.

Dauvilliers, Y.A., and Laberge, L. (2012). Myotonic dystrophy type 1, daytime sleepiness and REM sleep dysregulation. Sleep medicine reviews *16*, 539-545.
de Almeida, S.F., and Carmo-Fonseca, M. (2012). Design principles of interconnections between chromatin and pre-mRNA splicing. Trends in biochemical sciences *37*, 248-253.

De Ambroggi, L., Raisaro, A., Marchiano, V., Radice, S., and Meola, G. (1995). Cardiac involvement in patients with myotonic dystrophy: characteristic features of magnetic resonance imaging. European heart journal *16*, 1007-1010.

de Die-Smulders, C.E., Howeler, C.J., Thijs, C., Mirandolle, J.F., Anten, H.B., Smeets, H.J., Chandler, K.E., and Geraedts, J.P. (1998). Age and causes of death in adult-onset myotonic dystrophy. Brain *121 (Pt 8)*, 1557-1563.

DeJesus-Hernandez, M., Mackenzie, I.R., Boeve, B.F., Boxer, A.L., Baker, M., Rutherford, N.J., Nicholson, A.M., Finch, N.A., Flynn, H., Adamson, J.*, et al.* (2011). Expanded GGGGCC hexanucleotide repeat in noncoding region of C9ORF72 causes chromosome 9p-linked FTD and ALS. Neuron *72*, 245-256.

Du, H., Cline, M.S., Osborne, R.J., Tuttle, D.L., Clark, T.A., Donohue, J.P., Hall, M.P., Shiue, L., Swanson, M.S., Thornton, C.A.*, et al.* (2010). Aberrant alternative splicing and extracellular matrix gene expression in mouse models of myotonic dystrophy. Nature structural & molecular biology *17*, 187-193.

Dubois, N.C., Hofmann, D., Kaloulis, K., Bishop, J.M., and Trumpp, A. (2006). Nestin-Cre transgenic mouse line Nes-Cre1 mediates highly efficient Cre/loxP mediated recombination in the nervous system, kidney, and somite-derived tissues. Genesis *44*, 355-360.

Etchegaray, J.P., Machida, K.K., Noton, E., Constance, C.M., Dallmann, R., Di Napoli, M.N., DeBruyne, J.P., Lambert, C.M., Yu, E.A., Reppert, S.M.*, et al.* (2009). Casein kinase 1 delta regulates the pace of the mammalian circadian clock. Mol Cell Biol *29*, 3853-3866.

Fardaei, M., Larkin, K., Brook, J.D., and Hamshere, M.G. (2001). In vivo co-localisation of MBNL protein with DMPK expanded-repeat transcripts. Nucleic acids research *29*, 2766-2771.

Fardaei, M., Rogers, M.T., Thorpe, H.M., Larkin, K., Hamshere, M.G., Harper, P.S., and Brook, J.D. (2002). Three proteins, MBNL, MBLL and MBXL, co-localize in vivo with nuclear foci of expanded-repeat transcripts in DM1 and DM2 cells. Human molecular genetics *11*, 805-814.

Ferraro, E., Molinari, F., and Berghella, L. (2012). Molecular control of neuromuscular junction development. Journal of cachexia, sarcopenia and muscle *3*, 13-23.

Fu, Y.H., Pizzuti, A., Fenwick, R.G., Jr., King, J., Rajnarayan, S., Dunne, P.W., Dubel, J., Nasser, G.A., Ashizawa, T., de Jong, P.*, et al.* (1992). An unstable triplet repeat in a gene related to myotonic muscular dystrophy. Science *255*, 1256-1258.

Fugier, C., Klein, A.F., Hammer, C., Vassilopoulos, S., Ivarsson, Y., Toussaint, A., Tosch, V., Vignaud, A., Ferry, A., Messaddeq, N.*, et al.* (2011). Misregulated alternative splicing of BIN1 is associated with T tubule alterations and muscle weakness in myotonic dystrophy. Nature medicine *17*, 720-725.

Gehman, L.T., Meera, P., Stoilov, P., Shiue, L., O'Brien, J.E., Meisler, M.H., Ares, M., Jr., Otis, T.S., and Black, D.L. (2012). The splicing regulator Rbfox2 is required for both cerebellar development and mature motor function. Genes Dev *26*, 445-460.

Gehman, L.T., Stoilov, P., Maguire, J., Damianov, A., Lin, C.-H., Shiue, L., Ares, M., Jr., Mody, I., and Black, D.L. (2011). The splicing regulator Rbfox1 (A2BP1) controls neuronal excitation in the mammalian brain. Nature genetics *43*, 706-711.

Gehrmann, J., and Berul, C.I. (2000). Cardiac electrophysiology in genetically engineered mice. J Cardiovasc Electrophysiol *11*, 354-368.

Gomes-Pereira, M., Cooper, T.A., and Gourdon, G. (2011). Myotonic dystrophy mouse models: towards rational therapy development. Trends in molecular medicine *17*, 506-517.

Gomes-Pereira, M., Foiry, L., Nicole, A., Huguet, A., Junien, C., Munnich, A., and Gourdon, G. (2007). CTG trinucleotide repeat "big jumps": large expansions, small mice. PLoS genetics *3*, e52.

Groh, W.J., Groh, M.R., Saha, C., Kincaid, J.C., Simmons, Z., Ciafaloni, E., Pourmand, R., Otten, R.F., Bhakta, D., Nair, G.V.*, et al.* (2008). Electrocardiographic abnormalities and sudden death in myotonic dystrophy type 1. N Engl J Med *358*, 2688-2697.

Han, S., Nam, J., Li, Y., Kim, S., Cho, S.H., Cho, Y.S., Choi, S.Y., Choi, J., Han, K., Kim, Y.*, et al.* (2010). Regulation of dendritic spines, spatial memory, and embryonic development by the TANC family of PSD-95-interacting proteins. J Neurosci *30*, 15102-15112.

Hao, M., Akrami, K., Wei, K., De Diego, C., Che, N., Ku, J.H., Tidball, J., Graves, M.C., Shieh, P.B., and Chen, F. (2008). Muscleblind-like 2 (Mbnl2) -deficient mice as a model for myotonic dystrophy. Developmental dynamics : an official publication of the American Association of Anatomists *237*, 403-410.

Harmon, E.B., Harmon, M.L., Larsen, T.D., Yang, J., Glasford, J.W., and Perryman, M.B. (2011). Myotonic dystrophy protein kinase is critical for nuclear envelope integrity. J Biol Chem *286*, 40296-40306.

Harper, P.S. (2001). Myotonic Dystrophy, 3rd edn (London: WB Saunders).

Heatwole, C., Bode, R., Johnson, N., Quinn, C., Martens, W., McDermott, M.P., Rothrock, N., Thornton, C., Vickrey, B., Victorson, D.*, et al.* (2012). Patient-reported impact of symptoms in myotonic dystrophy type 1 (PRISM-1). Neurology *79*, 348-357.

Hernandez-Hernandez, O., Guiraud-Dogan, C., Sicot, G., Huguet, A., Luilier, S., Steidl, E., Saenger, S., Marciniak, E., Obriot, H., Chevarin, C.*, et al.* (2013). Myotonic dystrophy CTG expansion affects synaptic vesicle proteins, neurotransmission and mouse behaviour. Brain *136*, 957-970.

Hino, S., Kondo, S., Sekiya, H., Saito, A., Kanemoto, S., Murakami, T., Chihara, K., Aoki, Y., Nakamori, M., Takahashi, M.P.*, et al.* (2007). Molecular mechanisms responsible for aberrant splicing of SERCA1 in myotonic dystrophy type 1. Human molecular genetics *16*, 2834-2843.

Ho, T.H., Bundman, D., Armstrong, D.L., and Cooper, T.A. (2005). Transgenic mice expressing CUG-BP1 reproduce splicing mis-regulation observed in myotonic dystrophy. Human molecular genetics *14*, 1539-1547.

Ho, T.H., Charlet, B.N., Poulos, M.G., Singh, G., Swanson, M.S., and Cooper, T.A. (2004). Muscleblind proteins regulate alternative splicing. The EMBO journal *23*, 3103-3112.

Holt, I., Jacquemin, V., Fardaei, M., Sewry, C.A., Butler-Browne, G.S., Furling, D., Brook, J.D., and Morris, G.E. (2009). Muscleblind-like proteins: similarities and differences in normal and myotonic dystrophy muscle. The American journal of pathology *174*, 216-227.

Huguet, A., Medja, F., Nicole, A., Vignaud, A., Guiraud-Dogan, C., Ferry, A., Decostre, V., Hogrel, J.Y., Metzger, F., Hoeflich, A.*, et al.* (2012). Molecular, physiological, and motor performance defects in DMSXL mice carrying >1,000 CTG repeats from the human DM1 locus. PLoS genetics *8*, e1003043.

Irimia, M., and Blencowe, B.J. (2012). Alternative splicing: decoding an expansive regulatory layer. Current opinion in cell biology *24*, 323-332.

Jansen, G., Groenen, P.J., Bachner, D., Jap, P.H., Coerwinkel, M., Oerlemans, F., van den Broek, W., Gohlsch, B., Pette, D., Plomp, J.J.*, et al.* (1996). Abnormal myotonic dystrophy protein kinase levels produce only mild myopathy in mice. Nature genetics *13*, 316-324.

Jiang, H., Mankodi, A., Swanson, M.S., Moxley, R.T., and Thornton, C.A. (2004). Myotonic dystrophy type 1 is associated with nuclear foci of mutant RNA, sequestration of muscleblind proteins and deregulated alternative splicing in neurons. Human molecular genetics *13*, 3079-3088.

Jin, P., Duan, R., Qurashi, A., Qin, Y., Tian, D., Rosser, T.C., Liu, H., Feng, Y., and Warren, S.T. (2007). Pur alpha binds to rCGG repeats and modulates repeat-mediated neurodegeneration in a Drosophila model of fragile X tremor/ataxia syndrome. Neuron *55*, 556-564.

Kaliman, P., and Llagostera, E. (2008). Myotonic dystrophy protein kinase (DMPK) and its role in the pathogenesis of myotonic dystrophy 1. Cellular signalling *20*, 1935-1941.

Kalsotra, A., and Cooper, T.A. (2011). Functional consequences of developmentally regulated alternative splicing. Nature reviews Genetics *12*, 715-729.

Kanadia, R.N., Johnstone, K.A., Mankodi, A., Lungu, C., Thornton, C.A., Esson, D., Timmers, A.M., Hauswirth, W.W., and Swanson, M.S. (2003a). A muscleblind knockout model for myotonic dystrophy. Science *302*, 1978-1980.

Kanadia, R.N., Shin, J., Yuan, Y., Beattie, S.G., Wheeler, T.M., Thornton, C.A., and Swanson, M.S. (2006). Reversal of RNA missplicing and myotonia after muscleblind overexpression in a mouse poly(CUG) model for myotonic dystrophy. Proc Natl Acad Sci U S A *103*, 11748-11753.

Kanadia, R.N., Urbinati, C.R., Crusselle, V.J., Luo, D., Lee, Y.J., Harrison, J.K., Oh, S.P., and Swanson, M.S. (2003b). Developmental expression of mouse muscleblind genes Mbnl1, Mbnl2 and Mbnl3. Gene expression patterns : GEP *3*, 459-462.

Kasahara, H., Wakimoto, H., Liu, M., Maguire, C.T., Converso, K.L., Shioi, T., Huang, W.Y., Manning, W.J., Paul, D., Lawitts, J.*, et al.* (2001). Progressive atrioventricular conduction defects and heart failure in mice expressing a mutant Csx/Nkx2.5 homeoprotein. J Clin Invest *108*, 189-201.

Kashiwai, A., Suzuki, T., and Ogawa, S. (2012). Sensitivity to rocuronium-induced neuromuscular block and reversibility with sugammadex in a patient with myotonic dystrophy. Case reports in anesthesiology *2012*, 107952
.
Kim, H.J., Kim, N.C., Wang, Y.D., Scarborough, E.A., Moore, J., Diaz, Z., MacLea, K.S., Freibaum, B., Li, S., Molliex, A.*, et al.* (2013). Mutations in prion-like domains in hnRNPA2B1 and hnRNPA1 cause multisystem proteinopathy and ALS. Nature *495*, 467-473.

Kim, J.S., Coon, S.L., Weller, J.L., Blackshaw, S., Rath, M.F., Moller, M., and Klein, D.C. (2009). Muscleblind-like 2: circadian expression in the mammalian pineal gland is controlled by an adrenergic-cAMP mechanism. Journal of neurochemistry *110*, 756-764.

Kim, S., Yun, H.M., Baik, J.H., Chung, K.C., Nah, S.Y., and Rhim, H. (2007). Functional interaction of neuronal Cav1.3 L-type calcium channel with ryanodine receptor type 2 in the rat hippocampus. J Biol Chem *282*, 32877-32889.

Kimura, T., Nakamori, M., Lueck, J.D., Pouliquin, P., Aoike, F., Fujimura, H., Dirksen, R.T., Takahashi, M.P., Dulhunty, A.F., and Sakoda, S. (2005). Altered mRNA splicing of the skeletal muscle ryanodine receptor and sarcoplasmic/endoplasmic reticulum Ca2+-ATPase in myotonic dystrophy type 1. Human molecular genetics *14*, 2189-2200.

Kiyan, E., Okumus, G., Cuhadaroglu, C., and Deymeer, F. (2010). Sleep apnea in adult myotonic dystrophy patients who have no excessive daytime sleepiness. Sleep Breath *14*, 19-24.

Koshelev, M., Sarma, S., Price, R.E., Wehrens, X.H., and Cooper, T.A. (2010). Heart-specific overexpression of CUGBP1 reproduces functional and molecular abnormalities of myotonic dystrophy type 1. Human molecular genetics *19*, 1066-1075.

Krahe, R., Ashizawa, T., Abbruzzese, C., Roeder, E., Carango, P., Giacanelli, M., Funanage, V.L., and Siciliano, M.J. (1995). Effect of myotonic dystrophy trinucleotide repeat expansion on DMPK transcription and processing. Genomics *28*, 1-14.

Kummer, T.T., Misgeld, T., Lichtman, J.W., and Sanes, J.R. (2004). Nerve-independent formation of a topologically complex postsynaptic apparatus. J Cell Biol *164*, 1077-1087.

Kuyumcu-Martinez, N.M., Wang, G.S., and Cooper, T.A. (2007). Increased steady-state levels of CUGBP1 in myotonic dystrophy 1 are due to PKC-mediated hyperphosphorylation. Mol Cell *28*, 68-78.

La Spada, A.R., and Taylor, J.P. (2010). Repeat expansion disease: progress and puzzles in disease pathogenesis. Nature reviews Genetics *11*, 247-258.

Laberge, L., Gagnon, C., and Dauvilliers, Y. (2013). Daytime sleepiness and myotonic dystrophy. Current neurology and neuroscience reports *13*, 340.

Laurent, F.X., Sureau, A., Klein, A.F., Trouslard, F., Gasnier, E., Furling, D., and Marie, J. (2012). New function for the RNA helicase p68/DDX5 as a modifier of MBNL1 activity on expanded CUG repeats. Nucleic acids research *40*, 3159-3171.

Lebre, A.S., Jamot, L., Takahashi, J., Spassky, N., Leprince, C., Ravise, N., Zander, C., Fujigasaki, H., Kussel-Andermann, P., Duyckaerts, C.*, et al.* (2001). Ataxin-7 interacts with a Cbl-associated protein that it recruits into neuronal intranuclear inclusions. Human molecular genetics *10*, 1201-1213.

Lee, J.E., and Cooper, T.A. (2009). Pathogenic mechanisms of myotonic dystrophy. Biochem Soc Trans *37*, 1281-1286.

Lehnart, S.E., Mongillo, M., Bellinger, A., Lindegger, N., Chen, B.X., Hsueh, W., Reiken, S., Wronska, A., Drew, L.J., Ward, C.W.*, et al.* (2008). Leaky Ca2+ release channel/ryanodine receptor 2 causes seizures and sudden cardiac death in mice. J Clin Invest *118*, 2230-2245.

Lesniewski, L.A., Hosch, S.E., Neels, J.G., de Luca, C., Pashmforoush, M., Lumeng, C.N., Chiang, S.H., Scadeng, M., Saltiel, A.R., and Olefsky, J.M. (2007). Bone marrow-specific Cap gene deletion protects against high-fat diet-induced insulin resistance. Nature medicine *13*, 455-462.

Li, S., Czubryt, M.P., McAnally, J., Bassel-Duby, R., Richardson, J.A., Wiebel, F.F., Nordheim, A., and Olson, E.N. (2005). Requirement for serum response factor for skeletal muscle growth and maturation revealed by tissue-specific gene deletion in mice. Proc Natl Acad Sci U S A *102*, 1082-1087.

Lia, A.S., Seznec, H., Hofmann-Radvanyi, H., Radvanyi, F., Duros, C., Saquet, C., Blanche, M., Junien, C., and Gourdon, G. (1998). Somatic instability of the CTG repeat in mice transgenic for the myotonic dystrophy region is age dependent but not correlated to the relative intertissue transcription levels and proliferative capacities. Human molecular genetics *7*, 1285-1291.

Licatalosi, D.D., and Darnell, R.B. (2006). Splicing regulation in neurologic disease. Neuron *52*, 93-101.

Lin, P.T., Gleeson, J.G., Corbo, J.C., Flanagan, L., and Walsh, C.A. (2000). DCAMKL1 encodes a protein kinase with homology to doublecortin that regulates microtubule polymerization. J Neurosci *20*, 9152-9161.

Lin, W.H., Huang, C.J., Liu, M.W., Chang, H.M., Chen, Y.J., Tai, T.Y., and Chuang, L.M. (2001). Cloning, mapping, and characterization of the human sorbin and SH3 domain containing 1 (SORBS1) gene: a protein associated with c-Abl during insulin signaling in the hepatoma cell line Hep3B. Genomics *74*, 12-20.

Lin, X., Miller, J.W., Mankodi, A., Kanadia, R.N., Yuan, Y., Moxley, R.T., Swanson, M.S., and Thornton, C.A. (2006). Failure of MBNL1-dependent post-natal splicing transitions in myotonic dystrophy. Human molecular genetics *15*, 2087-2097.

Liquori, C.L., Ricker, K., Moseley, M.L., Jacobsen, J.F., Kress, W., Naylor, S.L., Day, J.W., and Ranum, L.P. (2001). Myotonic dystrophy type 2 caused by a CCTG expansion in intron 1 of ZNF9. Science *293*, 864-867.

Lopez Castel, A., Nakamori, M., Tome, S., Chitayat, D., Gourdon, G., Thornton, C.A., and Pearson, C.E. (2011). Expanded CTG repeat demarcates a boundary for abnormal CpG methylation in myotonic dystrophy patient tissues. Hum Mol Genet *20*, 1-15.

Luco, R.F., Allo, M., Schor, I.E., Kornblihtt, A.R., and Misteli, T. (2011). Epigenetics in alternative pre-mRNA splicing. Cell *144*, 16-26.

Luco, R.F., and Misteli, T. (2011). More than a splicing code: integrating the role of RNA, chromatin and non-coding RNA in alternative splicing regulation. Current opinion in genetics & development *21*, 366-372.

Luco, R.F., Pan, Q., Tominaga, K., Blencowe, B.J., Pereira-Smith, O.M., and Misteli, T. (2010). Regulation of alternative splicing by histone modifications. Science *327*, 996-1000.

Lukong, K.E., Chang, K.W., Khandjian, E.W., and Richard, S. (2008). RNA-binding proteins in human genetic disease. Trends in genetics : TIG *24*, 416-425.

Machuca-Tzili, L.E., Buxton, S., Thorpe, A., Timson, C.M., Wigmore, P., Luther, P.K., and Brook, J.D. (2011). Zebrafish deficient for Muscleblind-like 2 exhibit features of myotonic dystrophy. Disease models & mechanisms *4*, 381-392.

Mahadevan, M., Tsilfidis, C., Sabourin, L., Shutler, G., Amemiya, C., Jansen, G., Neville, C., Narang, M., Barcelo, J., O'Hoy, K.*, et al.* (1992). Myotonic dystrophy mutation: an unstable CTG repeat in the 3' untranslated region of the gene. Science *255*, 1253-1255.

Mairet-Coello, G., Courchet, J., Pieraut, S., Courchet, V., Maximov, A., and Polleux, F. (2013). The CAMKK2-AMPK Kinase Pathway Mediates the Synaptotoxic Effects of Abeta Oligomers through Tau Phosphorylation. Neuron *78*, 94-108.

Mankodi, A., Logigian, E., Callahan, L., McClain, C., White, R., Henderson, D., Krym, M., and Thornton, C.A. (2000). Myotonic dystrophy in transgenic mice expressing an expanded CUG repeat. Science *289*, 1769-1773.

Mankodi, A., Takahashi, M.P., Jiang, H., Beck, C.L., Bowers, W.J., Moxley, R.T., Cannon, S.C., and Thornton, C.A. (2002). Expanded CUG repeats trigger aberrant splicing of ClC-1 chloride channel pre-mRNA and hyperexcitability of skeletal muscle in myotonic dystrophy. Mol Cell *10*, 35-44.

Mankodi, A., Teng-Umnuay, P., Krym, M., Henderson, D., Swanson, M., and Thornton, C.A. (2003). Ribonuclear inclusions in skeletal muscle in myotonic dystrophy types 1 and 2. Annals of neurology *54*, 760-768.

Marteyn, A., Maury, Y., Gauthier, M.M., Lecuyer, C., Vernet, R., Denis, J.A., Pietu, G., Peschanski, M., and Martinat, C. (2011). Mutant human embryonic stem cells reveal neurite and synapse formation defects in type 1 myotonic dystrophy. Cell stem cell *8*, 434-444.

Mathieu, J., Allard, P., Gobeil, G., Girard, M., De Braekeleer, M., and Begin, P. (1997). Anesthetic and surgical complications in 219 cases of myotonic dystrophy. Neurology *49*, 1646-1650.

Matynia, A., Ng, C.H., Dansithong, W., Chiang, A., Silva, A.J., and Reddy, S. (2010). Muscleblind1, but not Dmpk or Six5, contributes to a complex phenotype of muscular and motivational deficits in mouse models of myotonic dystrophy. PLoS One *5*, e9857.

McKinney, B.C., Sze, W., Lee, B., and Murphy, G.G. (2009). Impaired long-term potentiation and enhanced neuronal excitability in the amygdala of Ca(V)1.3 knockout mice. Neurobiology of learning and memory *92*, 519-528.

Meola, G., and Sansone, V. (2007). Cerebral involvement in myotonic dystrophies. Muscle Nerve *36*, 294-306.

Meredith, A.L., Wiler, S.W., Miller, B.H., Takahashi, J.S., Fodor, A.A., Ruby, N.F., and Aldrich, R.W. (2006). BK calcium-activated potassium channels regulate circadian behavioral rhythms and pacemaker output. Nature neuroscience *9*, 1041-1049.

Miller, J.W., Urbinati, C.R., Teng-Umnuay, P., Stenberg, M.G., Byrne, B.J., Thornton, C.A., and Swanson, M.S. (2000). Recruitment of human muscleblind proteins to (CUG)(n) expansions associated with myotonic dystrophy. The EMBO journal *19*, 4439-4448.

Modoni, A., Silvestri, G., Vita, M.G., Quaranta, D., Tonali, P.A., and Marra, C. (2008). Cognitive impairment in myotonic dystrophy type 1 (DM1): a longitudinal follow-up study. Journal of neurology *255*, 1737-1742.

Montgomery, J.R., Whitt, J.P., Wright, B.N., Lai, M.H., and Meredith, A.L. (2013). Mis-expression of the BK K(+) channel disrupts suprachiasmatic nucleus circuit rhythmicity and alters clock-controlled behavior. American journal of physiology Cell physiology *304*, C299-311.

Mori, K., Lammich, S., Mackenzie, I.R., Forne, I., Zilow, S., Kretzschmar, H., Edbauer, D., Janssens, J., Kleinberger, G., Cruts, M.*, et al.* (2013). hnRNP A3 binds to GGGGCC repeats and is a constituent of p62-positive/TDP43-negative inclusions in the hippocampus of patients with C9orf72 mutations. Acta neuropathologica *125*, 413-423.

Moseley, M.L., Zu, T., Ikeda, Y., Gao, W., Mosemiller, A.K., Daughters, R.S., Chen, G., Weatherspoon, M.R., Clark, H.B., Ebner, T.J.*, et al.* (2006). Bidirectional expression of CUG and CAG expansion transcripts and intranuclear polyglutamine inclusions in spinocerebellar ataxia type 8. Nature genetics *38*, 758-769.

Motta, J., Guilleminault, C., Billingham, M., Barry, W., and Mason, J. (1979). Cardiac abnormalities in myotonic dystrophy. Electrophysiologic and histopathologic studies. Am J Med *67*, 467-473.

Nagrani, T., Siyamwala, M., Vahid, G., and Bekheit, S. (2011). Ryanodine calcium channel: a novel channelopathy for seizures. The neurologist *17*, 91-94.

Nelson, D.L., Orr, H.T., and Warren, S.T. (2013). The unstable repeats--three evolving faces of neurological disease. Neuron *77*, 825-843.

Nguyen, H.H., Wolfe, J.T., 3rd, Holmes, D.R., Jr., and Edwards, W.D. (1988). Pathology of the cardiac conduction system in myotonic dystrophy: a study of 12 cases. J Am Coll Cardiol *11*, 662-671.

Nishi, M., Itoh, H., Tsubokawa, T., Taniguchi, T., and Yamamoto, K. (2004). Effective doses of vecuronium in a patient with myotonic dystrophy. Anaesthesia *59*, 1216-1218.

Nomura, K., Takeuchi, Y., Yamaguchi, S., Okamura, H., and Fukunaga, K. (2003). Involvement of calcium/calmodulin-dependent protein kinase II in the induction of mPer1. Journal of neuroscience research *72*, 384-392.

O'Rourke, J.R., and Swanson, M.S. (2009). Mechanisms of RNA-mediated disease. J Biol Chem *284*, 7419-7423.

Orengo, J.P., Chambon, P., Metzger, D., Mosier, D.R., Snipes, G.J., and Cooper, T.A. (2008). Expanded CTG repeats within the DMPK 3' UTR causes severe skeletal muscle wasting in an inducible mouse model for myotonic dystrophy. Proc Natl Acad Sci U S A *105*, 2646-2651.

Pal, R., Agbas, A., Bao, X., Hui, D., Leary, C., Hunt, J., Naniwadekar, A., Michaelis, M.L., Kumar, K.N., and Michaelis, E.K. (2003). Selective dendrite-targeting of mRNAs of

NR1 splice variants without exon 5: identification of a cis-acting sequence and isolation of sequence-binding proteins. Brain research *994*, 1-18.

Pan, Q., Shai, O., Lee, L.J., Frey, B.J., and Blencowe, B.J. (2008). Deep surveying of alternative splicing complexity in the human transcriptome by high-throughput sequencing. Nature genetics *40*, 1413-1415.

Pascual, M., Vicente, M., Monferrer, L., and Artero, R. (2006). The Muscleblind family of proteins: an emerging class of regulators of developmentally programmed alternative splicing. Differentiation; research in biological diversity *74*, 65-80.

Peters, M., Mizuno, K., Ris, L., Angelo, M., Godaux, E., and Giese, K.P. (2003). Loss of Ca2+/calmodulin kinase kinase beta affects the formation of some, but not all, types of hippocampus-dependent long-term memory. J Neurosci *23*, 9752-9760.

Petri, H., Vissing, J., Witting, N., Bundgaard, H., and Kober, L. (2012). Cardiac manifestations of myotonic dystrophy type 1. International journal of cardiology *160*, 82-88.

Pfeffer, M., Muller, C.M., Mordel, J., Meissl, H., Ansari, N., Deller, T., Korf, H.W., and von Gall, C. (2009). The mammalian molecular clockwork controls rhythmic expression of its own input pathway components. J Neurosci *29*, 6114-6123.

Philips, A.V., Timchenko, L.T., and Cooper, T.A. (1998). Disruption of splicing regulated by a CUG-binding protein in myotonic dystrophy. Science *280*, 737-741.

Polymenidou, M., Lagier-Tourenne, C., Hutt, K.R., Bennett, C.F., Cleveland, D.W., and Yeo, G.W. (2012). Misregulated RNA processing in amyotrophic lateral sclerosis. Brain research *1462*, 3-15.

Poulos, M.G., Batra, R., Charizanis, K., and Swanson, M.S. (2011). Developments in RNA splicing and disease. Cold Spring Harbor perspectives in biology *3*, a000778.

Proenca, C.C., Gao, K.P., Shmelkov, S.V., Rafii, S., and Lee, F.S. (2011). Slitrks as emerging candidate genes involved in neuropsychiatric disorders. Trends in neurosciences *34*, 143-153.

Puymirat, J., Bouchard, J.P., and Mathieu, J. (2012). Efficacy and tolerability of a 20-mg dose of methylphenidate for the treatment of daytime sleepiness in adult patients with myotonic dystrophy type 1: a 2-center, randomized, double-blind, placebo-controlled, 3-week crossover trial. Clin Ther *34*, 1103-1111.

Ranum, L.P., and Cooper, T.A. (2006). RNA-mediated neuromuscular disorders. Annual review of neuroscience *29*, 259-277.

Ranum, L.P., and Day, J.W. (2002). Dominantly inherited, non-coding microsatellite expansion disorders. Current opinion in genetics & development *12*, 266-271.

Ranum, L.P., and Day, J.W. (2004). Myotonic dystrophy: RNA pathogenesis comes into focus. American journal of human genetics *74*, 793-804.

Ranum, L.P., Rasmussen, P.F., Benzow, K.A., Koob, M.D., and Day, J.W. (1998). Genetic mapping of a second myotonic dystrophy locus. Nature genetics *19*, 196-198.

Ravel-Chapuis, A., Belanger, G., Yadava, R.S., Mahadevan, M.S., DesGroseillers, L., Cote, J., and Jasmin, B.J. (2012). The RNA-binding protein Staufen1 is increased in DM1 skeletal muscle and promotes alternative pre-mRNA splicing. J Cell Biol *196*, 699-712.

Renton, A.E., Majounie, E., Waite, A., Simon-Sanchez, J., Rollinson, S., Gibbs, J.R., Schymick, J.C., Laaksovirta, H., van Swieten, J.C., Myllykangas, L.*, et al.* (2011). A hexanucleotide repeat expansion in C9ORF72 is the cause of chromosome 9p21-linked ALS-FTD. Neuron *72*, 257-268.

Ricker, K., Koch, M.C., Lehmann-Horn, F., Pongratz, D., Otto, M., Heine, R., and Moxley, R.T., 3rd (1994). Proximal myotonic myopathy: a new dominant disorder with myotonia, muscle weakness, and cataracts. Neurology *44*, 1448-1452.

Roig, M., Balliu, P.R., Navarro, C., Brugera, R., and Losada, M. (1994). Presentation, clinical course, and outcome of the congenital form of myotonic dystrophy. Pediatric neurology *11*, 208-213.

Sahashi, K., Hua, Y., Ling, K.K., Hung, G., Rigo, F., Horev, G., Katsuno, M., Sobue, G., Ko, C.P., Bennett, C.F.*, et al.* (2012). TSUNAMI: an antisense method to phenocopy splicing-associated diseases in animals. Genes Dev *26*, 1874-1884.

Sansone, V., Gandossini, S., Cotelli, M., Calabria, M., Zanetti, O., and Meola, G. (2007). Cognitive impairment in adult myotonic dystrophies: a longitudinal study. Neurological sciences : official journal of the Italian Neurological Society and of the Italian Society of Clinical Neurophysiology *28*, 9-15.

Santos, K., Palmini, A., Radziuk, A.L., Rotert, R., Bastos, F., Booij, L., and Fernandes, B.S. (2013). The impact of methylphenidate on seizure frequency and severity in children with attention-deficit-hyperactivity disorder and difficult-to-treat epilepsies. Developmental medicine and child neurology.

Savkur, R.S., Philips, A.V., and Cooper, T.A. (2001). Aberrant regulation of insulin receptor alternative splicing is associated with insulin resistance in myotonic dystrophy. Nature genetics *29*, 40-47.

Sergeant, N., Sablonniere, B., Schraen-Maschke, S., Ghestem, A., Maurage, C.A., Wattez, A., Vermersch, P., and Delacourte, A. (2001). Dysregulation of human brain microtubule-associated tau mRNA maturation in myotonic dystrophy type 1. Human molecular genetics *10*, 2143-2155.

Seznec, H., Agbulut, O., Sergeant, N., Savouret, C., Ghestem, A., Tabti, N., Willer, J.C., Ourth, L., Duros, C., Brisson, E.*, et al.* (2001). Mice transgenic for the human myotonic dystrophy region with expanded CTG repeats display muscular and brain abnormalities. Human molecular genetics *10*, 2717-2726.

Seznec, H., Lia-Baldini, A.S., Duros, C., Fouquet, C., Lacroix, C., Hofmann-Radvanyi, H., Junien, C., and Gourdon, G. (2000). Transgenic mice carrying large human genomic sequences with expanded CTG repeat mimic closely the DM CTG repeat intergenerational and somatic instability. Human molecular genetics *9*, 1185-1194.

Shin, J., Charizanis, K., and Swanson, M.S. (2009). Pathogenic RNAs in microsatellite expansion disease. Neuroscience letters *466*, 99-102.

Slawson, S.E., Roman, B.B., Williams, D.S., and Koretsky, A.P. (1998). Cardiac MRI of the normal and hypertrophied mouse heart. Magn Reson Med *39*, 980-987.

Sofola, O.A., Jin, P., Qin, Y., Duan, R., Liu, H., de Haro, M., Nelson, D.L., and Botas, J. (2007). RNA-binding proteins hnRNP A2/B1 and CUGBP1 suppress fragile X CGG premutation repeat-induced neurodegeneration in a Drosophila model of FXTAS. Neuron *55*, 565-571.

Suenaga, K., Lee, K.Y., Nakamori, M., Tatsumi, Y., Takahashi, M.P., Fujimura, H., Jinnai, K., Yoshikawa, H., Du, H., Ares, M., Jr.*, et al.* (2012). Muscleblind-like 1 knockout mice reveal novel splicing defects in the myotonic dystrophy brain. PLoS One *7*, e33218.

Swanson, M.S., and Orr, H.T. (2007). Fragile X tremor/ataxia syndrome: blame the messenger! Neuron *55*, 535-537.

Takasawa, S., Kuroki, M., Nata, K., Noguchi, N., Ikeda, T., Yamauchi, A., Ota, H., Itaya-Hironaka, A., Sakuramoto-Tsuchida, S., Takahashi, I.*, et al.* (2010). A novel ryanodine receptor expressed in pancreatic islets by alternative splicing from type 2 ryanodine receptor gene. Biochem Biophys Res Commun *397*, 140-145.

Takeuchi, Y., Yamamoto, H., Matsumoto, K., Kimura, T., Katsuragi, S., Miyakawa, T., and Miyamoto, E. (1999). Nuclear localization of the delta subunit of Ca2+/calmodulin-dependent protein kinase II in rat cerebellar granule cells. Journal of neurochemistry *72*, 815-825.

Tang, Z.Z., Yarotskyy, V., Wei, L., Sobczak, K., Nakamori, M., Eichinger, K., Moxley, R.T., Dirksen, R.T., and Thornton, C.A. (2012). Muscle weakness in myotonic dystrophy associated with misregulated splicing and altered gating of Ca(V)1.1 calcium channel. Human molecular genetics *21*, 1312-1324
.
Timchenko, L.T., Miller, J.W., Timchenko, N.A., DeVore, D.R., Datar, K.V., Lin, L., Roberts, R., Caskey, C.T., and Swanson, M.S. (1996a). Identification of a (CUG)n triplet repeat RNA-binding protein and its expression in myotonic dystrophy. Nucleic acids research *24*, 4407-4414.

Timchenko, L.T., Timchenko, N.A., Caskey, C.T., and Roberts, R. (1996b). Novel proteins with binding specificity for DNA CTG repeats and RNA CUG repeats: implications for myotonic dystrophy. Human molecular genetics *5*, 115-121.

Timchenko, N.A., Patel, R., Iakova, P., Cai, Z.-J., Quan, L., and Timchenko, L.T. (2004). Overexpression of CUG triplet repeat-binding protein, CUGBP1, in mice inhibits myogenesis. J Biol Chem *279*, 13129-13139.

Ule, J., Stefani, G., Mele, A., Ruggiu, M., Wang, X., Taneri, B., Gaasterland, T., Blencowe, B.J., and Darnell, R.B. (2006). An RNA map predicting Nova-dependent splicing regulation. Nature *444*, 580-586.

Valdez, G., Tapia, J.C., Kang, H., Clemenson, G.D., Jr., Gage, F.H., Lichtman, J.W., and Sanes, J.R. (2010). Attenuation of age-related changes in mouse neuromuscular synapses by caloric restriction and exercise. Proc Natl Acad Sci U S A *107*, 14863-14868.

Vukojevic, V., Gschwind, L., Vogler, C., Demougin, P., de Quervain, D.J., Papassotiropoulos, A., and Stetak, A. (2012). A role for alpha-adducin (ADD-1) in nematode and human memory. The EMBO journal *31*, 1453-1466.

Wahbi, K., and Duboc, D. (2012). Arrhythmia management in myotonic dystrophy type 1-reply. Jama *308*, 337-338.

Wahbi, K., Meune, C., Porcher, R., Becane, H.M., Lazarus, A., Laforet, P., Stojkovic, T., Behin, A., Radvanyi-Hoffmann, H., Eymard, B.*, et al.* (2012). Electrophysiological study with prophylactic pacing and survival in adults with myotonic dystrophy and conduction system disease. Jama *307*, 1292-1301.

Wahl, M.C., Will, C.L., and Luhrmann, R. (2009). The spliceosome: design principles of a dynamic RNP machine. Cell *136*, 701-718.

Wang, E.T., Cody, N.A.L., Jog, S., Biancolella, M., Wang, T.T., Treacy, D.J., Luo, S., Schroth, G.P., Housman, D.E., Reddy, S.*, et al.* (2012). Transcriptome-wide Regulation of Pre-mRNA Splicing and mRNA Localization by Muscleblind Proteins. Cell *150*, 710-724.

Wang, E.T., Sandberg, R., Luo, S., Khrebtukova, I., Zhang, L., Mayr, C., Kingsmore, S.F., Schroth, G.P., and Burge, C.B. (2008). Alternative isoform regulation in human tissue transcriptomes. Nature *456*, 470-476.

Wang, G.-S., and Cooper, T.A. (2007). Splicing in disease: disruption of the splicing code and the decoding machinery. Nature reviews Genetics *8*, 749-761.
Wang, G.S., Kearney, D.L., De Biasi, M., Taffet, G., and Cooper, T.A. (2007). Elevation of RNA-binding protein CUGBP1 is an early event in an inducible heart-specific mouse model of myotonic dystrophy. J Clin Invest *117*, 2802-2811.

Wang, G.S., Kuyumcu-Martinez, M.N., Sarma, S., Mathur, N., Wehrens, X.H., and Cooper, T.A. (2009). PKC inhibition ameliorates the cardiac phenotype in a mouse model of myotonic dystrophy type 1. J Clin Invest *119*, 3797-3806.

Wang, Z., and Burge, C.B. (2008). Splicing regulation: from a parts list of regulatory elements to an integrated splicing code. RNA *14*, 802-813.

Wang, Z.J., and Huang, X.S. (2011). Images in clinical medicine. Myotonia of the tongue. N Engl J Med *365*, e32.

Ward, A.J., Rimer, M., Killian, J.M., Dowling, J.J., and Cooper, T.A. (2010). CUGBP1 overexpression in mouse skeletal muscle reproduces features of myotonic dystrophy type 1. Human molecular genetics *19*, 3614-3622.

Weatheritt, R.J., and Gibson, T.J. (2012). Linear motifs: lost in (pre)translation. Trends in biochemical sciences *37*, 333-341.

Wells, R.D., and Ashizawa, T. (2006). Genetic Instabilities and Neurological Diseases, 2nd edn (Burlington: Elsevier Inc.).

Wheeler, T.M., Krym, M.C., and Thornton, C.A. (2007a). Ribonuclear foci at the neuromuscular junction in myotonic dystrophy type 1. Neuromuscular disorders : NMD *17*, 242-247.

Wheeler, T.M., Leger, A.J., Pandey, S.K., MacLeod, A.R., Nakamori, M., Cheng, S.H., Wentworth, B.M., Bennett, C.F., and Thornton, C.A. (2012). Targeting nuclear RNA for in vivo correction of myotonic dystrophy. Nature *488*, 111-115.

Wheeler, T.M., Lueck, J.D., Swanson, M.S., Dirksen, R.T., and Thornton, C.A. (2007b). Correction of ClC-1 splicing eliminates chloride channelopathy and myotonia in mouse models of myotonic dystrophy. J Clin Invest *117*, 3952-3957.

Wheeler, T.M., Sobczak, K., Lueck, J.D., Osborne, R.J., Lin, X., Dirksen, R.T., and Thornton, C.A. (2009). Reversal of RNA dominance by displacement of protein sequestered on triplet repeat RNA. Science (New York, N Y) *325*, 336-339.

Xu, X., Yang, D., Ding, J.H., Wang, W., Chu, P.H., Dalton, N.D., Wang, H.Y., Bermingham, J.R., Jr., Ye, Z., Liu, F.*, et al.* (2005). ASF/SF2-regulated CaMKIIdelta alternative splicing temporally reprograms excitation-contraction coupling in cardiac muscle. Cell *120*, 59-72.

Xu, Z., Poidevin, M., Li, X., Li, Y., Shu, L., Nelson, D.L., Li, H., Hales, C.M., Gearing, M., Wingo, T.S.*, et al.* (2013). Expanded GGGGCC repeat RNA associated with amyotrophic lateral sclerosis and frontotemporal dementia causes neurodegeneration. Proc Natl Acad Sci U S A.

Yamamoto, H., Kokame, K., Okuda, T., Nakajo, Y., Yanamoto, H., and Miyata, T. (2011). NDRG4 protein-deficient mice exhibit spatial learning deficits and vulnerabilities to cerebral ischemia. J Biol Chem *286*, 26158-26165.

Yokota, S., Yamamoto, M., Moriya, T., Akiyama, M., Fukunaga, K., Miyamoto, E., and Shibata, S. (2001). Involvement of calcium-calmodulin protein kinase but not mitogen-activated protein kinase in light-induced phase delays and Per gene expression in the suprachiasmatic nucleus of the hamster. Journal of neurochemistry *77*, 618-627.

Yu, H., Laberge, L., Jaussent, I., Bayard, S., Scholtz, S., Raoul, M., Pages, M., and Dauvilliers, Y. (2011). Daytime sleepiness and REM sleep characteristics in myotonic dystrophy: a case-control study. Sleep *34*, 165-170.

Zhang, C., Frias, M.A., Mele, A., Ruggiu, M., Eom, T., Marney, C.B., Wang, H., Licatalosi, D.D., Fak, J.J., and Darnell, R.B. (2010). Integrative modeling defines the Nova splicing-regulatory network and its combinatorial controls. Science *329*, 439-443.

Zu, T., Gibbens, B., Doty, N.S., Gomes-Pereira, M., Huguet, A., Stone, M.D., Margolis, J., Peterson, M., Markowski, T.W., Ingram, M.A.C.*, et al.* (2011). Non-ATG-initiated translation directed by microsatellite expansions. Proc Natl Acad Sci U S A *108*, 260-265.

BIOGRAPHICAL SKETCH

Kuang-Yung (Kyle) Lee was born in Taipei, Taiwan, in 1968. Besides an elder sister, he is the only son born to Hsin-Min Lee and Shu-Jen Chen. Kyle attended Medical School in China Medical University at Taichung, Taiwan from 1987 to 1994 and earned M.D. degree in 1994. After two years of military service as a lieutenant physician, he started his residency at Taipei Municipal Jen-Ai Hospital and Chang-Gung Memorial Hospital (CGMH) Keelung branch. During 2000-2005, Kyle became a board-certified neurologist and was an attending physician in Department of Neurology at the Keelung branch of CGMH. Kyle committed himself to medical research and started his career in Dr. Jin-Moo Lee's lab at Washington University in St. Louis during 2005-2007. In 2007, Kyle was recruited by Interdisciplinary Program in Biomedical Science at the University of Florida, College of Medicine. During the past six years, Kyle did his graduate research with Dr. Maurice Swanson in the Department of Molecular Genetics and Microbiology and completed his Ph.D. dissertation in August, 2013. Kyle plans to return to CGMH at Keelung, Taiwan, and continue his biomedical research career as a physician scientist.